

Functional Analysis of Mammalian Coronin 3

INAUGURAL-DISSERTATION

zur

Erlangung des Doktorgrades

der Mathematisch-Naturwissenschaftlichen Fakultät

der Universität zu Köln

Vorgelegt von

Ziqiang Spoerl

Aus Shanghai, China

**Druck u. Verarbeitung: Hundt Druck GmbH, Köln
July, 2003**

Referees/Berichtererstatter

Prof. Dr. Angelika A. Noegel
Prof. Dr. Helmut W. Klein

Date of oral examination/
Tag der mündlichen Prüfung

03.07.2003

The present research work was carried out under the supervision of the direction of Professor Dr. Angelika A. Noegel and Dr. Andreas Hasse in the Institute of Biochemistry, Medical Faculty, University of Cologne, Germany, from August 2000 to April 2003.

Diese Arbeit wurde von August 2000 bis April 2003 am Biochemischen Institut I der medizinischen Fakultät der Universität zu Köln unter der Betreuung von Professor Dr. Angelika A. Noegel und der Leitung von Dr. Andreas Hasse durchgeführt.

Abbreviations

APS	ammonium persulphate
ATP	adenosintriphosphate
Bp	base pair(s)
BSA	bovine serum albumin
cAMP	cyclic adenosine monophosphate
cDNA	complementary DAN
<i>C. elegans</i>	<i>Caenorhabditis elegans</i>
CIAP	calf intertinal alkaline phosphatase
dNTP	deoxyribonucleotide triphosphate
DMSO	dimethylsulphoxide
DNA	deoxyribonucleic acid
DNase	deoxyribonuclease
ds DNA	double strand DNA
DTT	1,4-dithiothreitol
ECL	enhanced chemiluminescence
<i>E. coli</i>	<i>Escherichia coli</i>
EDTA	ethylenediaminetetraacetic acid
EGTA	ethyleneglycol-bis(2-amino-ethylene) N,N,N,N-tetraacetic acid
FCS	fetal calf serum
G418	geneticin
EGFP	enhanced green fluorescent protein
GST	glutathione S-transferase
HEPES	N-(2-hydroxyethyl)piperazine-N'-2-ethanesulphonic acid
HRP	horse radish peroxidase
IgG	immunoglobulin G
IPTG	iso-propylthio-galactopyranoside
Kb	kilobase pairs
kDa	kilodalton
MES	morpholinoethansulphonic acid
β -ME	beta-mercaptoethanol
MOPS	Morpholinopropanesulphonic acid
MW	molecular weight
NP-40	nonylphenylpolyethyleneglycol
OD	optical density
PAGE	polyacrylamide gel electrophoresis
PBS	phosphate buffer solution
PBG	phosphate buffer with fish gelatine
PIPES	piperazine-N,N'-bis(2-ethanesulphonic acid)
PMSF	phenylmethylsulphonylfluoride
RNA	ribonucleic acid
RNase	ribonuclease
rpm	rotations per minute
SDS	sodium dodecyl sulphate
ss DNA	single strand DNA
TE	Tris-EDTA
TEMED	N,N,N',N'-tetramethyl-ethylendiamine
Tris	Tris-(hydroxymethyl)aminomethane
TRITC	tetramethylrhodamine isothiocyanate

Triton X-100	t-Octylphenoxy polyoxyethanol
Tween 20	polyoxyethyl sorbitan monolaurate
UV	ultraviolet
vol.	volume
v/v	volume by volume
w/v	weight by volume
X-gal	5-bromo-4-chloro-3-indolyl-D-galactopyranoside

Units of measure and prefixes

Unit name	measure
°C	degree Celsius
D	Dalton
g	gram
h	hour
l	liter
μm	micrometer
min	minute
mg	milligram
μg	microgram
ng	nanogram
s	second
v	volt
μF	microfarad

Table of contents

I	Introduction1
1	The cytoskeleton1
1.1	Microtubules1
1.2	Intermediate filaments2
1.3	Actin filaments3
1.4	Actin-binding proteins4
2	Coronin6
3	Coronin function8
3.1	Coronin in <i>Dictyostelium discoideum</i>8
3.2	Coronin in <i>Saccharomyces cerevisiae</i>8
3.3	Coronin in mammals9
4	Coronins in the nerve system11
5	Aim of this work12
II	Materials and methods13
1	Materials13
1.1	Reagents13
1.2	Enzymes, inhibitors and antibodies14
1.3	Vectors15
1.4	Kits and reagents15
1.5	Bacterial host strains15
1.6	Media for <i>E. coli</i> culture15
1.7	Media for cell culture16
1.8	Mammalian cell lines16
1.9	Laboratory materials16
1.10	Instruments and equipments17
1.11	Computer analysis18
2	Molecular biological methods19
2.1	Plasmid preparation19
2.1.1	Boiling method for preparation of plasmid DNA19
2.1.2	Mini-preparation of plasmid DNA20
2.1.3	Midi and maxi preparation of plasmid of DNA20
2.2	DNA agarose gel electrophoresis20
2.3	Isolation of DNA fragments from agarose gels21
2.4	Quantification of DNA21
2.5	Digestion with restriction enzymes22
2.6	Generation of blunt ends in linearized plasmid DNA22
2.7	Dephosphorylation of DNA fragments23
2.8	Ligation of vectors and DNA fragments23
2.9	Transformation of <i>E. coli</i> cells23
2.9.1	Preparation of competent <i>E. coli</i> cells23
2.9.2	Transformation of <i>E. coli</i> cells24
2.9.3	Glycerol stock of bacterial cultures24
2.10	Construction of vectors24
2.10.1	Vector for expression of Hcoronin 3 as myc-6×His-fusion proteins24
2.10.2	Vector for expression of Hcoronin 3 as GST-fusion proteins25
2.10.3	Vector for expression of Hcoronin 3 as EGFP-fusion proteins25

2.10.4	Vector for expression of Hcoronin 3 fragments as 6×His-fusion proteins in <i>E. coli</i>25
2.11	DNA sequence analysis26
3	Protein analysis and immunological methods26
3.1	SDS-polyacrylamide gel electrophoresis26
3.2	Commassie blue staining of SDS-polyacrylamide gels27
3.3	Western blotting27
3.4	Ponceau S staining28
3.5	Immunodetection of nitrocellulose membrane-bound proteins28
3.6	Expression and purification of 6×His tagged NH ₂ - and COOH-terminal Hcoronin 3 fragments in <i>E. coli</i>29
3.6.1	Expression of 6×His tagged COOH-terminal Hcoronin 3 residues 315-444. 315-474 and NH ₂ -terminal Hcoronin 3 residues 1-7129
3.6.2	Purification of 6×His tagged COOH-terminal Hcoronin 3 fragments30
3.6.3	Purification of a 6×His tagged NH ₂ -terminal Hcoronin 3 (1-71) fragment30
3.7	Buffer exchange and concentration of proteins32
3.7.1	Quantification of protein concentration32
3.8	Generation of a Hcoronin 3 antibody32
3.9	Subcellular fractionation33
3.9.1	Differential centrifugation33
3.9.2	Isopycnic separation on discontinuous sucrose gradients33
3.10	Gel filtration chromatography34
3.10.1	Analysis of Hcoronin 3 oligomers <i>in vivo</i>34
3.10.2	Analysis of the domain requirements of Hcoronin 3 for the formation of cytosolic complexes35
3.10.3	Migration of recombinant COOH-terminal Hcoronin 3 fragments in gel filtration35
3.11	Immunoprecipitation36
3.12	Actin binding assay37
3.13	Light microscopic assay of F-actin suprastructures formed in the presence of different Hcoronin 3 COOH-terminal fragments38
3.14	2D-gel sample preparation39
4	Cell culture41
4.1	Cell lines41
4.2	Culture of adherent cell lines41
4.3	DMSO stocks of adherent cells41
4.4	Thawing and recovering mammalian cells41
4.5	Transfection of mammalian cells42
4.5.1	Lipid-mediated transfection42
4.5.2	Electroporation of Neuro-2a and HEK 293 cells42
4.6	Calculation of cell density43
4.7	Establishment of stable cell lines by G418 selection43
4.8	Differentiation of Neuro-2a cells44
4.9	Stimulation of Neuro-2a cells44
5	Cell biological methods44
5.1	Indirect immunofluorescence of mammalian cells44
5.1.1	Preparation of Neuro-2a cells44
5.1.2	Methanol fixation44
5.1.3	Paraformaldehyde fixation45
5.1.4	Immunolabelling of fixed cells45
5.1.5	Mounting of coverslips46
5.2	Fluorescence microscopy46

III	Results47
1	Sequence analysis of Hcoronin 347
1.1	Alignment of Hcoronin 3 with <i>Dictyostelium</i> coronin and yeast crn1p47
1.2	Alignment of Hcoronin 3 with <i>H. sapiens</i> coronin 1, 2, 3, 4, 5, <i>O. cuniculus</i> coronin 2 _{se} and <i>M. musculus</i> coronin 648
1.3	Phylogenetic relationship of Hcoronin 3 to conventional mammalian coronins48
2	Subcellular localization of endogenous and EGFP-Hcoronin 351
2.1	Localization of endogenous coronin 3 in undifferentiated and differentiated Neuro-2a cells52
2.2	Domain requirements for the colocalization of EGFP-Hcoronin 3 with neurite extensions53
3	Effect of the expression of different EGFP-Hcoronin 3 versions on neurite outgrowth in Neuro-2a cells58
4	Subcellular distribution of coronin 3 in undifferentiated and differentiated Neuro-2a cells60
5	Analysis of the cellular distribution by isopycnic sucrose step gradient centrifugation61
6	Gel filtration analysis of Hcoronin 363
6.1	Oligomerization of the recombinant Hcoronin 3 COOH-terminus <i>in vitro</i>	63
6.2	Oligomerization of Hcoronin 3 <i>in vivo</i>65
6.3	The domain requirement for the formation of Hcoronin 3 cytosolic complexes67
7	Phosphorylation of coronin 369
8	Effect of PMA and bisindolylmaleimide on the phosphorylation of coronin 3 in Neuro-2a cells <i>in vivo</i>72
9	Effect of PMA and bisindolylmaleimide on the subcellular localization of EGFP-Hcoronin 3 in undifferentiated and differentiated Neuro-2a cells74
10	Effect of colchicine and taxol on the subcellular localization of EGFP-Hcoronin 3 in differentiated Neuro-2a cells76
11	<i>In vitro</i> analysis of recombinant Hcoronin 3 fragments78
11.1	Expression and purification of 6×His-Hcoronin 3 fragments79
11.2	Actin binding assay80
11.2.1	<i>In vitro</i> binding of Hcoronin 3 NH ₂ - and COOH-terminal domains to actin80
11.2.2	The affinity of COOH-terminal Hcoronin 3 polypeptides to actin filaments82
11.2.3	COOH-terminal Hcoronin 3 polypeptide crosslink or bundle F-actin filaments <i>in vitro</i>83
11.2.4	Light microscopic observation of F-actin suprastructures formed in the presence of Hcoronin 3 COOH-terminal fragments84
11.2.5	Interaction of Hcoronin 3 NH ₂ - and COOH-terminal domains <i>in vitro</i>85
IV	Discussion88
1	Subcellular localization of coronin 389
2	Overexpression of full-length and a truncated EGFP-Hcoronin 3 changes cell morphology91
3	Oligomerization of the COOH-terminus92
4	Definition of an F-actin binding domain of coronin394
4.1	<i>In vitro</i> F-actin binding assay95
4.2	Interaction of the NH ₂ - and COOH-terminal region96
5	Phosphorylation of coronin 397

V	Summary100
VI	Zusammenfassung102
VII	References104
	Erklärung	
	Acknowledgements	
	Curriculum Vitae/Lebenslauf	

I. Introduction

1 The cytoskeleton

Cell motility and plasticity are crucial functions for many eukaryotic cells. The ability to adopt a variety of shapes and to move in a coordinated way relies on the cytoskeleton, a complex network of protein filaments. The cytoskeleton is a highly dynamic structure involved in different physiological events, like separation of chromosomes during mitosis (Alberts et al., 1994), development of axons and dendrites in nerve cells (Mullins et al., 2001), and chemotaxis of hematopoietic cells in response to infection (Ferrari et al., 1999). Another important function of the cytoskeleton is to traffic organelles inside cells (Alberts et al., 1994). The cytoskeleton is built up by three types of protein filaments: actin filaments or microfilaments, microtubules, and intermediate filaments. The common feature of these filaments is that they are composed of monomeric subunits that form linear polymeric arrays via non-covalent association.

1.1 Microtubules

Microtubules are found in all eukaryotes, and three essential functions of microtubules are well established. The first is their role as the primary structural component of the mitotic spindle. This apparatus is responsible for the translocation of one copy of each chromosome to each of the two spindle poles during cell division. A second role is the organization of the overall cell shape. In concert with actin filaments and intermediate filaments, cytoskeletal microtubules set up the internal cell architecture and maintain cellular morphology. The third role is in the transport of vesicles and organelles, which was first described in neurons. In nerve cells, the oriented microtubule array in axons serves as a “highway” along which vesicles and cell organelles such as mitochondria are transported from the cell body and back again, with the help of motor proteins and microtubule-associated proteins or MAPs (Alberts et al., 1994). Microtubules are assembled primarily from heterodimers of alpha- and beta-tubulin. The tubulin heterodimers are aligned into long parallel protofilaments. 13 protofilaments are bundled in parallel to form a cylinder-like structure. Since the two ends of a microtubule display different kinetics of subunit addition and loss, the faster growing end is defined arbitrarily as the “plus” end. In general, microtubules are organized in a polar fashion with the plus end pointing

toward the cell extremities and the minus ends attached to specific microtubule-organizing centers (MTOCs), located in most cases at the centrosome. This anchoring structure protects the minus ends of the filaments. Polymerization of microtubules is spontaneous, requires Mg^{2+} and GTP, which is hydrolyzed to GDP just after assembly, and is enhanced by elevated temperature and reversed by cooling. GTP binds to the β -tubulin subunit of heterodimeric tubulin molecules and stabilizes the polymers. Hydrolysis of GTP changes the conformation of the subunits and causes depolymerization of microtubules by weakening the bonds between the tubulin subunits in the microtubules. The nucleation, a process generating a microtubule *de novo*, determines the rate of polymerization. In the elongation phase, the rate of assembly depends on the concentration of tubulin monomers until a steady state is reached, in which polymerization and depolymerization are exactly balanced.

1.2 Intermediate filaments

The major function of the cytoplasmic intermediate filaments is to withstand mechanical stress force (Alberts et al., 1994). Intermediate filaments are relatively stable and rope-like protein fibers. They are found prominently in epithelia subjected to mechanical stress. They are also widely distributed in the axons of nerve cells as well as muscle cells. The nucleus of most animal cells is surrounded by a closely-woven network of intermediate filaments, spreading to the cell periphery, where they are connected to the plasma membrane. 5 different types of intermediate filaments are known: Type I and type II are also called the acidic and neutral/basic keratins, respectively. They are present in epithelia and associate to form heterodimers. Type III filaments are the vimentin-related proteins such as vimentin and desmin; vimentins are mainly found in mesoderm-derived cells, and desmin is abundantly expressed in muscle cells. Type IV are the neurofilaments which are found in axons of nerve cells. Type V are the nuclear lamins which form the fibrous lamina surrounding of nuclear envelope. The protein monomers of all intermediate filaments are elongated, fibrous polypeptides that dimerize via a coiled-coil structure. Two dimers interact with each other in an antiparallel way, and these tetramers associate laterally in an overlapping manner to form a nonpolarized intermediate filament (Fuchs & Weber, 1994). This overlapping lateral array is responsible for the high mechanical stability of intermediate filaments. In contrast to actin filaments and

microtubules, the polymerization of intermediate filaments is independent of cofactors and nucleotides.

1.3 Actin Filaments

Actin and its associated proteins constitute more than 25 % of the protein in non-muscle cells, in muscle cells even more than 60 %. The actin system is found in all eukaryotes, and actin is one of the most conserved and ubiquitous proteins, indicating its central role in various cellular processes. Actin monomers, called G-actin, are 375 amino acid globular proteins with a molecular mass of about 43 kDa. G-actin is found predominantly in the cytoplasm. When appropriate concentrations of K^+ and Mg^{2+} are added to purified G-actin in the presence of ATP, spontaneous assembly into actin filaments, F-actin, takes place *in vitro*. The filaments are structurally arranged in a helical form and have a diameter of about 8 nm. Similar to microtubules, the actin filaments reveal a polarity with two different ends, a slow growing (-) end and a fast growing (+) end. In contrast to G-actin, F-actin is present predominantly in the cortex of animal cells. Three isoforms of actin are found in higher eukaryotes, named the α -, β - and γ -isoforms in order of their increasing basicity. α -actin is found mainly in different types of muscles, while β - and γ -actin are essential components of non-muscle cells (Whalen et al., 1976). Actin filaments are thinner and more flexible than microtubules and intermediate filaments. F-actin can be isolated mainly as cross-linked bundles, whereas single filaments are instable. At dynamic cell-surface protrusions, actin molecules rapidly polymerize to push out the plasma membrane. This forward extension is a common feature of most shape changing processes in cells. Usually not only thin sheet-like lamellipodia but also microspikes are formed at these regions. Lamellipodia are composed of a dense meshwork of actin filaments. The bundles of the elongating actin filaments are inserted into the submembranous cytoplasm with their (+) end to form the motile apparatus. In contrast to this, actin stress fibers are long bundles of filaments that transverse the cell and are linked to integrins at sites called focal adhesions (Alberts, 1994). Also, the rate of actin polymerization depends on the nucleation, an initial phase for building up a trimer of actin molecules (Gärtner et al., 1989). As for microtubules, elongation is proportional to the concentration of free subunits. The critical concentration of G-actin for polymerization is around 0.2 μ M (about 8 μ g/ml). However, simple polymerization and depolymerization events are not sufficient to

form the diversity of F-actin structures found in different cell types. For example, lamellipodial actin in fibroblasts forms a meshwork of short branches. In contrast to this, the growing tips of developing nerve cell axons, called growth cones, contain different F-actin structures: A meshwork with less regularly branching, long filaments with their pointed ends oriented in various directions fills in the spaces between long bundles of 6-12 actin filaments that radiate from the membrane to the central zone of the growth cone (Lewis and Bridgman, 1992; Meyer and Feldman, 2002).

1.4 Actin-binding proteins

The diversity of actin structures and actin-dependent cellular processes can only be exerted with a large variety of actin binding proteins (Fig. 1). Briefly, these can be divided into 5 different groups according to their functions:

- G-actin sequestering proteins,
- F-actin capping and severing proteins,
- actin filament crosslinking and bundling proteins,
- motor proteins, and
- membrane anchor proteins.

Actin depolymerizing factor (ADF) and cofilin belong to the G-actin binding protein family and cause depolymerization of actin filaments from the pointed end. Profilin, a small globular, cytoplasmic protein is another member of the G-actin associated protein family. However, this protein binds released monomers and facilitates ADP/ATP exchange, providing new monomers for addition to the leading edge of the actin network. It also acts as an adapter protein, regulates actin polymerization, and potentially links transmembrane signaling to the actin cytoskeleton (Pollard 1999).

An example for actin filament severing proteins is gelsolin. Gelsolin cleaves an actin filament and forms a cap on the newly exposed (+) end of the filament, thus inhibiting further polymerization (Kwiatkowski et al., 1986). The F-actin severing protein family also includes villin, adseverin, CapG, severin/fragmin and several other members. CP, the capping protein, is a typical F-actin capping protein found in all eukaryotes (Schafer et al., 1995). Basically, the concentration of CP in a cell is comparable to the number of barbed ends and is responsible for keeping filaments short and increasing the amounts of G-actin (Hug et al., 1995).

Actin filament crosslinking proteins play a decisive role in the spatial arrangement of filaments. This protein family can be divided into three main classes, F-actin parallel

bundling proteins, F-actin contractile bundling proteins and F-actin gel-like network forming proteins. Fimbrin, for example, causes tight parallel bundling of F-actin and is found predominantly in microspikes and filopodia (Adams et al., 1995). It contains two actin-binding domains, that allows cross-linking of actin filaments. α -Actinin, a rod-shaped antiparallel homodimer also bundles F-actin and is enriched in stress fibers, where it is responsible for the loose cross-linking of actin filaments into contractile bundles (Condeelis, 1995). Filamin, as a representative of the third group, forms flexible homodimers that can build up polygonal F-actin networks (Weihing et al., 1985).

All F-actin motor proteins belong to the myosin subfamily with a conserved head domain, which are involved in the association with actin filaments and varying additional domains. In the cell cortex, actin filaments are linked to the plasma













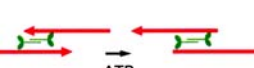


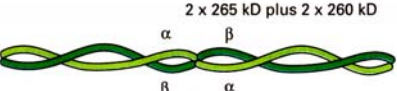



function of protein	example of protein	comparative shapes, sizes And molecular weight	Schematic drawing of Interaction with actin
form filament	actin		
strengthen filaments	Tropomyosin		
bundle filaments	Fimbrin		
		α -actinin	
crosslink filaments into gel	Filamin		
fragment filaments	Gelsolin		
slide filaments	Myosin II		
moves vesicles on filaments	Myosin I		
attach sides of filaments to plasma membrane	Spectrin		
sequester actin monomer	Thymosin		

Fig. 1. The types of actin-binding proteins found in most vertebrate cells. Actin is shown in red, while the actin binding proteins are presented in green. The molecular mass of each protein is given in kilo daltons (kD). Taken from "Molecular Biology of the Cell", Alberts et al. (1994).

membrane directly or indirectly by membrane anchors. Ponticulin, an integral membrane protein, binds directly to the side of actin filaments and nucleates actin polymerization at the cytoplasmic surface of the plasma membrane (Wuestehube & Luna, 1987). In contrast to this, talin forms a bridge between the cytoplasmic domain of integrin, a transmembrane protein, and vinculin which in turn binds to α -actinin, thus linking F-actin to the plasma membrane (Bolton et al., 1997). Other ABPs do not belong directly to one of these five types. The Arp2/3 complex consists of 7 subunits (Mullins et al., 1998) and is localized at the branching points of actin meshworks where it nucleates the formation of a new actin filament off the side of an existing filament. Arp2/3 complex is activated by N/WASP (neural-/Wiskott-Aldrich syndrome protein) or Scar (suppressor of cAMP receptor mutation), downstream of the small rho-like GTPases cdc42 and rac. This was the first mechanism directly coupling the rho GTPases to actin polymerization (Machesky et al., 1998). A variety of different proteins are involved in signaling to the Arp2/3 complex and eventually to the actin cytoskeleton. Actin and actin binding proteins can be seen as effectors of signal transduction cascades. However, the role and regulation of many F-actin interacting proteins still remains to be elucidated in detail. Generally, these proteins contain one or more protein-protein interaction domain(s) besides one or more actin binding site(s). Among them, coronin is assumed to play an important role (de Hostos et al., 1991).

2. Coronin

The prototype of coronin (Fig. 2) was identified in *Dictyostelium discoideum* (de Hostos et al., 1991). This protein is a component of actin-myosin complexes and could be isolated after dissociation under low ionotropic conditions. The protein was distributed predominantly in the region of actin-rich, crown-shaped extensions on the dorsal cell surface and less intense in the cytoplasm, suggesting that it exists in an actin-bound and a free state (de Hostos et al., 1991). In the meantime, coronins have been discovered in all eukaryotes examined so far. The structure of these proteins is quite similar. Basically, they are composed of 450-500 amino acids. A prominent structural feature, which is not found in most other ABPs is a highly conserved 5 WD (Trp-Asp)- repeat region in the central part (amino acids 50 to 291) of the molecule. The WD-repeat motif is found in different proteins in eukaryotes, for

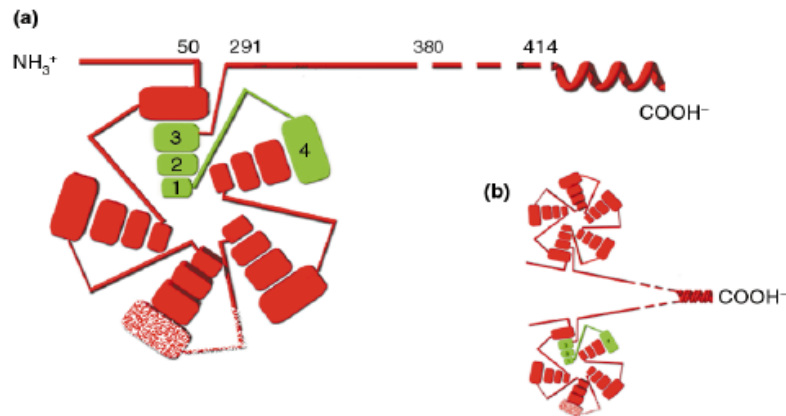


Fig. 2. Domain structure of coronin based on the beta-propeller structure of heterotrimeric G protein β -subunits. (a) Monomer. Numbers represent the approximate amino acid positions in *Dictyostelium* coronin. An individual WD (Trp-Asp) repeat (in green) appears to fold into four beta sheets (numbered) that lie between two 'propeller blades'. (b) Sheet 4 of the third repeat (mottled) is more variable than others among mammalian coronins. The conserved region (N-terminus to amino acid ~380) is followed by a unique region with variable length. The C-terminal ~32 amino acids are thought to form an α -helical coiled coil. (b) postulated dimer with subunits associated via the C-terminal coiled coil regions (taken from de Hostos, 1999).

example, in subunits of phosphatases and anchors for protein kinase C which are involved in signal transduction. The best characterized example, with a known crystal structure, is the G_{β} subunit of heterotrimeric G proteins, well-characterized components of the transmembrane signaling machinery. WD repeats consist of 44~60 residues typically, containing a GH(Gly-His)-di-peptide 11~24 residues from its N-terminus and a WD dipeptide at the C-terminus (Smith et al., 1999). According to X-ray structure data, the G_{β} subunit forms a propeller-like assembly. Each repeat contains 4 antiparallel β -sheets. One sequence repeat does not match a structural blade, rather, a repeat contains the first three strands of one blade and the last strand of the next (Fig. 2). It is assumed that WD-repeats are responsible for protein-protein interactions since it provides three large surfaces, the top, the bottom and the circumference (Smith et al., 1999). Since the sequence of the coronin WD repeats are highly similar to G_{β} , they are believed to fold into a five-bladed β -propeller. This core region is flanked by NH_2 - and $COOH$ -terminal domains. The N-terminus and the region C-terminal of the WD-repeats are conserved, too. At the C-terminus, a unique region with variable length, from 22 amino acids in *Dictyostelium* to 50 residues in mammals, is located, which shows no significant homology between different coronins. This unique region may confer specific functions to individual members of the family. A second, highly variable region is found in the β strand 4 of the third repeat. The last 30 amino acids in the C-terminus are predicted to fold into an α -

helical coiled-coil structure, which is assumed to mediate dimerization. The C-terminus of some coronins contains a leucine zipper motif.

3 Coronin functions

3.1 Coronin in *Dictyostelium discoideum*

Dictyostelium coronin is able to associate with the actin cytoskeleton in a Ca^{2+} - and pH-independent manner. It is enriched in the leading edge of actin-rich pseudopods and the cortical membrane extensions (Gerisch et al., 1995). This localization of coronin implies that it could be a component of the signal transduction cascade, involved in the reorganization of the actin cytoskeleton. The coronin null phenotype shows that many actin-dependent processes such as cytokinesis, cell locomotion, phagocytosis and macropinocytosis are partially impaired but not completely abolished in mutants (de Hostos et al., 1993; Maniak et al., 1995; Gerisch et al., 1995; Rauchenberger et al., 1997; Hacker et al., 1997). The exact function(s) of coronin in the regulation of the F-actin organization is controversial in *Dictyostelium*. On one hand, localization suggests that it plays a role in the formation or stability of actin filaments. On the other hand, Gerisch and coworkers envisioned a role for coronin in actin disassembly, since they found that an extension of the cortical cytoplasm was formed in coronin null mutants indicating accumulation of F-actin in the cortex. Alternatively, an actin-myosin II complex stabilizing function of coronin is postulated based on the recruitment of coronin to the cleavage furrow during cytokinesis (Fukui et al., 1999).

3.2 Coronin in *Saccharomyces cerevisiae*

The primary sequence of coronin (Crn1p) in *Saccharomyces cerevisiae* shows strong homology to other members of the family. This protein (M_r 72,5 kDa) contains an unusually long unique region which is distinct from other coronins. Two sequences in this unique region show high homology to the microtubule binding motif of MAP1B. *In vitro*, purified Crn1p binds to F-actin with high affinity (K_d 6 nM, Goode et al., 1999). Crn1p promotes rapid actin polymerization apparently by reducing the lag phase of actin assembly. Goode and his coworkers speculated that Crn1p acts by binding to the sides of actin dimers/trimers and by accelerating filament elongation. Crn1p is also capable of crosslinking actin filaments *in vitro* into branched networks or bundles. The C-terminal coiled coil domain is required for this bundling activity.

Furthermore, it is assumed that Crn1p forms a dimer through the predicted C-terminal coiled coil. Interestingly, Crn1p interacts with both F-actin and microtubules (Goode et al, 1999). The conserved region including the WD-repeats is required for actin binding activity, whereas the unique region is essential for microtubule interaction. Overexpression of Crn1p in yeast severely affects actin and microtubule organization and results in formation of aberrant tubulin-positive structures, abnormal actin loop structures and arrested cell growth (Goode et al., 1999; Humphries et al., 2002). This finding implied that Crn1p mediates the interaction between microtubules and cortical actin (Goode et al., 1999). Recently, two hybrid assays revealed that the C-terminal coiled coil domain of Crn1p interacts with Arc35/p35, a subunit of the Arp2/3 complex (Humphries et al., 2002). Crn1p inhibits the actin nucleation activity of Arp2/3 complex in the absence of actin filaments through its coiled coil domain and recruits the Arp2/3 complex to the sides of F-actin. Both activities may be involved in directing the formation of a branched F-actin network. Whether the coronin-Arp2/3 complex interaction is conserved in other organisms is unclear. There is evidence that could strengthen this assumption, because substoichiometric amounts of coronin copurified with Arp2/3 complex from human neutrophils (Machesky et al., 1997).

3.3 Coronin in mammals

In contrast to lower eukaryotes, which express unique coronins, metazoa possess several homologues. Seven different coronin-like proteins have been identified in human and mouse databases (Tab. 1). These proteins can be classified as coronins 1-7. Coronin 1-3 have been grouped as coronins 1A-1C and coronin 4 and 5 as 2A and 2B, according to their relative homology (Okumura et al., 1998; de Hostos 1999). Each family member is again distinguished from the others mainly by the unique region in the COOH-terminal extension. Their expression patterns show pronounced tissue preferences for each coronin. Coronin 1 (p57 or TACO, tryptophane-aspartate containing coat protein) is the best characterized mammalian family member (Suzuki et al., 1995). It is mainly expressed in human immune tissues, and weakly in lung and brain. In human neutrophils (phagocytic leukocytes), coronin 1 can be detected in cytoskeletal as well as in cytosolic fractions. Most of coronin 1 protein colocalizes with F-actin around phagocytic vacuoles, whereas soluble coronin 1 associates with

Table 1. mammalian coronins (based on de Hostos, 1999)

	Original name	Size (aa)	Animal	Tissue	Reference
coronin 1	p57	461	bovine, human, mouse	Haematopoietic lineage lung, brain	Suzuki et al., 1995
coronin 2	coronin 2	484	mouse, rat, H-EST	ubiquitous except muscle	Okumura et al., 1998
coronin _{se}	coronin _{se}	486	rabbit	Parietal mucosa, epithelia	Parente et al., 1999
coronin 3	coronin 3	474	mouse, H-EST	ubiquitous, strongest in brain, lung, kidney	Okumura et al., 1998
coronin 4	IR 10	480	human, M-EST	brain, mostly testes	Zaphiropoulos et al., 1996
coronin 5	ClipinC	475	human	brain	Nakamura et al., 1999
coronin 6	ClipinE	431/471 ^{1a)}	mouse	brain	Watanabe et al., unpublished
p70		443	rat	unknown	Muralikrishna et al., 1998
coronin 7		925	Human, mouse	strongly brain	Hasse et al., unpublished

Abbreviation: H=Human, EST=expressed sequence tag, M=mouse, a) different splicing variants

p40^{phox}, a cytosolic subunit of the NADPH oxidase complex (Grogan et al., 1997). This complex generates microbicidal superoxide in phagosomes. In the adherent neutrophils, activation of PKC results in a change in the subcellular localization of coronin 1. The protein is also found in the phagocytic vacuole of macrophages. Living mycobacteria in phagosomes inhibit the dissociation of coronin 1 and further transport to lysosomes (Ferrari et al., 1999). It is hypothesized that coronin 1 plays an important role in regulating phagocytosis in mammalian immune system, similar to the *Dictyostelium* protein.

Coronin_{se}, a variant of coronin 2, was initially identified as a PKC-dependent phosphoprotein in HCl-secreting gastric parietal cells (Brown et al., 1989; Chew et al., 1997). It is also highly expressed in the secretory cells of the kidney and the lung (Parente et al., 1999). Also, the phosphorylation of coronin_{se} is enhanced by PKC activators. This stimulation leads to formation of filopodia and redistribution of coronin_{se} to the leading edge. Different from coronin_{se}, coronin 2 is ubiquitously expressed in almost all tissues except muscle cells. Its function is less clear. Also coronin 2 localizes to dynamic actin-rich areas (Morrissette et al., 1999). Coronin 4 ("IR10") is mostly expressed in testis and also in brain (Zaphiropoulos et al., 1996). ClipinC is referred to as coronin 5 according to the suggestion by de Hostos (1999). This protein is relatively restricted to neuronal tissue, where it accumulates at growth

cones and colocalizes with focal adhesions as well as stress fibers (Nakamura et al., 1999). It coprecipitates with vinculin, a major component of focal contacts.

The cDNA for coronin 6, ClipinE, was published in the GenBank database recently (Accession BAB64361). This protein is found predominantly in brain and has 3 splicing variants (Watanabe et al., unpublished).

The sequence of p70, a 70 kDa-tumor specific antigen from a histiocytoma in rat, is only partially known and shows only 41% homology to coronin 1 and *Dictyostelium* coronin (Muralikrishna et al., 1998). However, it is 99% identical to mouse coronin 7. Coronin 7 was recently identified in the GenBank database of humans (Accession AK025674) and mouse (Accession BAB31380), suggesting that p70 and coronin 7 might be identical or splice variants. In contrast to all other mammalian coronins, coronin 7 contains two complete, degenerate copies of the conventional coronin sequence and thus has about the twice size (925 amino acids). Human coronin 7 is expressed strongly in thymus, spleen and brain, its function is as yet unknown (A. Schulze, 2001).

4. Coronins in the nerve system

Recent clinical investigations revealed that coronin 1 and the Arp2/3 complex 20 kDa subunit are significantly down-regulated in the fetal down syndrome (DS) brain cortex (Weitzdorfer et al., 2002). The authors proposed that the reduction of both proteins results - at least in part - in dysgenesis of the brain and the associated mental disabilities in DS patients by derangement of cytoskeletal elements. It is known that mouse coronin 1 is mainly expressed in immune tissues (thymus, spleen, bone marrow, lymph nodes) but weakly in brain (Suzuki et al., 1995) whereas coronin 3 demonstrates a strong expression in brain (Spoerl et al., 2002). It was speculated that the neuronal tissue-specific coronin 5 may be involved in neuronal migration as well as neurite extension. This protein may link F-actin to the plasma membrane and may play an important role in the rearrangement of neuronal actin structures during neuronal development and growth cone advance leading to synapse formation. (Nakamura et al., 1999). Coronin 4, coronin 6 (ClipinE) and coronin 7 have been found in brain tissue as well. Thus, except for coronin 2, all members of the mammalian coronin family are more or less expressed in brain, which might suggest that neuronal cells may have an elevated requirement for these proteins. However,

the role and molecular functions of coronins in the nerve system have not been studied in detail so far.

5. Aim of this work

The main goal of this work was to understand the biochemical and cellular functions of coronin 3. This protein is the most widely expressed coronin in mammals and may thus be important in many cell types. Since the specialized functions of different coronins are likely dependent on their unique regions, the properties of these parts of special interest.

One goal was, to study the involvement of coronin 3 domains in subcellular localization by the expression of different full-length and truncated EGFP fusion proteins. This was done by analysis of the colocalization in F-actin rich neurites of differentiated neuroblastoma cells, because coronin 3 is strongly expressed in neuronal tissue. Furthermore, this cell system served to analyze the distribution, oligomerization and possible covalent modification of the protein in different subcellular fractions. Translocation between cellular compartments during differentiation and a possible role of protein kinase C for subcellular coronin 3 localization were further topics. Finally, we asked whether coronin 3 is also a microtubule-binding protein *in vivo* similar to yeast Crn1p. To define the F-actin-binding domain of coronin 3, F-actin cosedimentation assays were performed with recombinant NH₂- and COOH-terminal fragments *in vitro*. Furthermore, for polypeptides binding to F-actin *in vitro*, quantitative studies were performed to determine the binding affinity for F-actin.

II. Materials and Methods

1 Materials

1.1 Reagents

acrylamide (Protogel: 30: 0.8 AA/Bis-AA)	National Diagnostics
agarose (electrophoresis grade)	Life Technologies
acetone	Riedel-de-Haen
APS (Ammoniumperoxodisulfate)	Fluka
Bacto-Agar, Bacto-Tryptone	Difco
benzamidine	Sigma-Aldrich
bromophenol blue (Na-salt)	Serva
BSA (bovine serum albumin)	Sigma-Aldrich
chloroform	Riedel-de-Haen
calcium chloride	Sigma-Aldrich
Coomassie-brilliant-blue R250	Serva
p-coumaric acid	Fluka
DMSO (Dimethyl sulfoxide)	Merck
DTT (1,4-dithiothreitol)	Gerbu
EDTA (Ethylenediaminetetraacetic acid)	Merck
EGTA [ethylene-glycol-bis(2-aminoethylether)-N,N,N',N'-tetraacetic acid]	Sigma-Aldrich
acetic acid	Riedel-de-Haen
ethanol	Riedel-de-Haen
ethidium bromide	Sigma-Aldrich
FCS (fetal calf serum)	Biochrom
fish gelatin	Sigma-Aldrich
formamide	Merck
formaldehyde	Sigma-Aldrich
glucose	
glycine	Degussa
glycerol	Oxoid
IPTG (isopropyl β -D-thiogalactopyranoside)	Sigma-Aldrich
isopropanol	Merck
HEPES [(N-2-hydroxyethyl)piperazine-N'-(2-ethansulfonic acid)]	Sigma-Aldrich
β -mercaptoethanol	Sigma-Aldrich
methanol	Riedel-de-Haen
mineral oil	Amersham Biosciences
MOPS (g-[Morpholino]propanesulfonic acid)	Gerbu
Ni-NTA agarose	Qiagen
nucleosidtriphosphate	Roche
Nonidet-P40 (Nonylphenyl-polyethylenglycerine)	Fluka
paraformaldehyde	Sigma-Aldrich
PIPES (1,4-piperazindiethansulfonic acid)	Sigma-Aldrich
Ponceau S-concentrate	Sigma-Aldrich
protein-A-sepharose	LifeTechnologies
phalloidin TRITC-conjugated	Sigma-Aldrich
SDS (sodium dodecylsulfate)	Serva
sucrose	Fluka
sodium azide	Merck

TEMED (tetramethylethylenediamine)	Merck
Tris (hydroxymethyl)aminomethane	Sigma-Aldrich
Triton-X-100 (t-octylphenoxyethoxyethanol)	Merck
Tween 20 (Polyoxyethylensorbitanmonolaurate)	Sigma-Aldrich
X-gal (5-bromo-4-chloro-3-indolyl- β -galactopyranoside)	Roth
yeast extract	Oxoid

1.2 Enzymes, inhibitors and antibodies

Enzymes for Molecular Biology:

lysozyme	Sigma-Aldrich
restriction endonucleases	Invitrogen
	Amersham Biosciences
T4 DNA ligase	Invitrogen
calf intestinal alkaline phosphatase (CIAP)	Roche
Klenow fragment (DNA polymerase)	Roche
Taq polymerase	Roche
Trypsin/EDTA 10 \times	Invitrogen

Inhibitors:

Complete mini protease inhibitor cocktail	Roche
PMSF (phenylmethylsulfonylfluoride)	Sigma-Aldrich

Antibiotics:

Ampicillin	Sigma-Aldrich
Kanamycin	Sigma-Aldrich
Geneticin G418	Invitrogen
Penicillin/streptomycin	Biochrom

Primary Antibodies:

Mouse-anti-GFP-antibody mAB K3-184-2	R. Müller and B. Gassen
Rabbit-anti-myc-antibody	Santa Cruz
Mouse-anti-tubulin-antibody	Noegel et al., 1999
Mouse-anti-annexin 7-antibody mAB 203-217	Clemen et al., 2000
Mouse-anti-pan-cadherin-antibody	Sigma-Aldrich
Mouse-anti- β -actin-antibody	Sigma-Aldrich
Goat-anti-GST-antibody	Amersham Biosciences
Mouse-anti-coronin 3 antibody K6-444-4	M. Stumpf and A. Hasse

Secondary antibodies:

Goat-anti-mouse-IgG, peroxidase-conjugated	Sigma-Aldrich
Goat-anti-rabbit-IgG, peroxidase-conjugated	Sigma-Aldrich
Goat-anti-mouse-IgG, Cy3-conjugated	Sigma-Aldrich
Rabbit-anti-mouse-IgG, Alexa 488-conjugated	Sigma-Aldrich
Rabbit-anti-mouse-IgG, Alexa 586-conjugated	Sigma-Aldrich
Goat-anti-rabbit-IgG, FITC-conjugated	Sigma-Aldrich

1.3 Vectors

pEGFP-C1	Clontech
pcDNA3.1/myc-His	Invitrogen
pQE-30	Qiagen
pGMEX-T	AMRAD BIOTECH

1.4 Kits and reagents

Nucleobond AX 100 and 500	Macherey & Nagel
NucleoSpin Extract 2 in 1	Macherey & Nagel
NucleoSpin Plus	Macherey & Nagel
1 kb DNA-marker	Gibco-BRL
High molecular weight protein marker	Amersham Biosciences
Prestained protein marker	Bio-Rad
Protein marker for gel filtration	Amersham Biosciences
Drystrip gel pl 3-10, 7 cm	Amersham Biosciences
IPG buffer	Amersham Biosciences
IPGphor isoelectric focusing units	Amersham Biosciences

1.5 Bacterial host strains

<i>E. coli</i> JM 109	Yanisch-Perron et al., 1985
<i>E. coli</i> DH5 α	Hanahan, 1983
<i>E. coli</i> M15	Qiagen

1.6 Media for *E. coli* culture

LB medium, pH 7.4	SOC-medium, pH 7.0
10 g bacto-tryptone	20 g bacto-tryptone
5 g yeast extract	5 g yeast extract
5 g (95.5 mmol) NaCl	0.5 g (9.5 mmol) NaCl
adjusted to pH 7.4	20 mM glucose
with 1 M NaOH	with 1 M NaOH
H ₂ O ad 1 l	H ₂ O ad 1 l

All media and buffers were prepared with deionised water, which was filtered through an ion exchanger (Membra Pure). The media and buffers were sterilized by autoclaving at 120 °C. The pH value of each solution was adjusted to 7.4 with NaOH. Antibiotics were added to the media after the solution was cooled down to 50°C, namely ampicillin in a final concentration of 100 μ g/ml and kanamycin in a final

concentration of 25 µg/ml. For making agar plates, a semi-automatic plate pouring machine (Technomat) was used. The plates were incubated at 37°C for at least 30 min before use.

1.7 Media for cell culture

DMEM (4,500 mg/l glucose)	Sigma-Aldrich
DMEM (1,000 mg/l glucose)	Sigma-Aldrich

1.8 Mammalian cell lines

Name	Species	Tissue	reference
Neuro-2a	<i>Mus musculus</i>	Neuroblastoma cells	Klebe et al., 1969
Cos-7	<i>Cercopithecus aethiops</i>	Kidney fibroblasts	Gluzman, 1981
HEK293	<i>Homo sapiens</i>	Human embryonic kidney	Graham et al., 1977

1.9 Laboratory materials

Centrifuge tubes, 15 ml	Greiner
Frozen tube 1.5 ml	Nunc
Coverslips Ø 12 mm, 18 mm	Assistant
Corex tube 15 ml, 50 ml	Corex
Cryo tube, 1 ml	Nunc
Electroporation cuvette, 4 mm electrode gap	Bio-Rad
Gel-drying frames	house made
Microcentrifuge tubes, 0.5 ml, 1.5 ml, 2.2 ml	Sarstedt
Micropipette, 1-20 µl, 10-200 µl, 100-1000 µl	Greiner
Micropipette tips	Greiner
Multiphor II electrophoresis Unit	Amersham Biosciences
3 MM filter paper	Whatman
Nitrocellulose transfer membrane, type BA85	Schleicher and Schüll
Nylon membrane	Gelman Science
Parafilm	American Nat Can
Pasteur pipette, 145 mm, 230 mm	Volac
Petri dish for cell culture Ø 60 mm×17 mm	Nunc
Petri dish for cell culture Ø 90 mm×17 mm	Nunc
Petri dish for cell culture Ø 140 mm×17 mm	Nunc
Petri dish 120×120×17 mm	Greiner
Plastic cuvette, semi-micro	Greiner
Quartz cuvette infrasil	Hellma
Quartz cuvette, semi-micro	Perkin Elmer
Slides 76×26 mm	Menzel
Sterile filter (Acrodisc) 0.2 µM, 0.45 µM	Gelman Science
Syringes (sterile) 1 ml, 5 ml, 10 ml, 50 ml	Amefa, Omnifix

Tissue culture flasks 25 cm ² , 75 cm ² , 175 cm ²	Nunc
Tissue culture dishes 6 wells, 24 wells, 96 wells	Nunc
X-ray film, X-omat AR-5, 18×24 mm	Kodak
15 ml tube	Greiner
50 ml tube	Greiner

1.10 Instruments and Equipments

Microcentrifuges

Centrifuge 5417 C	Eppendorf
Centrifuge Sigma-Aldrich B	Braun
Cold centrifuge Biofuge fresco	Heraeus Instruments

Centrifuges (table-top, cooling, low speed)

Centrifuge CS-6R	Beckman
Centrifuge RT7	Sorvall
Centrifuge Allegra 21R	Beckman

Centrifuges (cooling, high speed)

Beckman Avanti J25	Beckman
Sorvall RC 5C plus	Sorvall
Ultracentrifuge Optima L-70 K	Beckman
Ultracentrifuge Optima TLX	Beckman

Centrifuge rotors

JA-10	Beckman
JA-25.50	Beckman
SLA-1500	Sorvall
SLA-3000	Sorvall
SS-34	Sorvall
SW41	Beckman
TLA 45	Beckman
TLA 100.3	Beckman

Dounce homogenizer 10 ml

B. Braun

Dounce homogenizer 100 ml

B. Braun

Electrophoresis power supply, power-pac-200

Bio-Rad

Electrophoresis power supply, power-pac-300

Bio-Rad

Electroporation unit gene-pluser

Bio-Rad

X-ray-Film developing machine FPM 100A

Fuji Photo film Co. LTD

Freezer (-80°C)

Nunc

Gel-documentation unit

MWG-Biotech

Heating block

Störk Tronic

Incubator Lab-Therm

Kühner

Ice machine

Ziegra

Incubators

CO₂-incubator, BBD 6220, BB 6220

Heraeus

CO₂-incubator

WTC Binder Biotran

Incubator microbiological

Heraeus

Incubator with shaker Lab-Therm

Kühner

Magnetic stirrer, MR 3001K	Heidolph
Microscopes	
Light microscope, CH30	Olympus
Light microscope, DMIL	Leica
Light microscope, CK2	Olympus
Fluorescence microscope 1X70	Olympus
Confocal laser scanning microscope	
TSC CP	Leica
Stereomicroscope, SZ4045TR	Olympus
Oven, conventional	Heraeus
pH-meter pH 526	Wissen. Tech. Werkstätten Weinheim
Refrigerator	Liebherr
Semi-dry blot apparatus, Trans-Blot SD	Bio-Rad
Lab Shakers	Kühner
Sonicator, ultra turrax T25 basic	IKA Labortechnik
Speed-vac concentrator, DNA 110	Savant
Spectrophotometer, Ultraspec 2000 UV/visible	Amersham Biosciences Biotech
UV-transilluminator TFS-35 M	Faust
Vortex, REAY top	Heidolph
Waterbath Type 1002	GFL
Waterbath	Messgeräte-Werk Lauda

1.11 Computer Analysis

For alignment analysis, the program Bioedit was performed. The software BLAST (NCBI) was used to calculate the homology between two amino acid sequences. The programs ClustalW and TreeView were applied for the phylogenetic analysis of coronin-like proteins. The proteomics and sequence analysis tools from ExPASy were used to predict the possible protein pI and motifs (www.expasy.ch). A program supplied by the web site (bmerc-www.bu.edu/bioinformatics/wdrepeat.html) was applied to localize WD-repeats in protein sequences. Adobe Photoshop was applied to process scanned confocal images. The programs Word 2000, Excel 2000 and Powerpoint 2000 (Microsoft) were used for evaluation and presentation of the experimental data.

2. Molecular biological methods

2.1 Plasmid preparation

2.1.1 Boiling method for preparation of plasmid DNA (Holmes and Quigley, 1981)

The method is suitable to screen a large number of bacterial clones for the desired recombinant plasmid. It is based on the coagulation of proteins and denaturation of chromosomal DNA by short heating and separation by centrifugation, whereas RNA and plasmid-DNA are soluble and localized in supernatants. Briefly, single transformants were picked up from the culture plate and were grown overnight in 2 ml of LB media containing the appropriate antibiotic. *E. coli* cells were pelleted by centrifugation at 10.000×g in a microcentrifuge for 3 min. The pellet was resuspended in 200 µl STET-buffer with lysozyme and the suspension was subsequently incubated at room temperature for 10 min to lyse the bacterial cell wall. The lysate was then boiled at 95°C for 1 min and centrifuged at 13.000 rpm for 10 min at room temperature. The resulting sediments were separated from the supernatant with a tooth pick. The plasmid DNA present in the supernatant was precipitated by adding an equal volume of isopropanol and incubating at room temperature for another 10 min. The precipitated plasmid DNA was pelleted in the Eppendorf centrifuge at 12.000 rpm for 15 min and the DNA pellet was washed with 70% ethanol once. The purified plasmid DNA was dried in a speed-vacuum concentrator and finally resuspended in 30 ml TE-buffer, pH 8.0, containing RNAase (10 µg/ml)

STET/lysozyme buffer, pH 8.0	TE-buffer, pH 8.0
50 mM Tris/HCl, pH 8.0	10 mM Tris/HCl, pH 8.0
50 mM EDTA	1 mM EDTA
0.5 % Triton X-100	
8 % sucrose	
Add fresh lysozyme at 1 mg/ml before use	

2.1.2 Mini-preparation of plasmid DNA (Macherey & Nagel)

NucleoSpin plasmid is designed for the rapid, small-scale preparation of highly pure plasmid DNA (minipreps) and allows the isolation of up to 40 µg per preparation of plasmid DNA. The principle of this plasmid-DNA purification kit is based on the alkaline lysis method. Basically, overnight culture of bacteria containing the desired plasmid were pelleted by centrifugation and cells were then lysed by alkaline lysis. The plasmid DNA was subsequently absorbed on a silica column, washed with ethanol, and then eluted with TE buffer. This method avoids the use of caesium chloride or phenol/chloroform for isolation.

2.1.3 Midi and Maxi preparation of plasmid DNA (Macherey & Nagel)

For the transfection of eukaryotic cells by electroporation, high amounts of plasmid-DNA are needed (40 µg DNA/Transfection). The Kits Nucleobond AX 100 and 500 (Macherey & Nagel) were used for this purpose. The purity of the isolated plasmid DNA was sufficient for sequencing and transfection of mammalian culture cell lines. Purification was done as described by the manufacturer.

2.2 DNA agarose gel electrophoresis

Agarose gel electrophoresis was performed according to the method described by Sambrook et al. (1989) to separate and isolate the DNA fragments. DNA fragments of different molecular weight show different electrophoretic mobility in an agarose gel matrix. Optimal separation results were obtained using 0.5-1 % gels in 1×TAE buffer submerged in a horizontal electrophoresis tank containing 1×TAE buffer at 5-10 V/cm. Depending on the molecular weight and the number of the samples, the separation of DNA fragments was performed in different sizes of horizontal gel electrophoresis apparatuses (7.5 cm×8 cm or 11.5 cm×14 cm). Only for resolving fragments less than 1,000 bp, 1% (w/v) agarose gel in 1×TAE buffer were applied. Before loading of the sample, 1/10 volume of 10× DNA sample buffer was added. DNA size marker was always loaded along with the DNA samples in order to estimate the size of the separated DNA fragments. For visualizing the DNA fragments, gels were stained with 0.1 µg/ml ethidium bromide. The gel was visualized under UV light at 302 nm and was photographed using a gel documentation system (MWG-Biotec).

DNA molecular weight marker

1 kb DNA ladder (Invitrogen): 12,216; 11,198; 10,180; 9,162; 8,144
7,126; 6,108; 5,090; 4,072; 3,054; 2,036
1,636; 1,018; 506; 396; 344; 298; 220
201; 154; 134; 75 bp

50 × TAE-buffer pH 8.0	DNA sample buffer
2 M Tris	40 % Saccharose
1 M sodium acetate	0.5 % sodiumdodecylsulfate
50 mM EDTA	0.25 % bromophenol blue
	in TE buffer, pH 8.0

2.3 Isolation of DNA fragments from agarose gels

DNA from restriction enzyme digests was separated on 1 % agarose gel in TAE buffer. The gel piece containing the desired DNA fragment labelled with ethidium bromide was excised with a scalpel under a UV transilluminator. The DNA fragment was subsequently purified from the excised gel piece using the Macherey & Nagel gel elution kit (NucleoSpin Extract 2 in 1). Briefly, the gel piece was transferred to a 1.5 ml reaction tube and melted at 50 °C in binding buffer. The DNA bound specifically to a silica membrane column after centrifugation and was eluted with a low salt solution.

2.4 Quantification of DNA

The concentration of DNA was measured in a quartz cuvette by its absorbance at a wavelength of 260 nm in a spectrophotometer. An extinction value of 1 corresponds to a concentration of 50 µg ds (double strand) DNA/ml, 40 µg ss (single strand) DNA as well as RNA/ml or 33 µg oligonucleotides/ml. The purity of the DNA was estimated by the ratio of its absorption at 260 nm to 280 nm. If the ratio is more than 2.2, this could indicate a contamination by phenol. If it is less than 1.8, this suggests that the DNA sample is contaminated by proteins.

2.5 Digestion with restriction enzymes

Digestion of DNA with restriction endonucleases was performed in the buffer systems and at temperature conditions recommended by the manufacturers. Basically, 1U enzyme digests 1 μ g lambda-DNA in 1 h at the optimal temperature. Since the enzyme is stored in 50 % glycerol stock solution, it should be diluted at least 10 fold in the reaction mixture. The performance of the digestion was controlled by gel electrophoresis.

2.6 Generation of blunt ends in linearized plasmid DNA

For cloning experiments, it might be necessary to convert the 5' or 3' extensions generated by restriction endonucleases into blunt ends. Filling-in of 5' extensions was carried out by the polymerase activity of the Klenow fragment, while "blunting" of 3' extensions was carried out by the 3' to 5' exonuclease activity of the Klenow fragment.

Reaction mix for 5' extensions	Reaction-mix for 3' extensions
1-4 μ g linearized DNA	1-4 μ g linearized DNA
5 μ l 10 \times high salt buffer	5 μ l 10 \times high salt buffer
1 μ l 50 \times dNTP-mix (each 4 mM)	2 U Klenow fragment
2 U Klenow fragment	Add H ₂ O to 50 μ l
Add H ₂ O to 50 μ l	

10 \times high salt buffer

500 mM Tris/HCl, pH 7.5

1 M NaCl

100 mM MgCl₂

10 mM DTT

The reaction was carried out at 37°C for 25-30 min. After incubation, it was immediately stopped by heat-inactivating the enzyme at 75°C for 10 min or adding 1 μ l 0.5 M EDTA. This was followed by phenol/chloroform extraction and precipitation of DNA with 2 vol. ethanol.

2.7 Dephosphorylation of DNA fragments

To prevent linearized vector digested with a single restriction enzyme from religation, 5' ends of the linearized plasmid were dephosphorylated by calf intestinal alkaline phosphatases (CIAP). Basically, 1-5 μg of the linearized vector was incubated with 1 U calf intestinal alkaline phosphatase in CIAP buffer in a 50 μl reaction volume at 37 °C for 10 min. The dephosphorylated DNA was extracted once with phenol/chloroform and precipitated with 2 vol. ethanol and 1/10 vol. 2M sodium acetate, pH 5.2.

2.8 Ligation of vector and DNA fragments

The T4 DNA ligase catalyses the ligation of DNA fragments and linearized vector DNA. For the ligation of relative small DNA fragments (<1000 bp) about 10 fold excess of fragment was used in the reaction, while large fragments (>3000 bp) were used in two-fold excess. Briefly, T4 DNA ligase and ATP were added as indicated below and the ligation reaction left overnight at 10-12°C.

Ligation reaction

Linearized vector DNA (200-400 ng)

DNA fragments

4 μl 5 \times ligation buffer

1 μl 0.1 M ATP

1.5 U T4 ligase

Add H₂O to 20 μl

2.9 Transformation of *E. coli* cells

2.9.1 Preparation of competent *E. coli* cells

An overnight grown culture of *E. coli* (1 ml) was inoculated into 100 ml LB medium and incubated at 37 °C with vigorous shaking at 250 rpm until an OD₆₀₀ of 0.5-0.6 was reached. After incubation on ice for 30 min, the cells were pelleted at 4000 rpm for 5 min. Subsequently, the cells were resuspended in 15 ml of ice cold TFB I solution and incubated on ice for another 30 min. The cells were pelleted again and resuspended in 2 ml of ice cold TFB II solution. After incubation for 30 min on ice, the cells were then aliquoted at 100 μl /tube. The aliquots were shock-frozen in liquid N₂ and immediately stored at -80°C.

TFB I	TFB II
30 mM potassium acetate	10 mM MOPS
50 mM MnCl ₂ ×4H ₂ O	75 mM CaCl ₂
100 mM RbCl	10 mM RbCl
10 mM CaCl ₂	15 % glycerol
15 % glycerol	
before addition of MnCl ₂ , pH adjusted to 6.0 with 0.2 M acetic acid, then pH switched to 5.8, the solution filter-sterilized, stored at 4°C	pH 7.0 adjusted with NaOH solution filter-sterilized, stored at 4°C

2.9.2 Transformation of *E. coli* cells

Plasmid DNA (~50 ng of a ligase reaction or ~10 ng of a supercoiled plasmid) was mixed with 100 µl of competent *E. coli* cells and incubated on ice for 30 min. The cells were then heat-shocked at 42°C for 60-90 s and immediately transferred to ice for 10 min. The cells were mixed 1 ml prewarmed (37°C) SOC medium and incubated with shaking for 1 h. Finally, 50-150 µl of the transformation mix was plated onto selection plates and the transformants were grown overnight at 37°C.

2.9.3 Glycerol stock of bacterial cultures

Glycerol stocks of all bacterial strains/transformants were prepared for long-term storage. The culture was grown overnight in LB medium with the selective antibiotic. 850 µl of overnight culture was added to 150 µl of sterile glycerol in a 1.5 ml microcentrifuge tube, mixed carefully, the tube was frozen on dry ice and stored – 80°C.

2.10 Construction of vectors

2.10.1. Vector for expression of Hcoronin 3 as myc-6×His-fusion proteins

For expression of human coronin 3 (Hcoronin 3) as a myc/6×His double-tagged protein in mammalian cells, the pcDNA3.1-myc-His (version B, Invitrogen) vector was used. The cDNA fragment encoding coronin 3 was isolated from vector pEGFPN-Hcoronin 3 (provided by Dr. A. Hasse) with the restriction enzymes Bam HI and Hind

III. The overhanging 5' ends of digested DNA fragment were modified to blunt ends with Klenow enzyme. The pcDNA3.1-myc-His vector was linearized with the restriction enzyme EcoR V and dephosphorylated with CIAP prior to ligation. The DNA fragment was then cloned into the vector to generate a myc-His fusion to the COOH-terminus of Hcoronin 3.

2.10.2 Vector for expression of Hcoronin 3 as GST-fusion protein

For expression of GST-coronin 3 in mammalian cells, the DNA sequence encoding coronin 3 was excised from pEGFPC-Hcoronin 3 (provided by Dr. A. Hasse) using the restriction sites for Kpn I and Bgl II. The vector pGMEX-T (kindly given by Dr. M. Plomann) was linearized with Bam HI and Kpn I. The DNA sequence was inserted into GMEX-T to fuse to the NH₂-terminal of Hcoronin 3.

2.10.3 Vector for expression of Hcoronin 3 as an EGFP-fusion protein

For expression of EGFP-fusions of Hcoronin 3 and various truncated versions, DNA fragments coding for full-length or truncated Hcoronin 3 were inserted into the pEGFP-C-series of vectors (Clontech) to express proteins carrying a NH₂-terminal EGFP fusion. These constructs were constructed by Dr. A. Hasse and have been described (Spoerl et al., 2002).

2.10.4 Vectors for expression of Hcoronin 3 fragments as 6×His-tagged proteins in *E. coli*

The vector pQE30 (Qiagen) was used for expression of coronin 3 residues 1-71, 315-444 and 315-474 in *E. coli* as NH₂-terminal 6×His-tagged recombinant fragments. The purified 6×His-tagged COOH-terminus (315-474) was also used for immunization of female Balb/c mice by using immuneeasy kit (Qiagen). This gave rise to the monoclonal antibody K6-444 used for detection of coronin 3. This work was kindly performed by Dr. A. Hasse and Frau M. Stumpf.

2.11 DNA sequence analysis

The sequence of plasmid DNA was analyzed by the sequencing facility in the center for molecular medicine, university of Cologne (ZMMK), with the modified dideoxy nucleotide termination method using a Perkin Elmer ABI prism 377 DNA sequencer.

3. Protein analysis and immunological methods

3.1 SDS-polyacrylamide gel electrophoresis (Laemmli, 1970)

The proteins were separated in a polyacrylamide gel based on their molecular weights with the help of SDS-polyacrylamide gel electrophoresis (SDS-PAGE). The original charge of proteins can be neglected, because denatured proteins associate with SDS molecules, so that they carry predominantly negative charges dependent on their molecular weight. Discontinuous polyacrylamide gels (8-15 % resolving gel, 5 % stacking gel) were prepared using glass plates of 10 cm × 7.5 cm dimensions and spacers of 0.5 mm thickness. A 12-well comb was generally used for formation of the wells in the stacking gels. The composition of resolving and stacking gels is given in the table below. Protein samples were mixed with suitable volumes of 5× SDS sample buffer, denatured by heating at 95°C for 5 min and loaded into the wells of the stacking gel. A molecular weight marker, which was run simultaneously on the same gel in an adjacent well, was used as a standard to estimate the apparent molecular weights of proteins. The molecular weight markers were prepared according to the manufacturer's instructions. After loading the sample, electrophoresis was performed in 1× gel running buffer at a constant voltage of 100-180 V. After electrophoresis, the resolved proteins were visualized either by Coomassie blue staining or transferred onto a nitrocellulose membrane. For subsequent western blot analysis, a prestained marker (BioRad) was used as molecular weight marker.

Molecular weight marker

LMK-marker kDa (Amersham Biosciences)	94; 67; 43; 30; 24; 20.1; 14.4
Prestained marker kDa (Bio-Rad)	250; 150; 100; 75; 50; 25; 15; 10

5 × SDS-loading buffer	10 × SDS-PAGE-running buffer
2.5 ml 1M Tris/HCl, pH 6.8	0.25 M Tris
2 ml 98.5 % glycerol	2 M glycine
4 ml 10 % SDS	1 % SDS
200 ml 10 % bromophenol blue	
1.0ml 1.43 M β-mercaptoethanol	

	Resolving gel			Stacking gel
	8 %	10 %	12 %	5 %
Acrylamid ¹ [ml]	15.8	19.7	23.6	3.4
1.5 M Tris/HCl, pH 8.8 [ml]	16	16	16	
0.5 M Tris/HCl, pH 6.8 [ml]				2
10 % SDS [μl]	590	590	590	200
TEMED [μl]	23	23	23	8
10 % APS [μl]	240	240	240	360
Deionized H ₂ O [ml]	27.4	23.5	19.6	14.3

¹)Bisacrylamide 30:0.8

3.2 Coomassie blue staining of SDS-polyacrylamide gels

After electrophoresis, the resolved proteins were visualized by staining the gel with Coomassie blue staining solution at room temperature with gentle agitation for at least 30 min. The staining solution was replaced by destaining solution. The gel was incubated in the destaining solution at room temperature with gentle shaking. The destaining solution was replaced several times to wash away unbound Coomassie blue until protein bands were clearly visible.

Coomassie blue staining solution	Destaining solution
0.1 % Coomassie blue R250	7 % acetic acid
50 % ethanol	20 % ethanol
10 % acetic acid	
Filter the solution before use	

3.3 Western blotting

Western blotting and subsequent immunolabelling by specific antibodies allows the specific detection of proteins. The proteins were electrophoretically transferred from the SDS gel to a nitrocellulose membrane. Transfer of proteins larger than 100 kDa was performed by the wet transfer method. Briefly, one sponge cloth, three Whatman 3MM papers, the nitrocellulose membrane, the gel, three Whatman 3MM papers and

another sponge cloth were stacked in a sandwich array. These materials were soaked in cold transferring buffer before blotting. The membrane in the sandwich was oriented to the anode of the blotting tank filled with transfer buffer. The transfer was performed at constant current (0.1 A) for overnight or 0.4 A for 4 h at 4°C. The transfer buffer contained 25 mM Tris/HCl (pH 8.5), 190 mM glycine and 20 % methanol.

3.4 Ponceau S staining

To control the efficient transfer of the proteins to the nitrocellulose membrane, the membrane was incubated in Ponceau solution for 1 min and briefly washed with TBST-buffer. The positions of the standard marker proteins were labeled with a pencil. Afterwards, the membrane was destained in TBST buffer for several times until the red color was completely removed. For the preparation of the staining solution 2 g Ponceau S (Sigma-Aldrich) was dissolved in 100 ml 3 % trichloroacetic acid.

3.5 Immunodetection of nitrocellulose membrane-bound proteins

After protein transfer, Ponceau S staining and washing, the nitrocellulose membrane (blot) was blocked in TBST-buffer with 4% milk powder with gentle agitation at room temperature for at least 1 h. Then, the membrane was incubated for 1 h with primary antibodies in TBST-buffer or hybridoma supernatant at room temperature. The blot was then washed 4×5 min with TBST buffer. Following washings, the blot was incubated for 1 h at room temperature with an appropriate dilution (1:5,000 or 1:10,000) of secondary antibodies, usually a goat-anti-mouse IgG coupled to horse radish peroxidase, with gentle agitation. Subsequently, the blot was washed as described above. The enhanced chemi-luminescence (ECL) detection system was used for visualization of labeled proteins (blackening the X-ray film at 430 nm). For this, the blot was incubated in ECL-detection solution containing H₂O₂, a substrate of peroxidase-conjugated secondary antibodies for 1-2 min and then wrapped in saran wrap immediately after removing the excess ECL-detection solution. An X-ray film was exposed to the membrane for 1-30 min and the film was developed to detect the immunolabeled protein.

ECL-detection solution	TBST buffer
100 mM Tris/HCl, pH 8.5	10 mM Tris/HCl, pH 8.0
250 mM aminonaphthylhydrazide ^{a)}	150 mM NaCl
80 mM p-coumaric acid ^{a)}	0.2 % Tween 20
0.01 % H ₂ O ₂	

a) dissolved in DMSO

3.6 Expression and purification of 6×His tagged NH₂-terminal and COOH-terminal Hcoronin 3 fragments in *E. coli*

For expression of recombinant 6×His tagged Hcoronin 3 subdomains, the QIAexpress system (Qiagen) was used. Affinity chromatography was used for the purification of 6×His tagged fusion protein by Ni-NTA matrix. The host strain *E. coli* M15 was transformed with the pQE-30 vector encoding the His-tag fusion proteins and expression was induced by addition of IPTG, which leads to inactivation of the *lac* repressor protein.

3.6.1 Expression of 6×His tagged COOH-terminal Hcoronin 3 (315-444), (315-474) and NH₂-terminal Hcoronin 3 (1-71) fragments

For expression of 6×His tagged COOH-terminal Hcoronin 3 residues 315-444 as well as 315-474 recombinant proteins, a single bacterial colony was inoculated in 20 ml LB medium containing both ampicillin (100 µg/ml) and kanamycin (25 µg/ml), respectively, and was grown overnight at 37°C. The overnight culture was inoculated into 1L LB medium containing both antibiotics and incubated at 30°C by vigorous shaking (250 rpm) until cell density reached an OD₆₀₀ of 0,5-0,6. Subsequently, IPTG was added to the *E. coli* culture with a final concentration of 0.5 mM. The culture was continuously incubated for 5 h at 30°C. The cells were then harvested by centrifugation at 4000×g for 20 min at 4°C and cell pellets were washed with 10 ml lysis buffer and frozen at -20°C. The lysis buffer contained 50 mM NaH₂PO₄, 300 mM NaCl and 10 mM imidazole.

The same procedure was used for expression of 6×His tagged NH₂-terminal Hcoronin 3 residues 1-71 fragment. However, the expression was induced by a final concentration of 0,1 mM IPTG. Afterwards, the culture was grown at room temperature for only 2 h.

3.6.2 Purification of 6×His tagged COOH-terminal Hcoronin 3 fragments

Both bacterially expressed fragments were soluble in lysis buffer under native conditions. Affinity chromatography with Ni-NTA column was done as follows: The pellet was thawed on ice and resuspended in lysis buffer at 5 ml per gram wet weight. After freezing in liquid N₂ and thawing in a water bath at 37°C for three times, the lysate was homogenated with the help of a Dounce homogenizer and transferred into a 50 ml falcon tube. The homogenate was then sonicated on ice using 1-sec bursts at 0,5 amplitude (200 W) with a cooling period of 1 min between each impulse. The suspensions were centrifuged at 10,000×g for 30 min at 4°C. The clarified supernatant was incubated for 1 h at 4°C by gentle shaking with 2 ml of 50% Ni-NTA resin which was prewashed with 10 ml water and equilibrated with 10 ml lysis buffer for 30 min at 4°C. The lysate-Ni-NTA mixture was loaded into a column (BIO-RAD flow column 1 cm ID, 14 cm length) with the bottom outlet capped and incubated for another 20 min to settle down the resin. The column was washed with 10 ml wash buffer. The proteins were finally eluted with buffer containing 250 mM imidazole. The purified 6×His tagged COOH-terminal Hcoronin 3 fragments were used for actin binding assay and gel filtration. About 12 mg of 6×His-Hcoronin 3 (315-444) and 8 mg of 6×His-Hcoronin 3 (315-474) were purified from 1L of bacterial culture, respectively. For actin cosedimentation assays, the buffer conditions were changed from elution to polymerization buffer and the recombinant proteins were concentrated by Millipore filtration. They could be stored at 4°C for at least one week.

Lysis buffer	Wash buffer	Elution buffer
50 mM NaH ₂ PO ₄	50 mM NaH ₂ PO ₄	50 mM NaH ₂ PO ₄
300 mM NaCl	300 mM NaCl	300 mM NaCl
10 mM imidazole	20 mM imidazole	250 mM imidazole

3.6.3 Purification of a 6×His tagged NH₂-terminal Hcoronin 3 (1-71) fragment

Because of the low solubility of the NH₂-terminal Hcoronin 3 residues 1-71 in lysis buffer, the protocol for the isolation of this bacterially expressed fragment was modified. 5 ml of lysis buffer containing 20 mM NaCl, 10 mM NaH₂PO₄, 1 mM imidazole and 10 % glycerol were added per 1 g of washed cell pellet. The suspended cells were lysed as described by freeze-thawing cycles. The homogenate

was supplemented with 0.5% Triton X-100 (final concentration). After cell lysis, the suspension was further homogenized with a Dounce homogenizer on ice for 5 min and sonicated for 2 min at 4°C. A supernatant fraction was prepared from the homogenate by centrifugation at 10,000 g, 4°C for 30 min and loaded onto Ni-NTA matrix column preequilibrated with lysis buffer. The column was washed with 10 ml of lysis buffer containing 1 mM imidazole. The NH₂-terminal peptide was eluted with a step gradient of 1-250 mM imidazole in 50 mM Na₂HPO₄, pH 8.0, and 300 mM NaCl. The recombinant protein was eluted from the column in the very early fractions E1 and E2. This could result from the weak interaction of this 6×His tagged protein with the Ni-NTA matrix. Possibly, this 6×His tag was not exposed on the surface of the protein under native conditions so that it had no access to the Ni-NTA matrix. Since the protein was contaminated by other bacterial materials in the eluate, it was further purified by a cation exchanger. The fractions containing N-terminus were pooled and dialysed overnight against cation exchanger running buffer at 4°C. After dialysis, the solution was clarified by a centrifugation at 10,000 g for 30 min. The clarified dialysate was subjected to a Mono-S sulfonemethyl cation exchanger column (Amersham Biosciences) equilibrated with running buffer. The column was developed with a linear gradient of 0-200 mM NaCl. The elutions containing NH₂-terminus were collected and controlled by SDS-gel electrophoresis. For actin cosedimentation assays, the buffer conditions were changed from elution to polymerization buffer and the recombinant proteins were concentrated by Millipore filtration. Only 2 mg of N-terminal 6×His-Hcoronin 3 residues 1-71 were isolated per l of bacterial culture. They could be stored at 4°C for at least one week.

Homogenization buffer	Cation exchanger buffer
5 mM PIPES	25 mM MES
5 mM EGTA	0.5 mM EGTA
2 mM DTT	0.2 mM DTT
5 mM Benzamidine	pH 6.0
pH 7.0	

3.7 Buffer exchange and concentration of proteins

A 1 ml protein sample was applied to a ultrafree-4 centrifugal filter unit pre-equilibrated with protein buffer without touching the membrane surface and the cap was tightly closed. The filter units were placed into a 15 ml falcon and centrifuged at 4000×g for 30 min at 4°C. The protein sample was recovered from the bottom of the concentration pocket with a pipette once the desired concentration was achieved, otherwise the sample was loaded onto the filter units repeatedly. For exchange of the protein buffer, 500 µl protein sample were suspended in 3.5 ml of the desired protein buffer in ultrafree-4 centrifugal filter units. After centrifugation at 4000×g for 30 min, fresh protein buffer was added to the filter unit again, up to 4 ml total filter unit volume. This step was repeated for another 5 times until a dilution of 1:1000 is reached. Finally, the solution was concentrated by new centrifugation at 4000×g for 30 min.

3.7.1 Quantification of protein concentration (Bradford, 1976)

The Bradford method is based on quantification of the binding of Commassie “brilliant Blue” G 250 to an unknown protein and comparing this binding to that of different amounts of standard protein BSA. Briefly, the duplicate aliquots of 0.5 mg/ml BSA (0, 5, 10, 15, and 20 µl) were placed into ten microcentrifuge tubes and diluted each to 100 µl with protein solution. After addition of 1ml Bradford reagent (Sigma-Aldrich) to each aliquot, the samples were incubated at room temperature for 5 min. Subsequently, the absorbance of 1 ml of sample at 595 nm was measured to make a standard curve. The concentration of protein was quantified by comparing its absorbance to that of standard BSA.

3.8 Generation of a Hcoronin 3 antibody

The monoclonal antibody specific for coronin 3 was raised by immunizing mice with a recombinant His×6-tagged protein containing the COOH-terminal unique and coiled coil region, a 164 amino acids fragment of Hcoronin 3. The hybridoma clone K6-444 recognized a single endogenous protein of about 57 kDa in cell extracts from human, monkey and mouse cell line. The antibody was able to specifically react with EGFP-tagged Hcoronin 3 and not bind to the closely related EGFP-Hcoronin 1 and -Hcoronin 2 in transfected HEK293 cells in Western Blot analysis. Thus unpurified K6-444 hybridoma supernatant was used for Western blot analysis. The purified mAB K-

444 with protein sepharose G (Amersham Biosciences) proved useful also in immunofluorescence studies. After checking, a 1:200 dilution of the purified mAB K6-444 (5 µg/ml final concentration) was used for subcellular localization of coronin 3 in immunostaining studies.

3.9 Subcellular fractionation

The distribution of coronin 3 in different subcellular compartments was analyzed by subcellular fractionation studies in combination with subsequent Western blot analysis.

3.9.1 Differential centrifugation

For the analysis of coronin 3 oligomers in different subcellular fractions, cytosolic supernatants (100,000×g) and 10,000×g pellets were prepared from HEK 293 cells. The confluent cell monolayers (2×10^7 cells) of two culture dishes (Φ15 cm) were washed with PBS once and scraped off in HES buffer. Cells were then disrupted with the help of a tight-fitting Dounce homogenizer. Nuclei and intact cells were removed by centrifugation at 500×g for 10 min at 4°C. The subsequent pelleting steps were performed at 10,000×g (30 min) and 100,000×g (60 min) respectively. All pellet fractions were resuspended in HES buffer and recentrifuged to purify the pellets. The pellets were finally suspended in 500 µl of HES buffer and subjected to western analysis. The 500×g supernatant was designated “postnuclear cell extract”, the 10,000×g pellets contained membrane + cytoskeletal compartments. The supernatant of 100,000×g and the pellet of 100,000×g corresponded to cytosolic extract and microsome pellet, respectively. For the analysis of the distribution of coronin 3 in different subcellular compartments in un- and differentiated mouse neuroblastoma cells, coronin 3 in cytosolic and cytoskeletal fraction was extracted from undifferentiated and differentiated 2×10^7 Neuro-2a cells in four culture dishes (Φ15 cm), respectively.

3.9.2 Isopycnic separation on discontinuous sucrose gradients

For isopycnic separation on discontinuous sucrose gradients, total cell extracts were prepared from 2×10^8 - 10^9 HEK 293 cells stably transfected with EGFP-Hcoronin 3 and EGFP-Hcoronin 3 (72-404). First, the transfected cells were suspended and scraped off in HEPES-DTT buffer. The cells were disrupted with a tight-fitting Dounce

homogenizer. The homogenates were centrifuged at 500×g for 10 min at 4°C. The pellet was resuspended in lysis buffer and homogenized with the tight-fitting Dounce again. This step was repeated three times. The supernatants were pooled. 1 ml of the pooled supernatant was loaded on the top of gradients containing 1 ml steps of 5, 10, 15, 20, 25, 30, 35, 40, 45, 50 and 85% sucrose in a 12 ml ultracentrifuge tube. After centrifugation at 100,000×g in a Beckman SW 41 rotor for 17 h at 4°C, the fractions were collected from the top (22 fractions, 0.5 ml respectively) and subjected to SDS-PAGE and Western blot analysis.

HES buffer	HEPES-DTT buffer
0.25 M sucrose	1 mM DTT
1 mM EDTA	10 mM Hepes, pH 7.2
20 mM Hepes, pH 7.2	1 mM PMSF
1× complete protease inhibitor cocktail/10 ml	1× complete protease inhibitor cocktail/10 ml

3.10 Gel filtration chromatography

Gel filtration is a method to determine the apparent molecular mass of macromolecules under native conditions. In this work, it was used to analyze protein-protein interactions, thus providing information about protein complexes in different subcellular fractions.

3.10.1 Analysis of Hcoronin 3 oligomers *in vivo*

For the analysis of Hcoronin 3 oligomers *in vivo*, cytosolic supernatants (100.000×g) and cytoskeletal pellets (10.000×g) were prepared from two confluent dishes of HEK 239 cells (~2×10⁷ cells, see section 3.8.1). Both fractions were adjusted to 0.6 M KCl, incubated for 1 h at 4°C and centrifuged at 100,000×g for 60 min at 4°C. The highly ionotropic conditions were used to minimize interaction of coronin 3 with other proteins and to disintegrate cytoskeletal actin-myosin complexes (Berryman et al., 1995). 50 µl of the clarified supernatant were loaded on a Superdex 200 PC 3.2/30 column preequilibrated with a modified relaxation buffer containing 0.6 M KCl using the Smart system (Amersham Biosciences). Fractions (50 µl) were collected and analyzed by SDS-PAGE and Western blot. The elution profile of the gel filtration

column was calibrated using a set of protein markers (Amersham Biosciences) as described below.

3.10.2 Analysis of the domain requirements of Hcoronin 3 for the formation of cytosolic complexes

To analyze the domain requirements of Hcoronin 3 for the formation of cytosolic complexes *in vivo*, two culture dishes with confluent HEK 239 cell monolayers stably transfected with EGFP-Hcoronin 3 and various truncated constructs (about 2×10^7 cells) were used for each sample preparation. Cells were rinsed once with PBS and detached from the surface of the culture dish by squirting the solution onto the cells. The suspension was then transferred into a 15 ml falcon tube and cells were centrifuged at 1,000 rpm for 5 min. The supernatant was discarded and cell pellets were resuspended in relaxation buffer. Cells were then disrupted with the help of a tight-fitting Dounce homogenizer. Nuclei and intact cells were removed by centrifugation at $500 \times g$ for 10 min at 4°C . The postnuclear supernatant was subsequently centrifuged at $100,000 \times g$ for 30 min at 4°C in a Beckman TL-100 tabletop centrifuge. 50 μl -aliquots of the supernatants (cytosol) were separated on a Superdex 200 PC 3.2/30 column preequilibrated with relaxation buffer containing 0.1 M KCl mounted in a Smart system (Amersham Biosciences). Fractions (50 μl) were collected and analyzed by SDS-PAGE and Western blot. As control, the elution profile of EGFP was tested. The components and concentrations of the standard protein marker for the calibration of Superdex 200 column were as listed below.

3.10.3 Migration of recombinant COOH-terminal Hcoronin 3 fragments in gel filtration

To analyze the role of the coiled coil domain of COOH-terminal Hcoronin 3 in oligomerization, the recombinant proteins Hcoronin 3 (315-474) containing the unique region and coiled coil domain, and Hcoronin 3 (315-444) lacking the coiled coil domain were used for gel filtration experiments. The protein buffer was first changed from elution buffer to relaxation buffer by Millipore ultrafree-4 centrifugal filter units. The concentration was adjusted to $1 \mu\text{g}$ protein/ μl with relaxation buffer. After ultracentrifugation at $100,000 \times g$ for 30 min at 4°C in a Beckman TL-100 tabletop centrifuge, cleared aliquots (50 μl) of the supernatants were loaded onto a

Superdex 200 column preequilibrated with ice-cold relaxation buffer. Fractions (50 μ l) were collected and analyzed by SDS-PAGE and Western blot.

Relaxation buffer	Protein marker	
100 mM KCl	Thyreoglobulin	669 kDa, 3 mg/ml
3 mM NaCl	Ferritin	440 kDa, 0.15 mg/ml
3.5 mM MgCl ₂	Aldolase	158 kDa, 3 mg/ml
10 mM K ⁺ PIPES, pH 7.2	BSA	67 kDa, 2 mg/ml
1 mM DTT	Ovalbumin	43 kDa, 3,5 mg/ml
1 mM PMSF	Ribonuclease	13.7 kDa, 6 mg/ml
1 \times protease inhibitor cocktail		

3.11 Immunoprecipitation

Immunoprecipitation is a method to analyze the possible binding partners of a protein of interest. HEK 293 cells stably transfected with Hcoronin 3-myc-His were used for immunoprecipitation. First, the transfected confluent cells were washed 1 \times with PBS (37°C) and lysed with 1 ml RIPA buffer containing protease inhibitor cocktail per petri dish (Φ 140 mm) for 2 min at room temperature. The cells were then scraped from the culture dish and transferred into Eppendorf tubes with incubation on ice for 30 min. The cells were disrupted with the help of a tight-fitting Dounce homogenizer and nuclei and intact cells were removed by centrifugation at 500 \times g for 10 min at 4°C. The supernatant was centrifuged at 13,000 rpm for 15 min at 4°C again. The cleared supernatant was incubated with 50 μ l protein A-sepharose (1:1 in PBS) for at least 2 h with gentle agitation at 4 °C in order to remove unspecifically protein A-sepharose binding proteins from cell lysates. The protein A-sepharose was then pelleted by centrifugation at 2,000 rpm for 20 s (preclear pellet). Following this step, the supernatant was incubated with 5 μ l monoclonal rabbit anti-myc-antibodies (1 μ g/ μ l) for 2 h with gently rotation at 4°C. Then, 50 μ l protein A-sepharose were added and incubated further for at least 1 h. After sedimentation as above, the protein A-sepharose was washed with RIPA-buffer for 3 \times 5 min. The pellet was resuspended in 50 μ l RIPA buffer and subjected to SDS-PAGE.

RIPA buffer

150 mM NaCl

1 % Nonidet-40

0.5 % Na-deoxycholate

0.1 % SDS

50 mM Tris/HCl, pH 8.0

Before using, add 1 mM PMSF and

1× complete-mini protease inhibitor cocktail/10 ml

3.12 Actin binding assay

Actin filaments with a length more than 10 monomers of G-actin can be sedimented at 100,000×g (Brown et al., 1982). Proteins which interact with those filaments are also located in the actin pellet. Therefore, this so called spin down method allows to examine the binding of proteins to actin filaments. Purified 6×His tagged NH₂-terminal Hcoronin 3 (1-71) and COOH-terminal Hcoronin 3 (315-444) and Hcoronin 3 (315-474) fragments were transferred to polymerization buffer and concentrated as described above. For the cosedimentation assay, G-actin isolated from rabbit muscle (kindly provided by Dr. M. Schleicher and Dr. E. Korenbaum) stored in liquid nitrogen was carefully thawed on ice. G-actin and the bacterially expressed recombinant proteins were centrifuged at 125,000×g for 15 min at 4°C in order to remove precipitated or aggregated proteins. 10 μl of G-actin (2.2 μg/μl) at a final concentration of 10 μM was incubated with different amounts of purified recombinant protein in the polymerization buffer. The volume of the reaction was adjusted to 50 μl with polymerization buffer. As controls, either G-actin alone, or only recombinant proteins, or BSA with G-actin were mixed with polymerization buffer. The samples were gently mixed and incubated for 60 min at room temperature. After centrifugation at 100,000×g or at 10,000×g at 22 °C for 40 min, 40 μl of the supernatant were transferred to a fresh Eppendorf tube and 10 μl 5× SDS sample buffer was added. 10 μl remaining supernatants were carefully removed from the pellet. The pellet was resuspended in 50 μl of the polymerization buffer and 12.5 μl 5× SDS sample buffer. The samples were analyzed by 12 % - 15 % SDS-PAGE. To estimate the concentration of the recombinant proteins in the sample, known amounts of BSA were loaded on the same gels as standards. After Coomassie blue staining and

drying in the frame, the gels were scanned with a Molecular Dynamics scanner and ImageQuant software was used for quantification of the bands of interest. The amount of the recombinant 6×His tagged fusion proteins in the supernatant and pellet were calculated from the measured intensities of bands.

Polymerization buffer	G-buffer
2 mM MgCl ₂	0.5 mM Tris/HCl, pH 7.0
80 mM KCl	0.5 mM ATP
1 mM EGTA	0.1 mM CaCl ₂
20 mM Imidazole, pH 7.2	0.5 mM DTT
2 mM ATP	

3.13 Light microscopic assay of F-actin suprastructures formed in the presence of different Hcoronin 3 COOH-terminal fragments

The light microscopic assay of actin filament structure is based on a protocol by Korneeva and Jockusch (1996) with slight modifications. 10 μM G-actin was induced to polymerize in polymerization buffer at room temperature for 30 min. 5 μM coronin 3 COOH-terminal polypeptide 315-474 and fragment 315-444 lacking coiled coil domain were then incubated with F-actin at room temperature for an additional 1 h as described for the low-speed spin down assay. The final reaction volume was 50 μl. After centrifugation at 10,000×g for 30 min at room temperature, the pellets were resuspended in 25 μl polymerization buffer. The samples were applied to poly-L-lysine (200 μg/ml)-coated glass coverslips which were located in a 24-well tissue culture plate and incubated for 1 h at 4°C. The absorbed proteins were fixed with 3 % paraformaldehyde for 20 min at 4°C and washed with PBS. Actin filaments were stained with TRITC-phalloidin. The coverslips containing labelled F-actin were mounted with 10 μl gelvatol onto ethanol-cleaned glass slides in the direction of the sample side facing to downwards. Mounted slides were then stored overnight in the dark at 4°C. The slides were observed with a confocal laser scanning microscope.

3.14 2D-gel sample preparation

Two dimensional electrophoresis (2D-electrophoresis) is a widely used methods for the analysis of complex protein mixtures extracted from cells, tissue or other biological samples. This technique separates proteins according to two independent properties in two discrete steps: The first dimension is an isoelectric focusing which separates proteins according to their isoelectric points (pI); the second dimension is an SDS-PAGE which separates proteins according to their molecular weights. Thus, each spot in 2D-gels provides information about the protein's pI and molecular weight. Because the pI of unphosphorylated and phosphorylated proteins is different, whereas the molecular masses are only marginally different, this method allows also the detection of this covalent modification.

For isoelectric focusing, it was most important to solubilize coronin 3 under low salt conditions. Briefly, 4 dishes of 50% confluent Neuro-2a cells (about 2×10^7 cells) were used for each sample preparation. Cells were rinsed once with PBS and detached from the surface of the cell dish by squirting the solution onto the cells. The suspension was then transferred into a 15 ml falcon and cells were centrifuged at 1,000 rpm during 5 min. The supernatant was discarded and cell pellets were washed in TE buffer briefly. After centrifugation, the cell pellets were solubilized with 1 ml of HES-lysis buffer. The cells were disrupted with a tight fitting Dounce. Nuclei and intact cells were removed by centrifugation at $500 \times g$ for 10 min at $4^\circ C$. The postnuclear supernatant was subsequently centrifuged at $1,000 \times g$ for 10 min at $15^\circ C$, $10,000 \times g$ for 30 min at $15^\circ C$, and $100,000 \times g$ for 60 min. The $1,000 \times g$ supernatant, $10,000 \times g$ pellet and $100,000 \times g$ supernatant were designated postnuclear extract, cytoskeletal and membrane as well as cytosolic fraction, respectively, and the sample buffer was exchanged from HES to 2 ml of 2D-lysis buffer with Millipore filter units (see section 3.7). $100 \mu l$ of each fraction were mixed with $50 \mu l$ rehydration buffer. DTT and IPG buffer were added to the mixture at a final concentration of 2 % (v/v) immediately prior to use. Subsequently, a trace of bromophenol blue was supplied to the sample mixture. Following this step, IPG strips (pI 3-11, 7 cm, Amersham Biosciences) was preswollen in the sample solution for in-gel rehydration overnight in an IPG Strip-tray at room temperature. To minimize evaporation and urea crystallization, mineral oil was applied to cover the surface of the strip. Finally the strip tray was overlay with cover fluid. The rehydrated IPG strips containing the samples were cleaned with water and immediately transferred to

adjacent grooves of the aligner in the immobiline dry strips tray. The strips were placed with the pointed (acidic) end at the top of the tray near the red electrode (anode). The blunt end was positioned at the bottom of the tray near the black electrode (cathode). Afterwards, presoaked strips with water were placed across the cathodic and anodic ends of the aligned IPG gel strips. Following this step, the electrodes were properly aligned over the moistened strips. Isoelectric focusing with the Multiphor II system (Amersham Biosciences) was performed with a modified program described below. After running the first dimension, the IPG strips were washed with water and incubated with SDS equilibration buffer for at least 20 min at room temperature. The second dimension, the SDS PAGE step, was performed as described. After the second electrophoresis, the proteins were transferred from the gel to nitrocellulose membranes by electrostatic transfer. The proteins of interest were detected with Western blot.

2D-lysis buffer	Rehydration buffer	SDS equilibration buffer
8 M urea	8 M urea	6 M urea
4 % w/v CHAPS	4 % w/v CHAPS	30 % (v/v) glycerol
2 % DTT	1% IPG buffer	2 % SDS (w/v)
40 mM TrisHCl, pH 8,0	2 % DTT	2% DTT
2 % IPG buffer		50 mM Tris/HCl, pH 8.8
1×complete mini protease inhibitor		

PBS, pH 7.4

10 mM KCl

150 mM NaCl

16 mM NaH₂PO₄

32 mM KH₂PO₄

4 Cell culture

4.1 Cell lines

Different adherent cell lines were used in the studies. Each cell line required a special growth medium as follows:

Neuro-2a DMEM (1,000 g glucose/l), 10 % heat inactivated FBS, 1× non essential amino acids, 2 mM glutamine, 100 U/ml penicillin/100 µg/ml streptomycin (=P/S)

HEK (293/SF) DMEM (4,000 mg glucose/l), 10 % heat inactivated FBS, 2mM glutamine, 1 % pyruvate, P/S

COS-7 DMEM (1,000 mg glucose/l), 10 % heat inactivated FBS, 2 mM glutamine, 1 % pyruvate, P/S

4.2 Culture of adherent cell lines

Adherent cell lines were cultured in petri dishes or culture flasks with the suggested medium at 37°C in incubator supplied with 5 % CO₂, 95 % moisture. According to the generation time of the cell lines and cell densities in culture dish, cultures were split every two or three days and the medium was changed. To do this, cells were rinsed once with PBS and detached from the surface of the cell dish by squirting the solution onto the cells with PBS. Then, the detached cells were resuspended in the proper medium and pipetted up and down several times. The cells in suspension were plated at the desired density onto the new dish filled with fresh medium.

4.3 DMSO stocks of adherent cells

In order to keep cells in a long term, cells were detached from the dish, sedimented at 1,000 rpm for 5 min and transferred into a frozen medium. The frozen medium consists of the respective culture medium and supplied additionally with 10 % serum and 10 % DMSO. Cells were quickly pipetted in cryotubes and placed in a styropor box at -80°C. The following day, the tubes were transferred to liquid nitrogen.

4.4 Thawing and recovering mammalian cells

When cryopreserved cells were needed, they were thawed rapidly and plated at relatively high density to optimize recovery. Briefly, the frozen cells were quickly thawed in an incubator at 37°C. The suspension was then immediately transferred

into a 25 cm² cell culture flask. As soon as cells were adherent to the bottom of the flask (~2 h), the medium was replaced with fresh one in order to remove the DMSO rest in the frozen medium.

4.5 Transfection of mammalian cells

There are several methods available for transfecting mammalian cells with plasmid constructs. To obtain high amounts of transfected cells, electroporation was performed for Gel filtration and subcellular fractionation of HEK 293 cells. For immunofluorescence, transfection kits by Qiagen or Invitrogen were used for the transfection.

4.5.1 Lipid-mediated transfection

Effectene (Qiagen) and Lipofectamine Plus (Invitrogen) were used, both transfection kits contain cationic lipids. The cationic lipids form electrostatic interactions of their positive charges with the negative charges in the backbone of DNA and condensethem to a more to a compact structure. The lipophilic nature of the cationic lipids allows the complexes to enter the target cells.

If Effectene reagent was used, 0.4 µg DNA was diluted in a solution containing 1.6 µl enhancer and 60 µl enhancer buffer per well in a 24-well plate. After vortexing and incubation at room temperature for 5 min, 5 µl Effectene-reagent was added, vortexed again and incubated at room temperature for the same time to allow the formation of the DNA-micelle complex. During the formation of DNA-lipophilic complex, cells in a 24-well plate were washed with PBS once and 400 µl medium containing 10 % FBS were added. Subsequently, the suspension containing the DNA-effectene complex was supplied with 350 µl culture medium without antibiotic and FBS and the mixture was added to the cells. After 4-6 hours, the medium was replaced with normal culture medium, since the lipophilic complex has generally a toxic effect on the cells. The transfection with Lipofectamine Plus followed a similar protocol and was performed according to the manufacturer's specifications.

4.5.2 Electroporation of Neuro-2a and HEK 293 cells

Prior to electroporation, the cuvette (4 mm width) was washed with ethanol, PBS and water several times. About 10⁷ cells were washed with PBS and pelleted at 1,000 rpm at 4°C. The cell pellet was resuspended in 200 µl culture medium and

transferred into the electroporation cuvette. Afterwards, 40 μg plasmid DNA was added to the cells and gently pipetted up and down several times. The cells were incubated on ice for 10 min. The cells were then electroporated using a Gene pulser unit (Bio-Rad) set at 975 μF and 200 V. After the electrical shock, the cells were incubated at room temperature for 10 min and then seeded out in fresh medium. 2-3 h later, the medium was replaced in order to remove dead cells.

4.6 Calculation of cell density

It is important to determine the number of cells in a culture to standardize the experimental conditions. A hemocytometer was used for this. A cleaned coverslip was applied to the hemocytometer slide and the cell suspension was applied. The counting chamber contains four corner squares. The volume of each corner square corresponds to 0.1 μl . To determine the amount of cells per ml, the average number of cells per corner square was counted manually. The cells per ml was calculated as follows:

$$\text{cells/ml} = \text{average number of cells per corner square} \times \text{dilution factor} \times 10^4$$

10^4 is the volume correction factor for the hemocytometer, because each square corresponds to $1 \times 1 \times 0.1 \text{ mm}^3$.

4.7 Establishment of stable cell lines by G418 selection

HEK 293 cells were used to produce cell lines stably expressing Hcoronin 3-myc-His proteins. To generate these cells, HEK 293 cells were first transfected with pcDNA-Hcoronin 3-myc-His, which contains a neomycin phosphotransferase expression cassette. This selection marker was used for the selection of stably expressing. The neomycin-derivative geneticin (G418) was added to the culture medium at a final concentration of 0.5 mg/ml. The cells, which occasionally integrated the plasmid into their genome were resistant to neomycin and survived in the selection medium. They formed a cell colony after 1-2 weeks. These colonies were carefully transferred into a 24-well plate for further propagation with the help of a Pasteur pipette. The expression of Hcoronin 3-myc-His in HEK 293 cells was examined by Western blots.

4.8 Differentiation of Neuro-2a cells

To differentiate mouse Neuro-2a cells, this line was first washed with PBS and then supplied with FBS-reduced cell medium (at a final concentration of 0.2 % FBS). Transfection was performed one or two days before differentiation started. As soon as EGFP-Hcoronin 3 was expressed, the cells were washed with PBS once and supplied with medium containing only 0.2 % serum. The cells were observed microscopically everyday. Normally, after the two days differentiation, the cells developed long projected neurites.

4.9 Stimulation of Neuro-2a cells

Neuro-2a cells (4×10^7) in 10 ml PBS were incubated at 37°C for 5 min, stimulated with PMA (0.1 μ M) for 5 min and bisindolylmaleimide (1 μ M) for 10 min, which diluted in prewarmed PBS. The cells were centrifuged at $200 \times g$ for 5 min at 4°C. The cell pellet were used for subcellular fractionation and 2D gel electrophoresis.

5 Cell Biological methods

5.1 Indirect immunofluorescence of mammalian cells

5.1.1 Preparation of mouse Neuro-2a cells

For immunofluorescence studies, Neuro-2a cells were cultured on sterilized glass coverslips in a 24-well plate the day before transfection. At least 30 % - 40 % of confluent Neuro-2a per well were grown before starting transfection with lipophilic methods. Cells attached to coverslips were fixed by using one of the fixation techniques described below. For transfection of Neuro-2a cells, Effectene-transfection-kit (Invitrogen) was used by following the manufacturer's instructions. The expression of EGFP-Hcoronin 3 fusion proteins was observed under the fluorescence microscope after overnight incubation.

5.1.2 Methanol fixation

For microtubule staining, methanol fixation was performed. After transfection and differentiation, the cell medium was aspirated and cells were washed with PBS at 37°C once. Since traces of calcium ions in methanol can destroy the structure of microtubules, a solution of EGTA in methanol was used in the experiments. 500 μ l of pre-chilled (-20°C) methanol was first pipetted into the well and incubated further for

10 min at -20°C in the dark. This was followed by two washings with PBS, incubation with 500 μl of PBG for 30 min to block unspecific binding of primary antibodies and immunolabelling as described in the section below.

Methanol fixation solution	PBG pH 7.4
5 mM EGTA	0.5 % bovine serum albumin
95 % methanol	0.045 % gelatin (cold water fish skin)
filter and store at -20°C	in 1 \times PBS, pH 7.4

5.1.3 Paraformaldehyde fixation

For observation of the distribution of endogenous coronin 3 and actin filaments in Neuro-2a cells, paraformaldehyde fixation was performed. First, the medium was aspirated and cells were washed with PBS at 37°C once. Then, 500 μl of paraformaldehyde (3 %) in PBS was pipetted into the well and incubated for 20 min at room temperature in the dark. For the permeabilization of the cell membrane, the cells were incubated with 500 μl of 0.5 % Triton-X 100 in PBS for 5 min at room temperature. This was followed by wash and blocking steps as described above, and immunostaining as described below.

Paraformaldehyde solution

3 g paraformaldehyde was dissolved in 90 ml PBS by stirring at 40°C and adding 3-5 drops of 2 M NaOH. After dissolving, the pH was adjusted to 7.4 with NaOH and the volume was adjusted to 100 ml with PBS. The solution was sterile filtered, aliquoted and finally stored at -20°C .

5.1.4 Immunolabelling of fixed cells

Coverslips with fixed cells were incubated with 250 μl of the desired dilution (in PBG) of the commercially available primary antibody or with hybridoma culture supernatant (anti-coronin 3-antibody K6-444 or anti- β -tubulin-antibody) for 1 h at room temperature. After incubation, unbound antibodies were removed by washing the coverslip in the well 3 \times 5 min with PBG each. The coverslip was incubated for 1 h with 250 μl of a proper dilution (in PBG) of secondary antibody (usually goat anti-mouse IgG) labeled with Alexa 488 or Alexa 568 fluorophore (Molecular Probes), FITC or Cy3 (Sigma-Aldrich). F-actin was labeled subsequently by incubation for 1 h with 100

ng/ml TRITC-phalloidin (Sigma-Aldrich). Following this incubation, 3×5 min washing with PBS each were performed. The coverslip was mounted onto a glass slide described as below.

5.1.5 Mounting of coverslips

After immunolabelling of the fixed cells, the coverslip was swirled once in deionised water and the extra water soaked off on a soft tissue paper. 10µl of gelvatol was placed to the middle of an ethanol-cleaned glass slide and the coverslip was mounted (with the cells facing downwards) onto the drop of gelvatol, taking care not to trap air bubbles between the coverslip and glass slide. Mounted slides were then stored overnight in the dark at 4°C. Thereafter, the slides were observed under a confocal laser scanning microscope.

Gelvatol

2.4 g of polyvinyl alcohol (MW 30-70 kDa, Sigma-Aldrich) was added to 6 g glycerol in a 50 ml centrifuge tube and mixed by stirring. To the mixture, 6 ml of distilled water was added and the mixture was incubated at room temperature for 3 h. Thereafter, 12 ml of 0.2 M Tris/HCl, pH 8.5, was added and the mixture was warmed to 50 °C for 10 min with occasional mixing to completely dissolve polyvinyl alcohol. The solution was centrifuged at 5000 rpm for 15 min. After centrifugation, 0.45 ml of diazabicyclooctane (DABCO), an anti-oxidant agent, was added to reduce the bleaching of the fluorescence. The solution was aliquoted in 300 µl in 1.5 ml Eppendorf tubes and stored at -20°C.

5.2 Fluorescence microscopy

Images of immunolabeled cells were acquired with a confocal laser scanning microscope TCS-SP (Leica) equipped with TCSNT software. A 488 nm argon-ion laser for excitation of EGFP and Alexa 488 fluorescence and a 568-nm krypton-ion laser for excitation of TRITC, Cy3 and Alexa 568 fluorescence were simultaneously used. For the proper acquisition of both signals, the emission signals for green and red fluorophores were separated by using appropriate wavelength settings for each photomultiplier. The images from both channels were independently attributed with color codes and then superimposed using the accompanying TCSNT software. Image processing was done with Adobe Photoshop or TCSNT software, respectively.

III. Results

1. Sequence analysis of Hcoronin 3

1.1 Alignment of Hcoronin 3 with *Dictyostelium* coronin and yeast crn1p

The alignment was done with the program BioEdit. Hcoronin 3, a 57 kDa protein, has

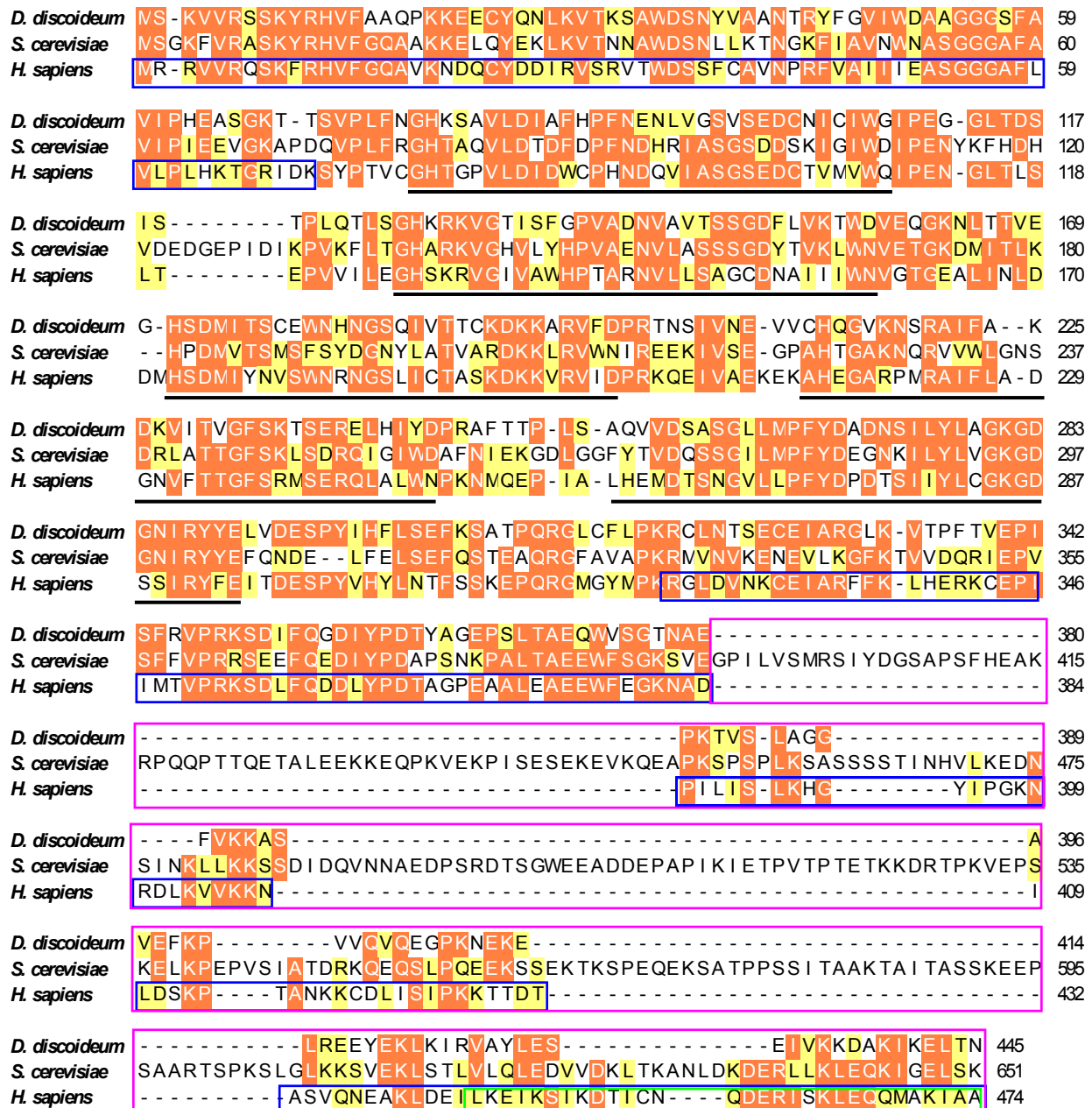


Fig. 3. Clustal alignment of *H. sapiens* coronin 3 (Genbank accession BAA83077) with *D. discoideum* coronin (P27133), and *S. cerevisiae* crn1p (Q06440). Identical amino acids are shown in orange and similar residues in yellow. The WD repeats are indicated by black lines. The boxes mark different features of the molecules as follows: violet, unique region; green, predicted coiled coil domain; blue, regions expressed as recombinant proteins for spin down assays with F-actin.

a similar domain structure to *D. discoideum* coronin and *S. cerevisiae* crn1p. Except for the unique region and the region between the first and the second WD40-repeats, the homology among them is relatively high from the NH₂-terminus to the part of the sequence following the WD40-repeats. There is 37% overall sequence identity among these three proteins. Among each pair, the sequence identities (and similarities) are as follows; 45% (65%) for *H. sapiens* coronin 3 and *D. discoideum* coronin; 37% (58%) for *H. sapiens* coronin 3 and *S. cerevisiae* crn1p; and 47% (63%) for *D. discoideum* coronin and yeast crn1p (Fig.3). The unique region between the conserved WD40-repeats and COOH-terminal coiled coil domain varies in length. This unique region is likely to be responsible for the diversity in the function of individual coronin family members (de Hostos, 2000). The unique region of *S. cerevisiae* crn1p, a 72.5 kDa protein, is considerably longer than that of other family members, suggesting that this protein might exhibit additional functions not shared by the others.

1.2 Alignment of Hcoronin 3 with *H. sapiens* coronin 1, 2, 3, 4, 5, *O. cuniculus* coronin 2_{se} and *M. musculus* coronin 6

Currently, 7 mammalian coronins are known. Due to its different structure, coronin 7 is not included in the alignment. At the amino acid level, the sequence of Hcoronin 3 shows 97% identity to mouse coronin 3, 65% identity to Hcoronin 1 and 73% identity to Hcoronin 2 and 58% identity to *M. musculus* coronin 6 (Fig.4). The alignment suggests that the unique region between the conserved WD40-repeats and COOH-terminal coiled coil part varies in length among them. Hcoronin 4 and 5 are more alike, as indicated by their 68% sequence identity. Their unique regions have low similarity to that of Hcoronin 1, 2, 3 and mouse coronin 6. The majority of the conserved amino acids are found in the first 391 amino acids of the molecules, whereas the C-terminal sequences are distinct.

1.3 Phylogenetic relationship of Hcoronin 3 to conventional mammalian coronins

The evolutionary tree of mammalian coronins was generated with the programs ClustalW and TreeView. This phylogenetic analysis suggests that Hcoronin 1, 2, 3 and *M. musculus* coronin 1, 2, 3, 6 are closely related to each other. They differ mainly in their unique region. In contrast, the sequences of Hcoronin 4 and 5 are

Hcoronin3	--MRRVVRQSKFRHVFGQAVKNDQCYYDIRVSRVTWDS	SFCVAVNPRFVAITIEASGGGAFLLVPLHKTGR	68
Mcoronin3	--MRRVVRQSKFRHVFGQAVKNDQCYYDIRVSRVTWDS	SFCVAVNPRFVAITIEASGGGAFLLVPLHKSGR	68
Hcoronin1	--MSRQVVRSSKFRHVFGQPAKADQCYEDVRSVQTWDS	SGFCVAVNPKFVALICEASGGGAFLLVPLGKTGR	69
Hcoronin2	MSFRKVVVRQSKFRHVFGQPVKNDQCYEDIRVSRVTWDS	STFCVAVNPKFLAVIVEASGGGAFLLVPLSKTGR	70
Mcoronin6	--MSRRVVRQSKFRHVFGQAAKADQAYEDIRVSKVTWDS	SAFCVAVNPKFLAVIVEAGGGGAFLLVPLAKTGR	69
Hcoronin4	MSWHPQYRSSKFRHVFGQKPAASKENCYDSSVPIITR	SVHNDHFCVAVNPHFI AVVT EASGGGAFLLVPLHQTGK	70
Hcoronin5	MSWHPQYRSSKFRNVYQKVANREHCFDGPITIKNVH	DNHFCVAVNTRFLAVT EASGGGSFLVIPLEQTGR	70
Hcoronin3	IDKSYPTVCGHTGTPVLDIDWC PHNDQVIASGSEDC	TMVMVQI PENGLT LSLTEPVVILEGH SKR VGI VAW	138
Mcoronin3	IDKSYPTVCGHTGTPVLDIDWC PHNDQVIASGSEDC	TMVMVQI PENGLT LSLTEPVVILEGH SKR VGI VAW	138
Hcoronin1	VDKNAPTVCGHTAPVLDIAWCPHNDNVIASGSEDC	TMVMVEIPDGGLMLPLREP VVITLEGH TKR VGI VAW	139
Hcoronin2	IDKAYPTVCGHTGTPVLDIDWC PHNDQVIASGSEDC	TMVMVQI PENGLT SPLTEPVVILEGH TKR VGI IAW	140
Mcoronin6	VDKNYPLVITGHTGTPVLDIDWC PHNDNVIASADDT	TMVMVQI PDYTPVRNIT E PVITLEGH SKR VGI LSW	139
Hcoronin4	LDPHYPKVCGHRGNVLDVKNPFDDEFIASCSEDA	TIKIWSIPKQLLTRNLTA YRKELVGHARRVGLVVEW	140
Hcoronin5	IEPNYKPCVCGHQGNVLDIKWNPFDNFIASCSEDT	SVRIWEIPEGGLKRNMTAALLEHGH SRVGLVVEW	140
Hcoronin3	HPTARNVLLSAGCDNAI I IWNVGTGEALIN---	LD-DMHSDMIYNVSWNRNGSLICTAS KD KKVRVIDPR	204
Mcoronin3	HPTARNVLLSAGCDNAI I IWNVGTGEALIN---	LD-DMHSDMIYNVSWNRNGSLICTAS KD KKVRVIDPR	204
Hcoronin1	HTTAQNVL L SAGCDNVI MVWDVGTGAAMLT---	LGPEVHPDTIYSVDWSRDGGLICTSGRDKRVR I I EPR	206
Hcoronin2	HPTARNVLLSAGCDNVLLIWNVGTAEELIYR---	LD-SLHPDLIYNVSWNHNGSLFC SAC KD KSVRI I DPR	206
Mcoronin6	HPTARNVLLSAGCDNVI I IWNVGTGEVLLS---	LD-DIHPDVIHSVCWN SNGSLATTC KD KTLRI I DPR	205
Hcoronin4	HPTAANILFSAGYDYKVM I WNLDTKESVI TSPMST	ISCHQDVI LMSMFNTNGSLLATTC KDRKI RVIDPR	210
Hcoronin5	HPTTNNILFSAGYDYKVL I WNLDTVGE-----	PVKMIDCHTDVILCMSFNTDGSLLTTC KD KKLRI I EPR	205
Hcoronin3	KQEI VAEKEKAHEGARPMRAIFLADGN-VFTTGF	SRMSERQLALWNPKNMQEPIALHEMDT SNGVLLPFY	273
Mcoronin3	KQEI VAEKEKAHEGARPMRAIFLADGN-VFTTGF	SRMSERQLALWNPKNMQEPIALHEMDT SNGVLLPFY	273
Hcoronin1	KGTVAEKDRPHEGTRPVRAVFVSEGN-ILTTGF	SRMSERQVALWDTKHL EEP LSLQELDTS SNGVLLPFY	275
Hcoronin2	RGTLVAERKAHEGARPMRAIFLADGK-VFTTGF	SRMSERQLALWDPENLEEP MALQELDSSNGALPFY	275
Mcoronin6	KSQVVAERARPHEGARPLRAVFTADGK-LLSTGF	SRMSERQLALWDPNFE E PVALQELMDT SNGVLLPFY	274
Hcoronin4	AGTVLQEEAS--YKGRASKVFLGNLKL MSTGT	SRWNNRQVALWQDNL SVPLMEEDLDGSSGVLFPFY	278
Hcoronin5	SCRVLQEEAN--CKNHRVNRVFLGNM KRLLTG	VSRWNTRQIALWQEDLSMPLIEE E I DGLSGLLFPFY	273
Hcoronin3	DPDTSIIYL CGKGDSSIRYFEITDES P YHYLNT	FSSKEPQRGMGYMPKRGLDVN KCEI ARFF KLHERK-	342
Mcoronin3	DPDTSIIYL CGKGDSSIRYFEITDES P YHYLNT	FSSKEPQRGMGYMPKRGLDVN KCEI ARFF KLHERK-	342
Hcoronin1	DPD T N I L V Y L C G K G D S S I R Y F E I T	S E A P F L H Y L S M F S S K E S Q R G M G Y M P K R G L E V N K C E I A R F Y K L H E R R -	344
Hcoronin2	DPD T S V V Y V C G K G D S S I R Y F E I T	E E P P Y I H F L N T F T S K E P Q R G M G S M P K R G L E V S K C E I A R F Y K L H E R K -	344
Mcoronin6	DPD S S I V Y L C G K G D S S I R Y F E I T	E E P P F V H Y L N T F S S K E P Q R G M G F M P K R G L D V S K C E I A R F Y K L H E R K -	343
Hcoronin4	D A D T S M L Y V V G K G D G N I R Y Y E V S A D	K P H L S Y L T E Y R S Y N P Q K G I G V M P K R G L D V S S C E I F R F Y K L I T T K S	348
Hcoronin5	D A D T H M L Y L A G K G D G N I R Y Y E T S T E	K P Y L S Y L M E F R S P A P Q K G L G V M P K H G L D V S A C E V F R F Y K L V T L K G	343
Hcoronin3	-CEPIIMTVPRKSDLFQDDL YPD TAGPEAL EAEWF	FECKNADPILISL K-----	391
Mcoronin3	-CEPIIMTVPRKSDLFQDDL YPD TAGPEAL EAEWF	FECKNADPILISL K-----	391
Hcoronin1	-CEPIAMTVPRKSDLFQEDLYPDTAGPD PALTAE	EWLGRDAGPLLISL K-----	393
Hcoronin2	-CEPIVMTVPRKSDLFQDDL YPD TAGPEAL EAEW	SGRDADPILISL R-----	393
Mcoronin6	-CEPIIMTVPRKSDLFQDDL YPD TPGPEPAL EAD	EWL SGQDAEPVLSL K-----	392
Hcoronin4	LIEPI SMIVPRRSSESYQEDI YPPTAGP S L T A Q	EWL SGMNRDPI LVSLR PGSELLRPHPLPAERPI FNS	398
Hcoronin5	LIEPI SMIVPRRSDSYQEDI YPMT PGTEPAL TPD	EWLGGI NRDPV LMSL K-----	393
Hcoronin3	-----HGYIPGKNRDLKVVKKNI---L-DSKPT	ANKKCDLISIPKKTDTASVQN--	437
Mcoronin3	-----HGYIPGKNRDLKVVKKNI---L-DSKPA	ANKKSEFSCAPKKTDTASVQN--	437
Hcoronin1	-----DGYVPPKSRRLRVNRG---LDTGRRRA	AP-----EASGTPSSDAVS--	431
Hcoronin2	-----EAYVPSKQRDLKISRRNV---LSDSRP	AMAPGSSHLGAPASTITAADATPSG	442
Mcoronin6	-----EGYVPPKHRRLRVTKRNI---L-DVRPP	AS-----PRRSQSA SEAPLS-	431
Hcoronin4	MAPASPRLLNQTEKLA AEDGWRSSSLLEEMPR	WAAEHL E EKKTWLTNGFDVFEC PPKTEN-ELLQM-	486
Hcoronin5	-----EGYKKS KMFVFKAP-----I KEK	KS VV VNGID LLENVPPRTEN-ELLRM-	436
Hcoronin3	-----EAKLDEILKEIKSIKDTICNQDERISK	LEQQMAKIAA-----	474
Mcoronin3	-----EAKLDEILKEIKSIKETICSQDERISK	LEQQ LAKMAA-----	474
Hcoronin1	-----RLEEEMRKIQATVQELQKRLDRLEET	VQAK-----	461
Hcoronin2	SLARAGEAGKLEEVMQELRALRALVKEQGDRI	CRL EEQLGRMENGDA--	489
Mcoronin6	-----QHTLETLL EETKALRDRVQAQ EERI	TAL ENMLCELVDGTD--	471
Hcoronin4	-----FYRQQEIRRLRELLTQRE VQAQLELEI	KNLRMGSEQL	525
Hcoronin5	-----FFRQQDEIRRLKEELAQKDIRIRQLQL	LELKNLRN SPKNC	475

Fig. 4. Alignment of mammalian coronin. The Genbank accession numbers are as follows: Hcoronin 1, P31146; Hcoronin 2, AAD32704; Hcoronin 3, BAA83077; Mcoronin 3, AAD32705; Hcoronin 4, Q92828; Hcoronin 5, BAA36341; Mcoronin 6, BAB64361. Identical amino acids are shown in orange and similar residues in yellow. The alignments were performed with the ClustalW and Bioedit programs. Note that the most divergent domain among the mammalian coronin family is their COOH-terminal unique region. The sequences from the NH₂-termini to the end of the WD-repeats show high homology throughout the mammalian coronin family.

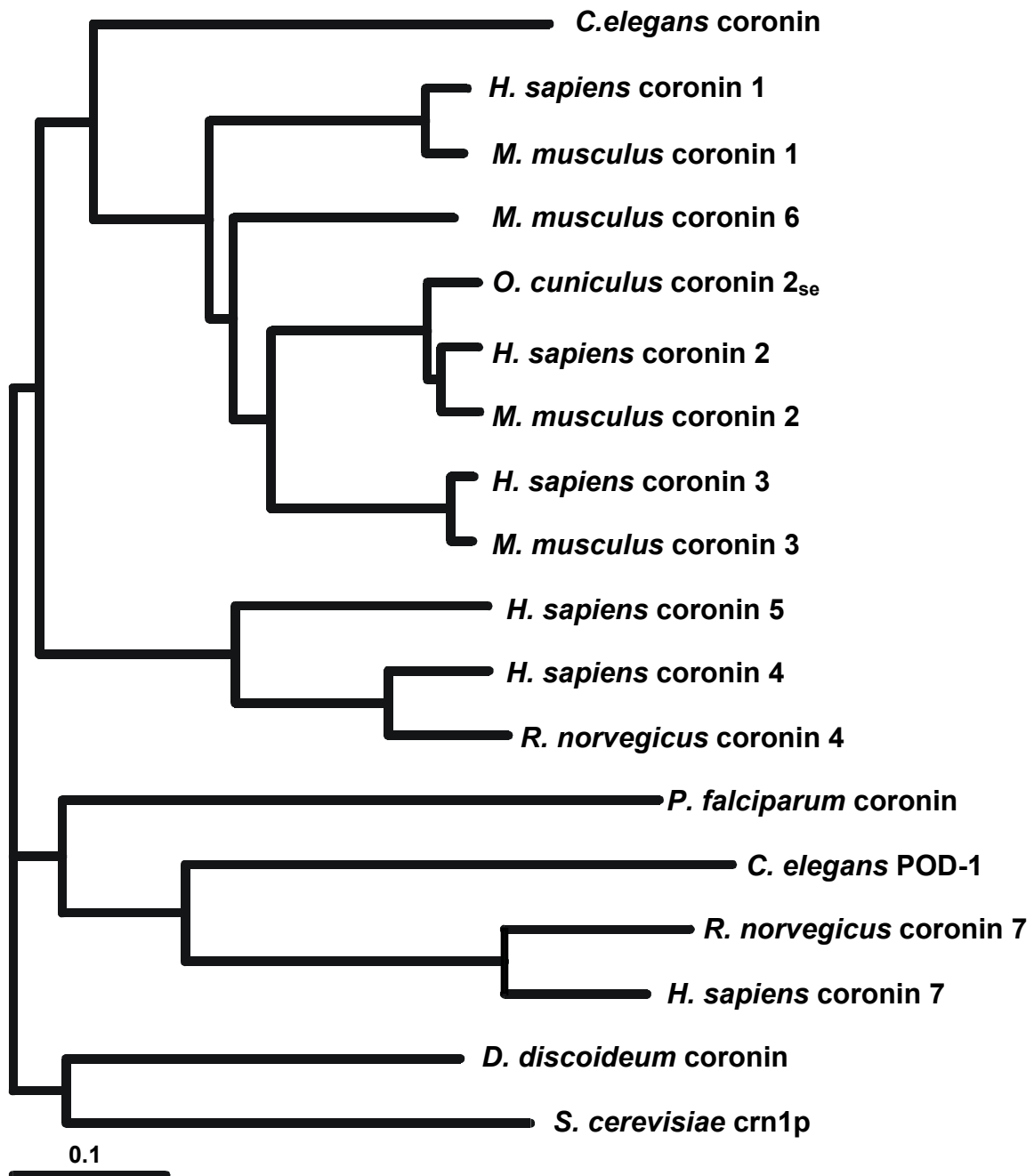


Fig. 5. Phylogenetic relationships of coronin-like proteins. *H. sapiens* coronin 1, 2, 3, *M. musculus* coronin 1, 2, 3, 6, *O. cuniculus* coronin 2_{se} are closely related to each other. *H. sapiens* coronin 4, 5 and *R. norvegicus* coronin 4 are similar to each other. *P. falciparum* coronin, *C. elegans* POD-1, *R. norvegicus* coronin 7 and *H. sapiens* coronin 7 show high similarity to each other and form a subgroup within the coronin family. Bar is 0.1 nucleotide substitutions per site.

more distantly related to this group, not only in the unique region, but also in the conserved parts (Fig. 5). It is evident from this evolutionary tree that there is a high degree of sequence conservation between mouse and human. It shows also that mammalian coronin has already evolved into divergent forms before the organisms underwent progressive evolution.

P. falciparum coronin, *C. elegans* POD-1, Rat coronin 7 and Human coronin 7 show high similarity to each other and form a subgroup in the coronin family that is distinguished from the rest of the family by its low homology and an unusual structure containing two WD40-domains in a tandem array (see introduction).

The accession number of the listed proteins is as follows:

protein	accession number
<i>H. sapiens</i> coronin 1	P31146
<i>M. musculus</i> coronin 1	AAD32703
<i>H. sapiens</i> coronin 2	NP_065174
<i>M. musculus</i> coronin 2	AAD32704
<i>O. cuniculus</i> coronin 2 _{se}	AAD23736
<i>H. sapiens</i> coronin 3	BAA83077
<i>M. musculus</i> coronin 3	AAD32705
<i>H. sapiens</i> coronin 4	Q92828
<i>H. sapiens</i> coronin 5	BAA36341
<i>M. musculus</i> coronin 5	BAC39865
<i>M. musculus</i> coronin 6	BAB64361
<i>H. sapiens</i> coronin 7	AK025674
<i>R. norvegicus</i> coronin 7	3123027
<i>D. discoideum</i> coronin	P27133
<i>S. cerevisiae</i> Crn1p	Q06440
<i>C.elegans</i> POD-1	AAD25089
<i>C.elegans</i> coronin	3878776
<i>P. falciparum</i> coronin	CAA05244

2. Subcellular localization of endogenous and EGFP-Hcoronin 3

In the previous tissue distribution studies, coronin 3 could be found in most organs of the mouse, like brain, lung, liver, kidney, spleen, ovary, thymus, muscle and heart (Spoerl et al., 2002, A. Hasse and M. Stumpf, personal communication). In brain, the protein, however, is expressed more abundantly than in other organs. Recent studies showed that the expression level of coronin 1 and the 20 kDa subunit of the actin related protein complex 2/3 is significantly reduced in the fetal Down's syndrome (DS) brain (Weitzdoerfer. et al., 2002). This could suggest a functional role of these actin-interacting proteins in neurogenesis. However, coronin 1 is not suggested to be

the major coronin in neuronal tissue. Rather, coronins 4 and 5 are highly expressed in brain, as is coronin 3. Thus, the possible functional involvement of coronin 3 in the rearrangement of actin filaments during the differentiation of neuronal cells was a major focus in the characterization of this protein. To study the influence of different truncated Hcoronin 3 proteins on differentiation, the neuroblastoma cell line Neuro-2a was chosen. These murine cells can be efficiently transfected by different methods and can be induced to form axon-like neurites by different methods (Olmsted et al., 1970).

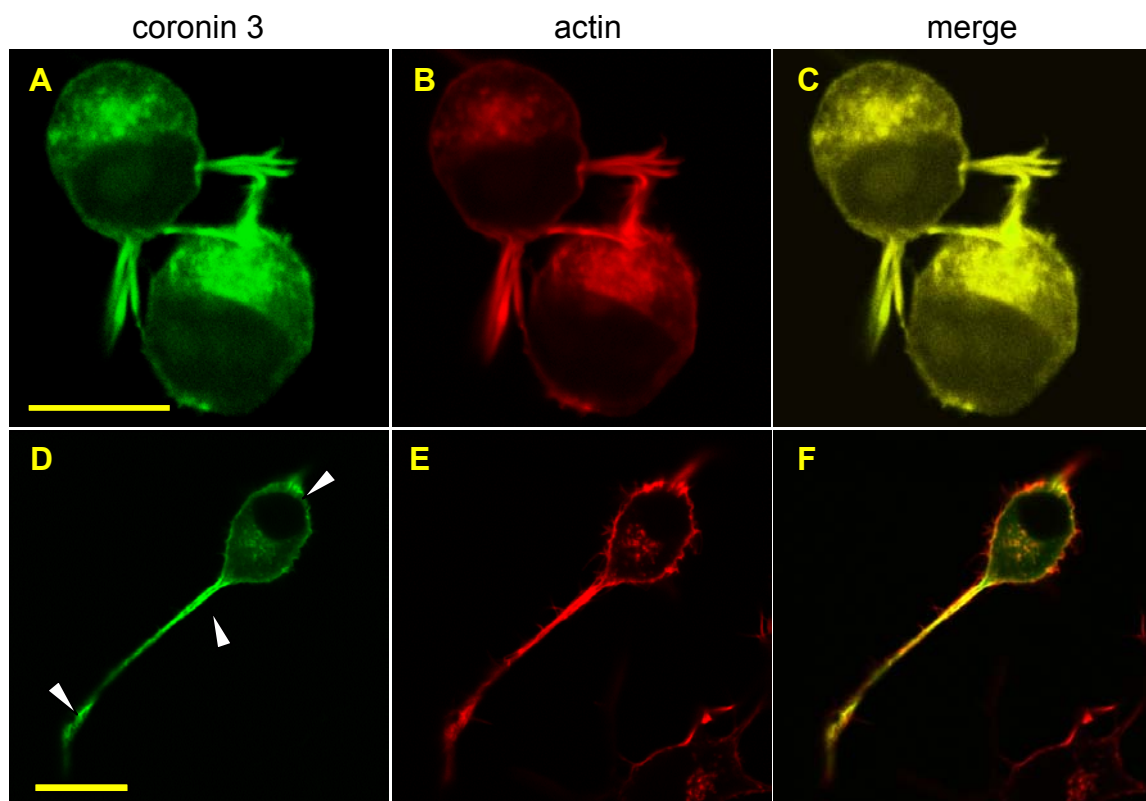


Fig. 6. Localization of endogenous coronin 3 in undifferentiated (A) and differentiated (D) Neuro-2a cells. A-C, Neuro-2a undifferentiated and 3-day-differentiated cells were fixed in 4 % paraformaldehyde in PBS and permeabilized with 0.5 % Triton at room temperature. Afterwards, the cells were incubated with primary antibody K6-444 and secondary goat anti-mouse-IgG, Alexa 488 conjugated. F-actin was labeled by 0.1 mg/ml TRITC-phalloidin (Sigma). Bars, 10 μ m.

2.1 Localization of endogenous coronin 3 in undifferentiated and differentiated Neuro-2a cells

Subcellular localization of endogenous coronin 3 in undifferentiated and differentiated Neuro-2a cells was detected by immunostaining with mouse monoclonal anti-coronin 3 antibody K6-444. F-actin was visualized with TRITC-phalloidin. In paraformaldehyde-fixed, undifferentiated cells (Fig. 6A), coronin 3 was found not only

in F-actin-rich protrusions but also in the cytosol (arrowheads) and colocalized with F-actin. In these differentiated Neuro-2a cells (Fig. 6D), coronin 3 antibodies labeled prominently sites of neurite projection (arrowheads). Coronin 3 was also strongly accumulated underneath the plasma membrane (right upper arrow). Staining could also be detected in the cytoplasm and was most prominent in punctate structures in the perinuclear area but not in the nucleus. F-actin labeled with TRITC-phalloidin was also found in these structures. The overlay of both images indicated that endogenous coronin 3 was colocalizing with actin filaments. The distribution of F-actin appeared to be more restricted to the cell cortex and surface extensions than that of coronin 3. However, not all of the coronin 3 immunoreactivity was found at F-actin rich regions, a considerable portion was also cytosolic.

2.2 Domain requirements for the colocalization of EGFP-Hcoronin 3 with neurite extensions

To identify the domain requirements for the colocalization of EGFP-Hcoronin 3 with actin filaments, different truncated variants were transfected into Neuro-2a cells (Fig. 7). The subcellular distribution of these EGFP fusion proteins was analyzed by fluorescence microscopy as described above. For this, the day before transfection, Neuro-2a cells were seeded on autoclaved glass coverslips in 24 well tissue culture plates. After overnight incubation for attachment, cells were transfected with pEGFPC1-Hcoronin 3 and different truncated constructs by using Lipotransfection kits. After 24 h, the transfected cells were induced to differentiation by reducing the serum concentration in DMEM medium from 10% to 0.2%. This treatment lasted 2-3 days. The cells were then fixed with paraformaldehyde in PBS and permeabilized with 0.5% Triton X-100. F-actin was labeled by TRITC-phalloidin. As a negative control, cells were also transfected with the pEGFPC1 vector. The EGFP protein was distributed throughout the cell including the nucleus. The morphology of the transfected cells showed no significant difference to that of untransfected Neuro-2a cells (Fig. 8).

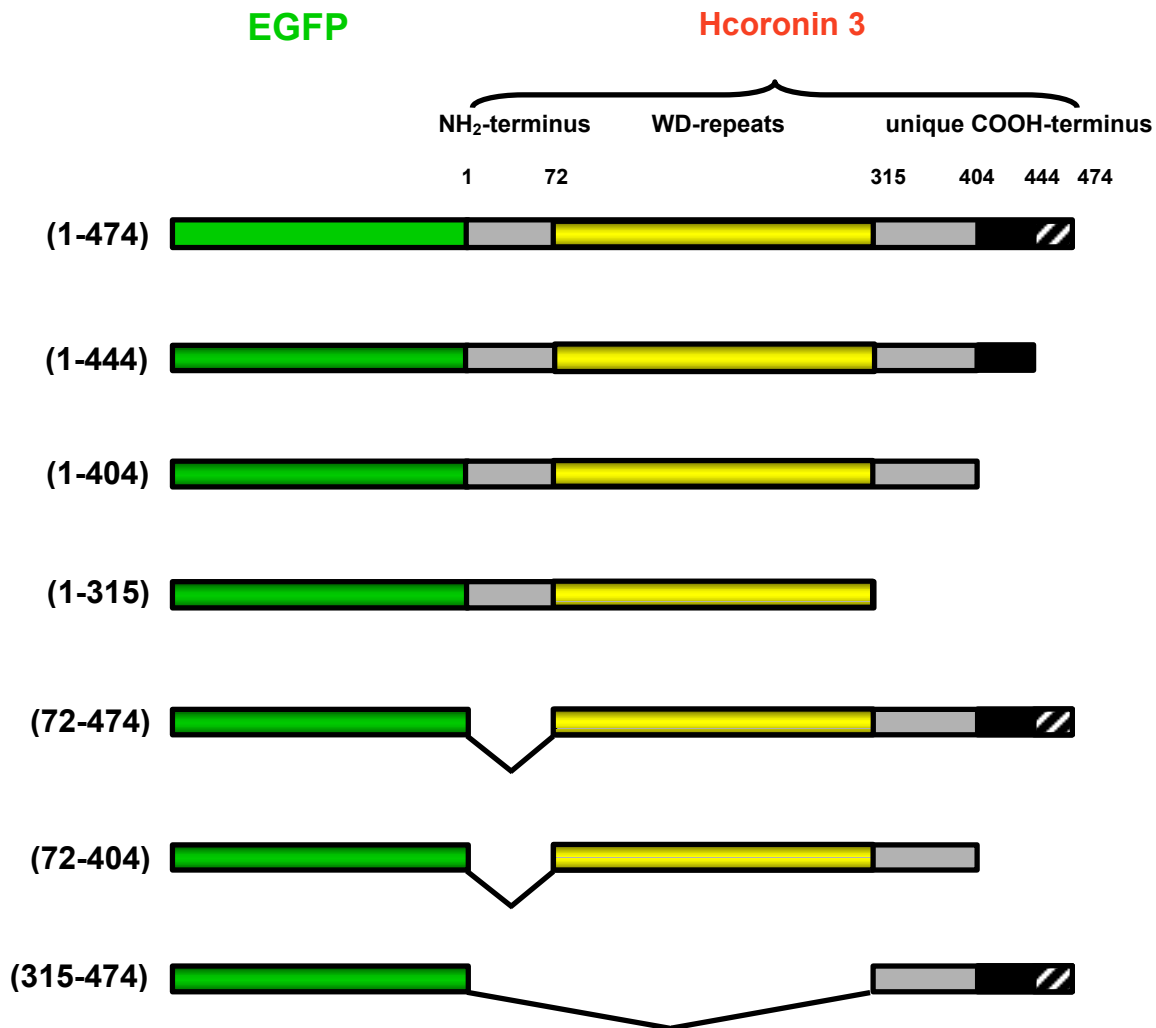


Fig. 7. Schematic view of EGFP-Hcoronin3 and different truncated constructs. The EGFP part is indicated by green boxes. Hcoronin 3 amino acid residues fused to EGFP are indicated by numbers. The yellow boxes represent the WD40-repeats. Hatched boxes indicated the coiled coil domain. The constructs were used for transfection of the Neuro-2a cell line to determine the domain requirement for neurite localization *in vivo*. The same constructs were also expressed stably in HEK 293 cells for the analysis of soluble complexes (see section 5.3).

A similar subcellular distribution to endogenous coronin 3 could also be observed for EGFP-Hcoronin 3. This protein was found prominently in the growth cone, which was highly enriched in F-actin (arrowhead in Fig. 8D). However, the amount of cytosolic protein was much higher for the EGFP fusion than for the endogenous protein. Furthermore, under the same differentiation conditions, the length of the neurites in cells expressing EGFP-Hcoronin 3 was slightly higher than that of untransfected cells. Also EGFP-Hcoronin 3 was not localized in the nucleus.

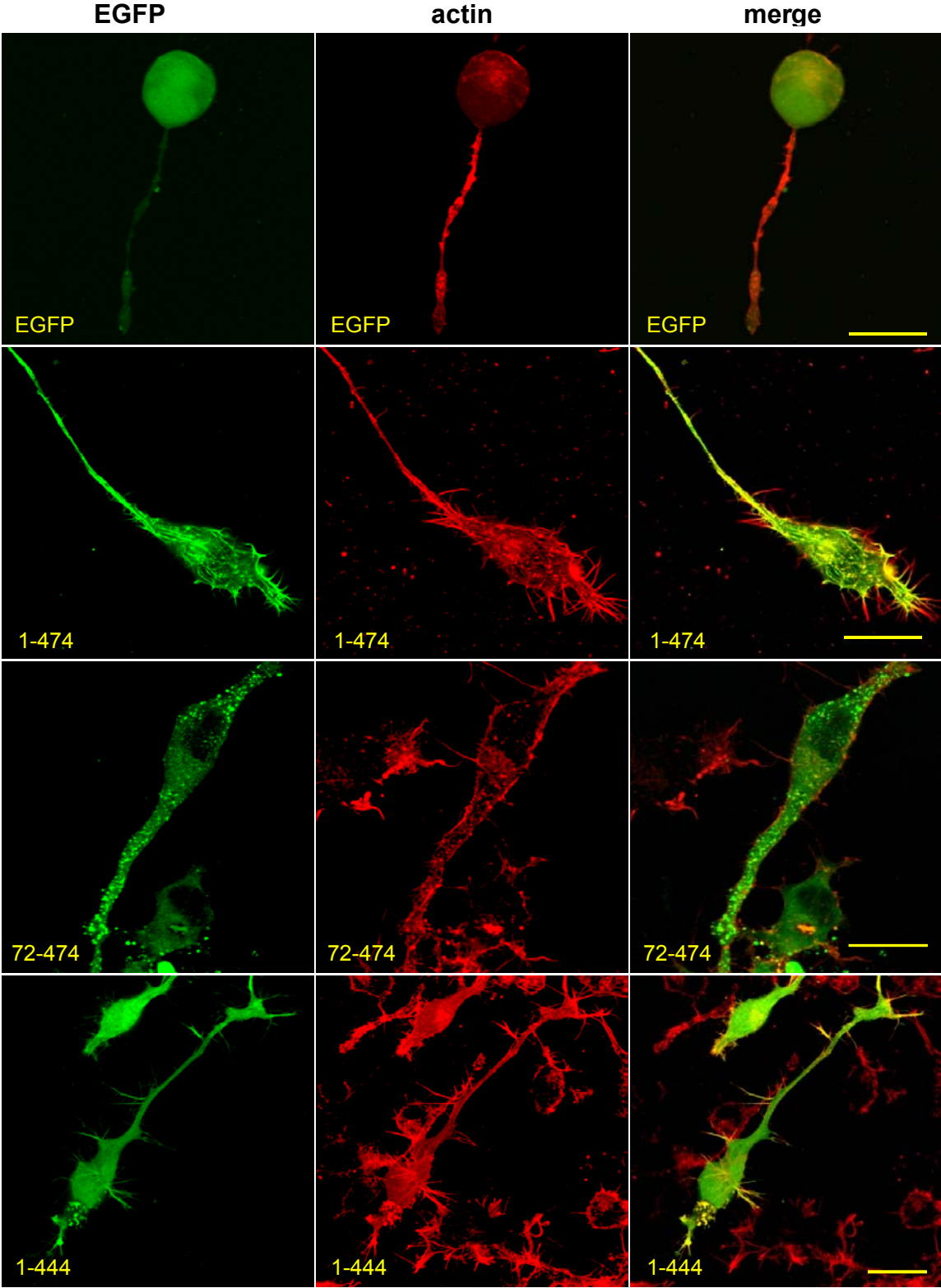


Fig. 8. Localization of full length and truncated EGFP-Hcoronin 3 in differentiated neuro-2a cells. Cells expressing the EGFP-fused regions of Hcoronin 3 containing the amino acids indicated were fixed in 3 % paraformaldehyde, permeabilized with 0.5 % Triton X-100, and F-actin was stained with TRITC-phalloidin. Bars, 10 μ m.

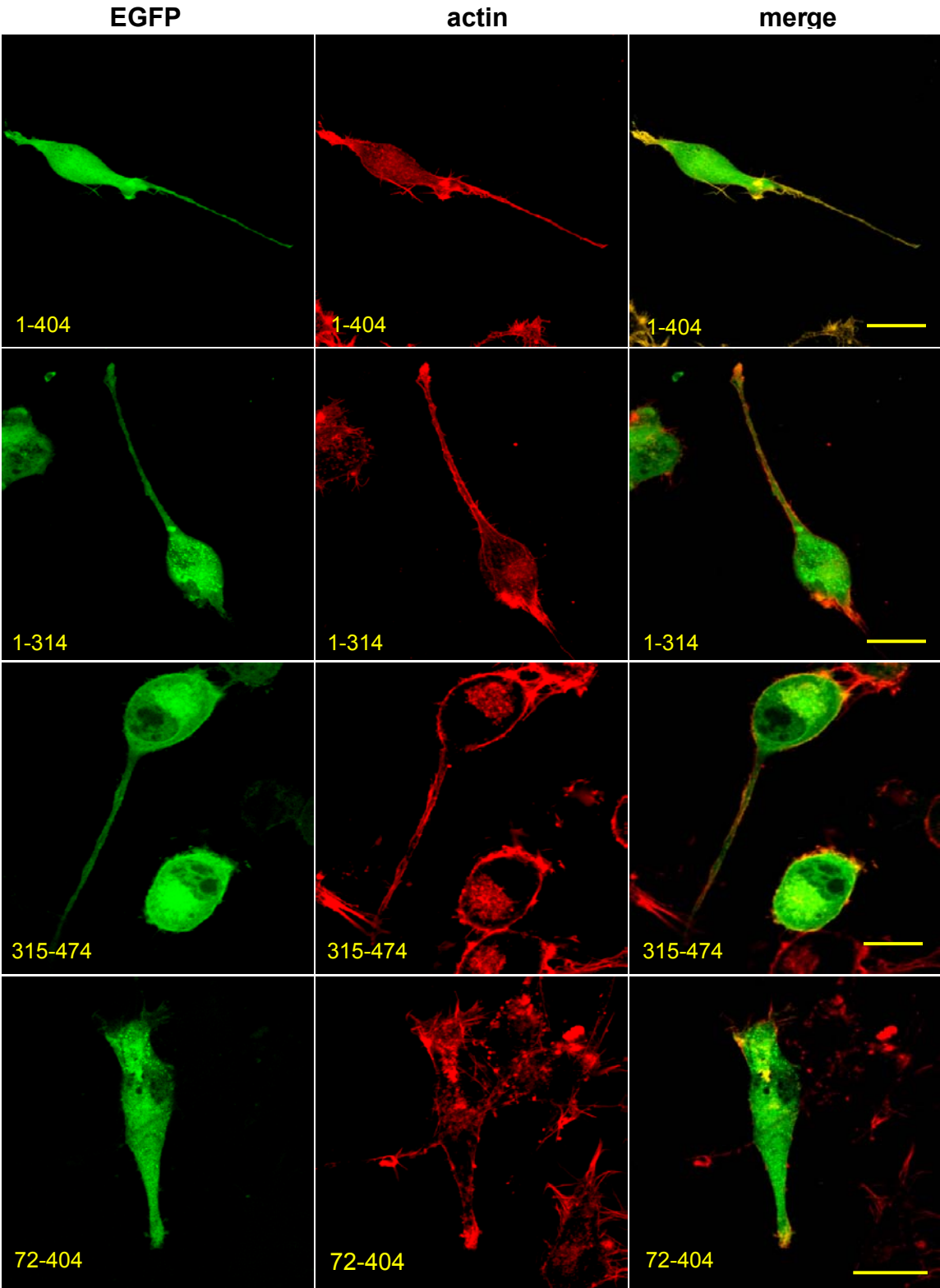


Fig. 9. Localization of full length and truncated EGFP-Hcoronin 3 in differentiated neuro-2a cells. Cells expressing the EGFP-fused regions of Hcoronin 3 containing the amino acids indicated were fixed in 3 % paraformaldehyde, permeabilized with 0.5 % Triton X-100, and F-actin was stained with TRITC-phalloidin. Bars, 10 μ m.

Overexpression of full length Hcoronin 3 resulted in the formation of many more filopodia or actin spikes as compared to untransfected cells. Not all actin filaments colocalized with EGFP-Hcoronin 3. In contrast to the full length EGFP fusion, the protein lacking the NH₂-terminus, EGFP-Hcoronin 3 (72-474) was diffusely distributed in the cytoplasm and showed primarily a punctate pattern which was neither enriched at sites of neurite extension nor at F-actin-rich sites underneath the membrane. These cells showed a “swollen” morphology, especially in the neurite projection areas as compared with the cells expressing full length EGFP-Hcoronin 3, indicating impaired actin organization. EGFP-Hcoronin 3 (1-444) lacking the C-terminal 30 amino acids showed partial colocalization with F-actin at the tip of growth cones and filopodia (Fig. 8), but the colocalization with actin filaments was less pronounced than with the full-length fusion. Rather, EGFP-Hcoronin 3 (1-444) displayed an increased cytoplasmic staining as compared with the wild type protein. Similar to EGFP-Hcoronin 3 (1-474), expression of EGFP-Hcoronin 3 (1-444) caused enhanced formation of filopodia at the peripheral regions of the cell. The distribution of EGFP-Hcoronin 3 (1-404) was only slightly different from that of EGFP-Hcoronin 3 (1-444). Only minor amounts of protein (1-404) were found at F-actin-rich sites, the vast majority was diffusely localized throughout the cytoplasm (Fig. 9). Moreover, this construct did not cause obvious changes in the F-actin structure of the cells. The shortest C-terminally truncated protein used here, EGFP-Hcoronin 3 (1-314), completely failed to colocalize with F-actin, since this fusion protein could not be observed at the site of neurite protrusions and was exclusively cytoplasmic in these cells (Fig. 9). Different from these observations, EGFP-Hcoronin 3 (315-474) carrying the sequences lacking in EGFP-Hcoronin 3 (1-314), retained a moderate F-actin colocalization, although this was much weaker than for full length EGFP-Hcoronin 3. Most interestingly, overexpression of EGFP-Hcoronin 3 (72-404) lacking the complete NH₂- and COOH-terminus resulted in a significant change of cell morphology (Fig. 9). This EGFP-tagged protein was localized throughout the cytoplasm including the nucleus. No colocalization with F-actin in neurites could be found in these cells. They did not attach to the culture dish properly, suggesting that the ability to adhere was impaired. Furthermore, neurite development in cells with this construct was weaker in comparison with untransfected cells and cells transfected with full length EGFP-Hcoronin 3.

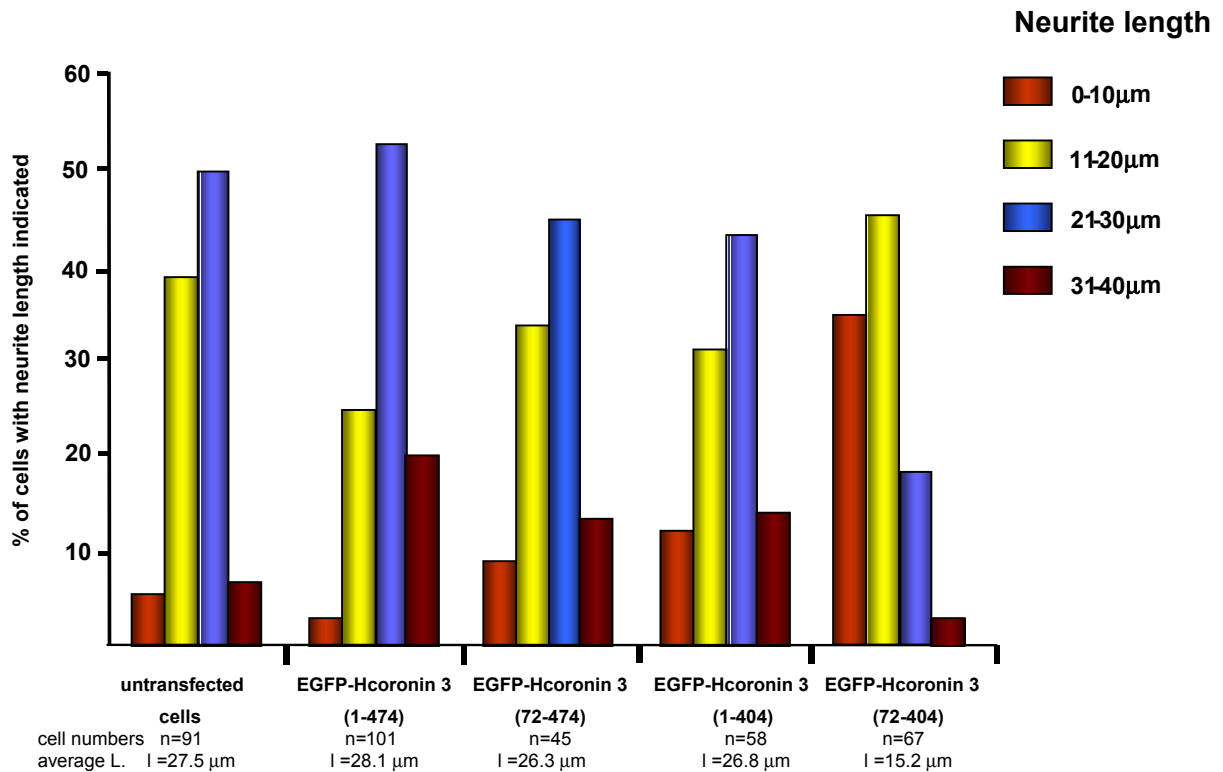


Fig. 10. Quantitation of the effect of expression of different EGFP-Hcoronin 3 proteins on neurite outgrowth in Neuro-2a cells. Cells were transfected with the constructs indicated and subjected to differentiation in low serum medium for 3 days. Cells were then fixed in 3 % paraformaldehyde. The actin structure was visualized with TRITC-phalloidin. Neurite length was determined by imaging cells with Leica confocal laser scanning microscopy (TCS SP) and TCSNT software. At least 45 cells for each group were chosen randomly from at least 4 different fields of each coverslip, and from 5 to 10 coverslips.

3. Effect of the expression of different EGFP-Hcoronin 3 versions on neurite outgrowth in Neuro-2a cells

Transfection experiments with EGFP-Hcoronin 3 (72-404) indicated that this protein might lead to abnormal neurite outgrowth in Neuro-2a cells. This phenomenon was not observed in cells transfected with other truncated constructs. Conversely, expression of EGFP-Hcoronin 3 appeared to enhance neurite extension, where cells started forming longer axon-like processes and filopodia. To test whether these opposite effects were representative and reproducible, neurite length was determined for differentiated untransfected Neuro-2a cells and cells transiently expressing EGFP-Hcoronin 3 (1-474), EGFP-Hcoronin 3 (72-404), EGFP-Hcoronin 3 (72-474) or EGFP-Hcoronin 3 (1-404). Transfection and differentiation were performed in parallel under the same experimental conditions. Similar amounts of cells were grown on the coverslips and transfected with the corresponding EGFP-Hcoronin 3 variants, and

after 24 h, cells were treated with low serum medium to induce neurite outgrowth. For evaluation, cells were chosen randomly from at least 4 different fields of each coverslip and from 5 to 10 coverslips. Images were acquired by confocal laser microscopy and (TCS SP) and TCSNT software, and neurite length was determined for at least 45 cells from each group.

The statistic results are presented in Figure 10. There were striking differences in the distribution of neurite length between untransfected cells and cells expressing EGFP-Hcoronin 3 (1-474) on one hand and EGFP-Hcoronin 3 (72-404) on the other. The other two constructs, EGFP-Hcoronin 3 (72-474) and EGFP-Hcoronin 3 (1-404), did not show dramatic differences to untransfected cells. The average neurite lengths were 28.1 μm for EGFP-Hcoronin 3 (1-474), 26.3 μm for EGFP-Hcoronin 3 (72-474), 26.8 μm for EGFP-Hcoronin 3 (1-404), and 15.2 μm for EGFP-Hcoronin 3 (72-404).

The differences between the groups were most obvious when the percentage of cells exhibiting neurites longer than 20 μm was compared. Of a total of 91 untransfected Neuro-2a cells, approximately 50% had neurites with a length between 21-30 μm and 7 % exhibited a neurite longer than 30 μm . EGFP-Hcoronin 3 full length protein slightly increased the length of neurites. Most of these cells (52 %) formed a neurite between 20 and 30 μm , but 19% generated a 31-40 μm long neurite. In the most interesting group, the cells transfected with EGFP-Hcoronin 3 (72-404), only 18 % showed neurites between 20 and 30 μm in length and only 3 % of the neurites were longer than 30 μm . The number of cells carrying a 0-10 μm neurite in this group was dramatically increased to 34%, as compared to 5 % in the untransfected cells and 3 % in the cells expressing full length EGFP-Hcoronin 3. These observations strongly suggested that expression of EGFP-Hcoronin 3 (72-404) had a strong inhibitory effect on neurite outgrowth in this cell system. The lack of this phenotype in the cells which were transfected with either EGFP-Hcoronin 3 polypeptide 72-474 or 1-404 excluded the possibility that the shorter neurites were due to toxic effects of the transfection reagent or to manipulation during transfection.

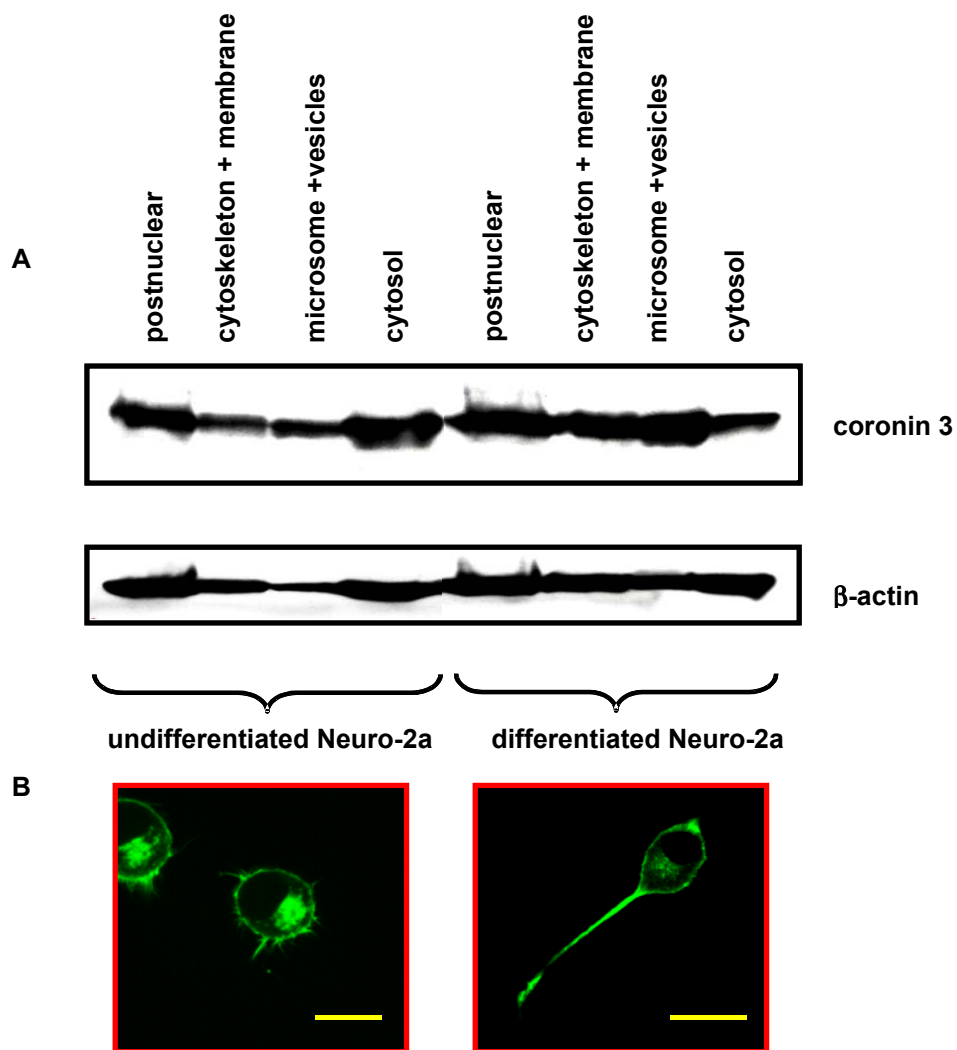


Fig. 11. Translocation of coronin 3 from the cytosol to a particulate fraction during differentiation of Neuro-2a cells. **A.** Endogenous coronin 3 in different subcellular fractions of undifferentiated and differentiated Neuro-2a cells was analyzed in a Western blot with monoclonal anti-coronin 3 antibody K6-444. β -actin was assayed to observe whether its distribution also changed during differentiation. Postnuclear cell extract, 2,000 \times g supernatant; cytoskeleton and membranes, 10,000 \times g pellet; microsomes and vesicles, 100,000 \times g pellet; cytosol, 100,000 \times g supernatant. **B.** Distribution of endogenous coronin 3 in undifferentiated and differentiated Neuro-2a cells. Cells were fixed with paraformaldehyde and stained with mAb K6-444 and polyclonal goat anti-mouse IgG conjugated with Alexa 488.

4. Subcellular distribution of coronin 3 in undifferentiated and differentiated Neuro-2a cells

When the distribution of endogenous coronin 3 in undifferentiated and differentiated cells was compared, immunofluorescence studies indicated that the protein was presented not only in actin-rich neurite protruding regions but also in the perinuclear cytoplasm. The latter staining was more pronounced in undifferentiated cells, whereas the former was stronger in differentiated cells (Fig. 11B). This significant

difference of the subcellular distribution raised the question whether coronin 3 is translocated during morphogenetic processes like neurite outgrowth. In order to answer this question, the amount of endogenous coronin 3 in different cell compartments of undifferentiated and differentiated cells was analyzed by Western blotting. β -actin was also assayed in these fractions in order to test whether its distribution was changed during differentiation.

The Western blot showed that endogenous coronin 3 was indeed predominantly found in the cytoplasmic fraction of undifferentiated cells (Fig. 11A). The amount of coronin 3 in the membrane/cytoskeletal and microsomal fractions was approximately one third of that in the cytoplasm, whereas in differentiated cells, coronin 3 accumulated mainly in the particulate fractions. The amount of cytosolic coronin 3 was obviously decreasing during neurite formation. Interestingly, the content of coronin 3 in vesicle and microsome fraction was even higher than that in the cytoskeleton fraction. The distribution of actin in the different fractions was more or less comparable in differentiated and undifferentiated cells. This was also supported by the immunofluorescence data (Fig. 11B). The increase of the coronin 3 amount in the 10,000xg pellet and its decrease in the cytosol of differentiated cells strongly support that translocation from a cytosolic pool of coronin 3 to cytoskeletal and microsomal compartments takes place during Neuro-2a cell differentiation. However, these experiments did not answer the question how this shift is induced *in vivo*.

5. Analysis of the cellular distribution by isopycnic sucrose step gradient centrifugation

Fluorescence microscopy showed that full length EGFP-coronin 3 was found not only in F-actin-rich neurites and in the cell periphery underneath the membrane but also in the cytosol, whereas EGFP-Hcoronin 3 (72-404) lacking NH₂- and COOH-termini was distributed in the cytosol. Impaired localization might explain the effect of EGFP-Hcoronin 3 (72-404) on neurite outgrowth. To confirm this subcellular distribution of EGFP-Hcoronin 3 *in vivo*, isopycnic sucrose step gradient centrifugation of total cell extracts from HEK 293 cells stably transfected with EGFP-Hcoronin 3 (1-474) and EGFP-Hcoronin 3 (72-404) lacking both NH₂- and COOH-terminus was performed to determine the subcellular distribution of Hcoronin 3.

It is difficult to establish stably transfected Neuro-2a cells expressing EGFP-Hcoronin 3. The transiently transfected cells are not suitable for the experiments,

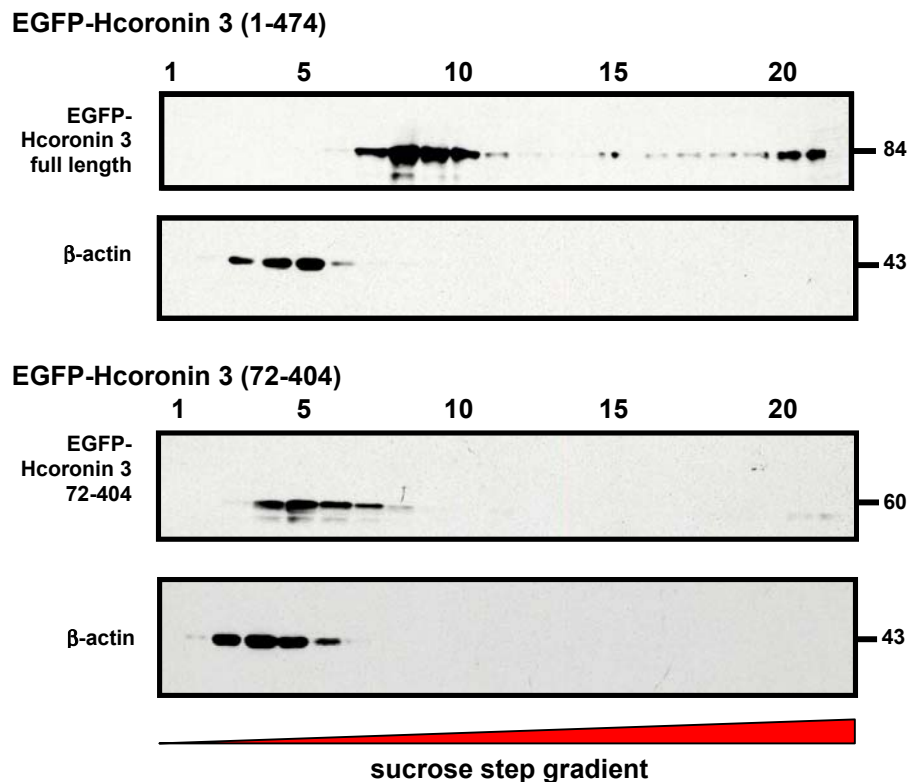


Fig. 12. Isopycnic centrifugation of total cell extracts from HEK 293 cell lines stably transfected with EGFP-Hcoronin 3 (1-474) and EGFP-Hcoronin 3 (72-404). Total cell lysates in HES buffer were loaded on the top of gradients containing 1 ml steps of 5, 10, 15, 20, 25, 30, 35, 40, 45, 50, and 85% sucrose. Centrifugation was done in a swing-out rotor for 20 h at 100,000 \times g. 0.5 ml fractions were collected from the top of the gradients and subjected to Western blotting with mAb K6-444 or monoclonal anti- β actin antibodies.

since transiently transfected cells contained also untransfected cells. After total homogenates were separated, EGFP-Hcoronin 3 (1-474) was found in two distinct peaks (Fig. 12). The main peak in the fractions 7 to 10 is likely to represent the cytosolic protein, as judged by the distribution of G-actin at the similar low density. The second peak was found in fractions 20-22, at relatively high density. In experiments not shown here, this fraction was shown to contain the plasma membrane marker protein E-cadherin (Spoerl et al., 2002). The high-density peak was not observed in cells stably expressing EGFP-Hcoronin 3 (72-404) which contains only the 5 WD40-repeats (Fig. 12). The fact that EGFP-Hcoronin 3 (72-404) appeared only in the fractions 4 to 7 support the data obtained by laser scanning microscopy that showed EGFP fluorescence of this truncated protein exclusively in the cytosol and no colocalization with F-actin or the plasma membrane. Another

outcome of this experiment is, that the two EGFP fusion proteins were found in different cytosolic fractions, although the difference of the theoretical molecular weight between these two EGFP fusion proteins is only 24 kDa. Migration of EGFP-Hcoronin 3 (72-404) exhibited a substantial shift to low density fractions compared to that of full length EGFP-Hcoronin 3. Gel filtration experiments indicate that cytosolic EGFP-coronin 3 is present in a large complex with an apparent molecular weight of 250-200 kDa. It seems likely that the large complex formed by full-length-EGFP-Hcoronin 3 migrated to high densities during centrifugation.

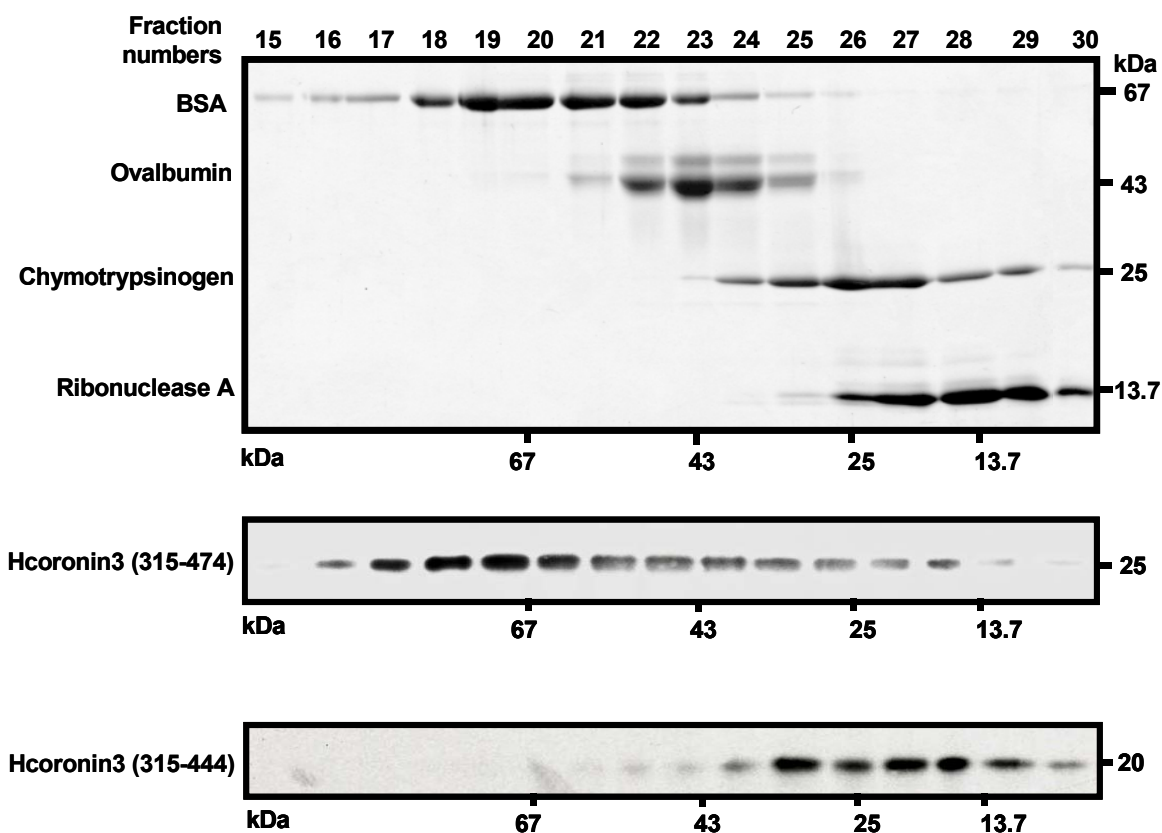


Fig. 13. Gel filtration analysis of recombinant Hcoronin 3 residues 315-474 and 315-444. 50 μ l of the purified Hcoronin 3 fragments 315-474 and 315-444 (0.1 μ g/ μ l) were subjected to superdex 200 gel filtration. Fractions (50 μ l) were collected and analysed by SDS-PAGE and Western Blot with mAb K6-444. The elution profile of the gel filtration column was calibrated using a set of marker proteins (Amersham Biosciences): BSA (67 kDa); ovalbumin (43 kDa); chymotrypsinogen (25 kDa); ribonuclease A (13.7 kDa) under the same conditions. Fractions were collected, analyzed by SDS-PAGE and gels were stained with Coomassie blue.

6 Gel filtration analysis of Hcoronin 3

6.1 Oligomerization of the recombinant Hcoronin 3 COOH-terminus *in vitro*

Gel filtration analysis is a method used for the analysis of the apparent size of proteins or protein complexes under native conditions. In contrast to native PAGE,

this approach is suitable for the analysis of relatively large macromolecules and oligomeric complexes, depending on the exclusion size of the gel matrix used. For purified recombinant proteins, gel filtration provides evidence about the formation of di-, tri-, or oligomers if the elution of the protein of interest is compared to that of marker molecules of known molecular mass.

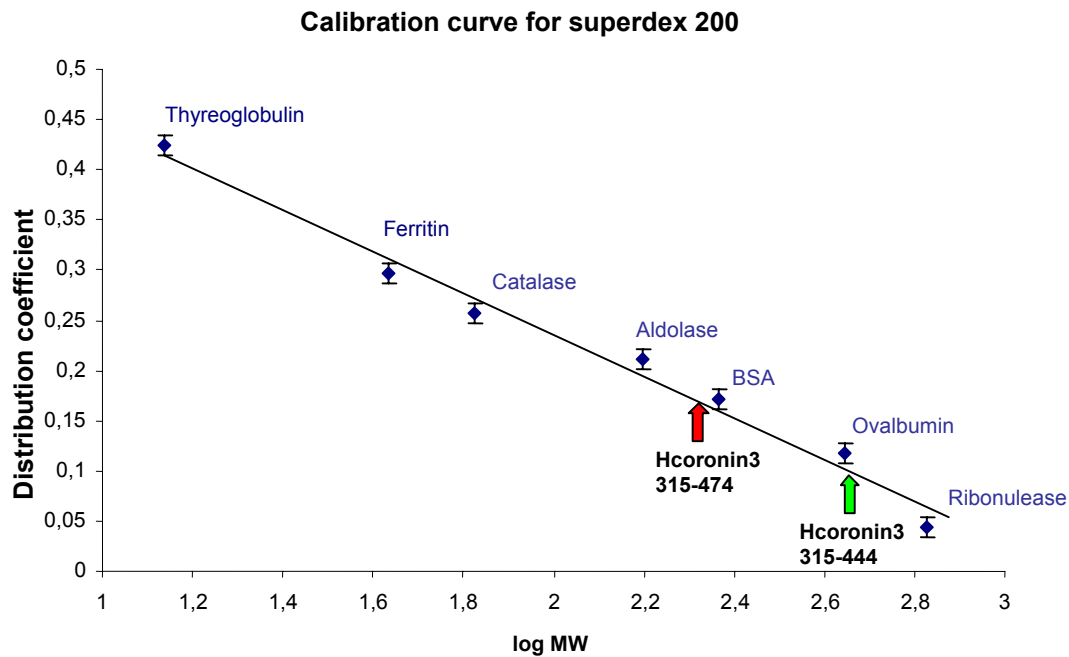


Fig. 14. Plot of the distribution coefficient K_{av} versus log MW in gel filtration. V_e : protein elution volume; V_0 : matrix column; V_x : total volume. 50 μ l of the purified Hcoronin 3 (315-474) and (315-444) with a concentration of 0.1 μ g protein/ μ l were loaded onto a superdex 200-gel filtration column. Fractions (50 μ l) were collected. 50 μ l of molecular protein marker mixture were used to set up a calibration curve. The elution volume of dextran 200 represents the matrix volume and the elution volume of KCl, as determined by measurement of electric conductivity, corresponds to the total volume of the column.

Asano and Nishida (2001) reported that *Xenopus* coronin forms dimers and that its COOH-terminal coiled coil domain is responsible for dimerization. Sequence analysis predicts that the C-terminal 30 amino acids of Hcoronin 3 fold into a coiled coil structure that is likely to form a trimer instead of dimer in *Xenopus* coronin (0.61 trimer versus 0.15 dimer). In order to analyze the role of the coiled coil domain in the multimerization of Hcoronin 3, the recombinant COOH-terminal fragments 315-474 and 315-444 were used for gel filtration analysis.

Fig.13 shows a typical elution profile obtained for recombinant Hcoronin 3 residues 315-474 and 315-444. Compared with the elution profile of the standard molecular weight marker on the superdex 200 gel filtration column, the majority of fragment

315-474 migrated with an apparent molecular mass of 85-60 kDa while most of the polypeptide 315-444 eluted with an apparent mass of 40-20 kDa. The distribution coefficient of the fragment 315-474 was examined to exclude the influence of buffer and FPLC-system on the elution profile of the proteins. The distribution coefficient of Hcoronin 3 (315-474) was 2.32, which corresponds to 78 kDa from the plot of the distribution coefficient against log MW, whereas Hcoronin 3 (315-444) exhibits a distribution coefficient of 2.67 which represents a molecular mass of 35 kDa (Fig.14). The calculated molecular weight of Hcoronin 3 (315-474) is 20.2 kDa and that of Hcoronin 3 (315-444) is 16.8 kDa. The results indicate that the polypeptide (315-474) formed a complex by self-association with an apparent molecular mass of more than 60 kDa, most likely representing tri- or tetramers rather than dimers, whereas the polypeptide (315-444) migrated with an apparent mass less than 40 kDa, suggesting a dimer. These results indicate that the recombinant COOH-terminal fragment 315-474 oligomerizes *in vitro*. Since the elution profile of the COOH-terminus lacking the coiled coil domain showed a significant difference from that of the complete COOH-terminus, the last 30 amino acids (coiled coil domain) seem to be responsible for this effect.

6.2 Oligomerization of Hcoronin 3 *in vivo*

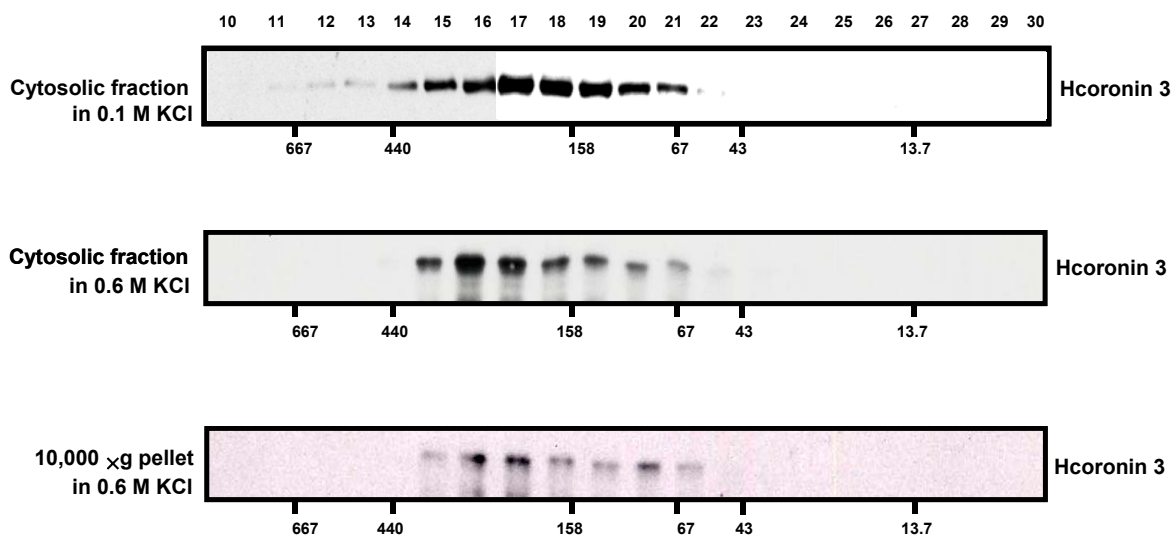


Fig. 15. Oligomerization of cytosolic and particle-associated Hcoronin 3 in HEK 293 cells. 10,000xg cytoskeletal/membrane pellets and 100,000xg cytosolic supernatant of HEK 293 cells were incubated in HES buffer with 0.1 M KCl or 0.6 M KCl, respectively, for 1 h. After centrifugation at 100,000xg for 30 min, the supernatants were fractionated on a superdex 200 gel filtration column equilibrated with HES buffer containing 0.6 M KCl. Fractions were subjected to 10% SDS-PAGE. Hcoronin 3 was detected with mouse anti-Hcoronin3 antibody K6-444 by Western blots. The elution of the molecular weight marker is indicated at the bottom of each blot. The fraction numbers are indicated above.

The fact that recombinant COOH-terminal fragment 315-474 oligomerized *in vitro* raised the question whether coronin 3 forms oligomers also *in vivo*. Therefore, the oligomerization state of endogenous Hcoronin 3 was tested in extracts of HEK 293 cells that express high levels of this protein (Spoerl et al., 2002). Previous experiments have shown that full-length EGFP-Hcoronin 3 is located not only in the actin-rich cell cortex but also in the cytoplasm *in vivo*, and cortical localization was impaired for EGFP-Hcoronin 3 lacking the coiled-coil (Spoerl et al., 2002, and immunofluorescence data in this work, see section 2.2). Thus, oligomerization might be involved in the regulation of subcellular localization and it was interesting to analyze the oligomerization state of Hcoronin 3 in different subcellular fractions. The knowledge about the state of Hcoronin 3 in different cell compartments could help to understanding the function of Hcoronin 3 *in vivo*. For this, Hcoronin 3 from cytosolic and particulate compartments was first separated from lysates of about 2×10^7 HEK 293 cells by differential centrifugation. 10,000×g, cytoskeletal pellets and 100,000×g cytosolic supernatants in HES buffer were prepared. The concentration of KCl in HES buffer was adjusted to 0.6 M. These highly ionotropic conditions were used to minimize interactions with other proteins and have been used successfully to solubilize other actin-binding protein oligomers from cytoskeletal preparations (Berryman et al., 1995). For comparison, the cytosolic fraction was treated with low KCl concentrations (0.1 M). After centrifugation at 100,000×g, 50 µl of each fraction was loaded on a gel filtration column. The fractions were analyzed by SDS-PAGE and probed on Western blots with anti-coronin 3 monoclonal antibodies. The results showed that under high ionotropic conditions, the majority of endogenous Hcoronin 3 both from cytosolic and particulate compartments migrated with an apparent molecular mass of 200-150 kDa (Fig. 15), much higher than its molecular weight (57 kDa). Thus, the oligomerization state of endogenous Hcoronin 3 in HEK 293 seems to be the same in both compartments. The stability of these complexes under high-salt conditions suggests that oligomerization occurs mainly by non-ionic interactions. Furthermore, cytosolic Hcoronin 3 treated with low KCl concentrations migrated similar to that from high-salt extracts, suggesting that the majority of Hcoronin 3 oligomers do not form stable complexes with other proteins.

6.3 The domain requirement for the formation of Hcoronin 3 cytosolic complexes

To test which Hcoronin 3 domains are required for the formation of soluble complexes, stably transfected HEK 293 cells expressing EGFP-Hcoronin 3 and various truncated constructs were used because it is difficult to establish stably transfected Neuro-2a cells expressing coronin 3 various constructs. The transiently transfected cells are not suitable for the experiments. 100,000xg supernatants were prepared and loaded onto a gel filtration column (superdex 200 coupled with Smart FPLC-system) as described above. The collected fractions were subjected to SDS-PAGE and Hcoronin 3 was detected with monoclonal anti-coronin 3 antibodies or anti-EGFP antibodies by Western blot analysis. As a control for a possible aggregation of the EGFP part of the fusion proteins, the migration pattern of EGFP in the gel filtration column was also analyzed as described above. The column was calibrated with a set of standard protein markers in relaxation buffer (Fig 16).

Standard protein elution profile on a Superdex 200 PC3.2/30

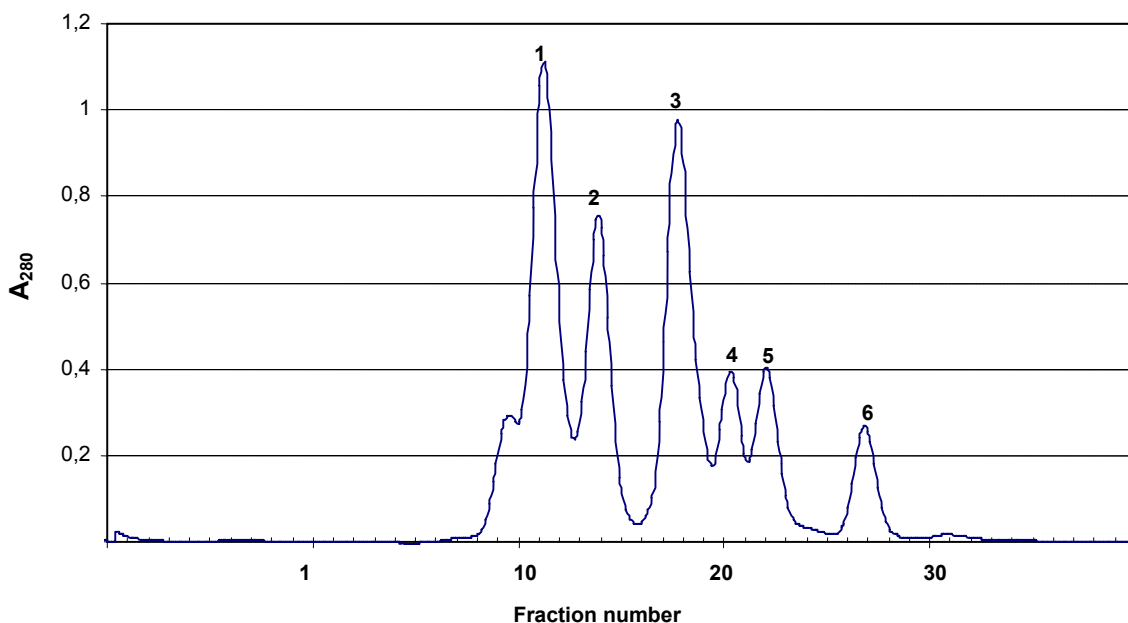


Fig. 16. Elution profile of standard molecular weight markers on a gel filtration column superdex 200 3.2/30. The X-axis gives fraction numbers and the Y axis shows the absorbance of the protein at 280 nm in the corresponding fraction. Each peak represents the elution maximum of a standard molecular weight marker protein (Amersham Pharmacia) fractionated on a Superdex 200 gel filtration column in a FPLC Smart system (Amersham Pharmacia). The peaks correspond to, 1: thyroglobulin, 669 kDa (3 mg/ml); 2: ferritin, 440 kDa (0.175 mg/ml); 3: aldolase, 158 kDa (3 mg/ml); 4: BSA, 67 kDa, 2 mg/ml; 5: ovalbumin 43 kDa (3.5 mg/ml); 6: ribonuklease A, 13.7 kDa (3 mg/ml).

The EGFP-control revealed that only one elution peak was found in fractions 24-25 which corresponds to monomer EGFP polypeptide with an apparent molecular mass of 27-30,000 showing that EGFP alone did not form stable aggregates

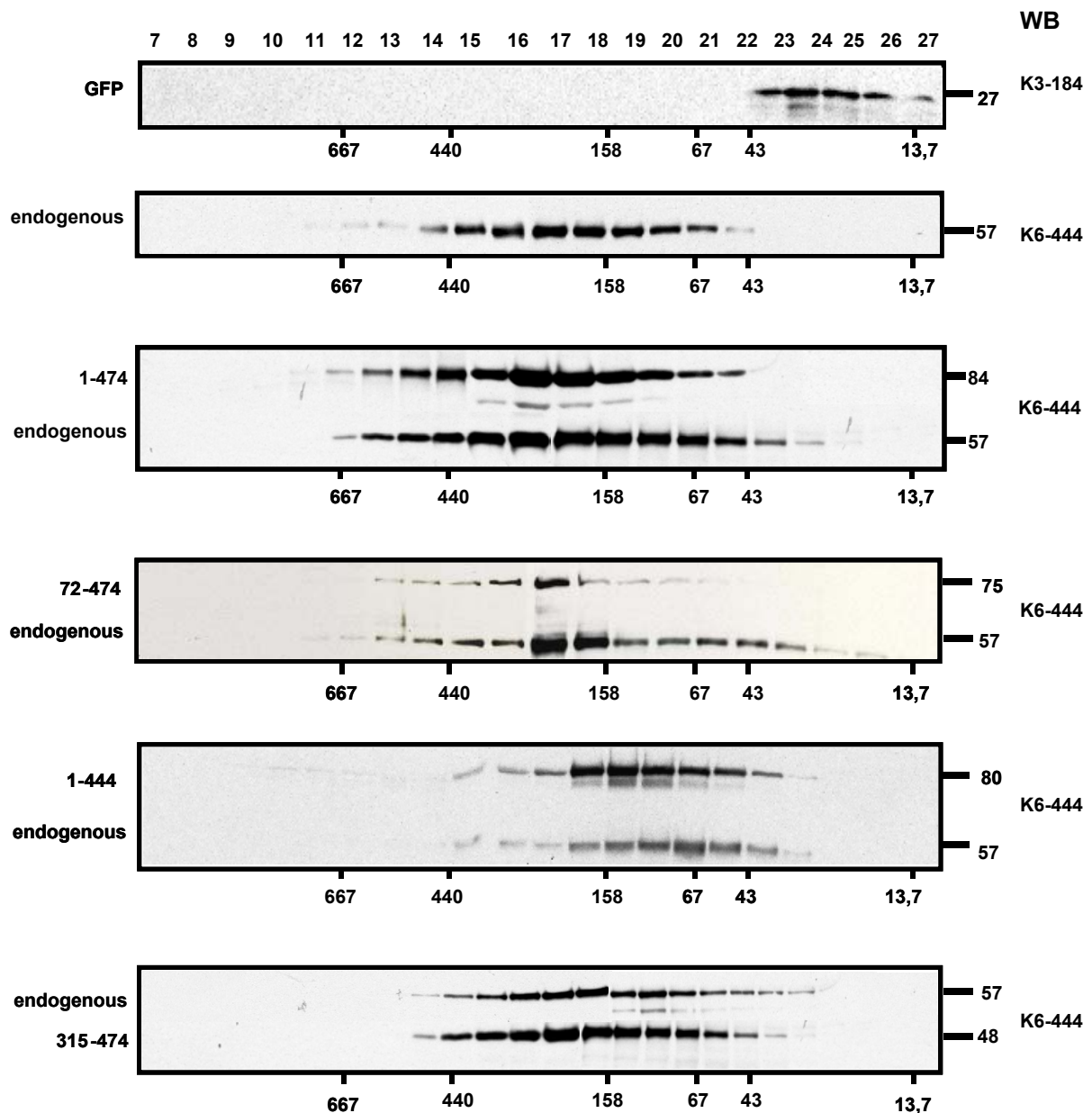


Fig.17. The domain requirements for Hcoronin 3 complex formation in the cytosol of HEK 239 cells. 100,000×g cytosolic supernatants in the relaxation buffer were prepared from HEK 293 cells stably transfected with the EGFP-Hcoronin 3 versions indicated and fractionated on a superdex 200 gel filtration column. Fractions were subjected to 10% SDS-PAGE analysis. Endogenous Hcoronin 3 was detected with monoclonal anti-Hcoronin 3 antibody K6-444 by Western blots. As control, the elution profile of EGFP extracted from stably transfected HEK 293 cells was detected with anti-EGFP monoclonal antibodies. K3-184. The elution of the molecular weight marker is indicated at the bottom of each blot. The fraction numbers are indicated above.

(Fig.17). Therefore, EGFP-Hcoronin 3 and truncated versions appear suitable for analysis of the domain requirements of complex formation. The peak in the EGFP-Hcoronin 3 elution profile was found in the fractions 16 to 19, which was quite similar to the findings for endogenous Hcoronin 3.

The majority of EGFP-Hcoronin 3 (72-474) was found in the elution fractions from 16 to 18, which corresponds to a protein size of 250-150 kDa and showed no significant difference from that of the full length EGFP-Hcoronin 3 as well as endogenous protein. Therefore, most likely the N-terminus is not involved in the formation of the complexes detected in these experiments. Likewise, the shift of EGFP-Hcoronin 3 (1-444) to lower molecular weight fractions was also observed for endogenous Hcoronin 3 in the cell line stably expressing this construct. It may be important that the expression level of EGFP-Hcoronin 3 (1-444) was considerably higher than that of its endogenous counterpart.

Taken together, these results suggest that the COOH-terminal part is sufficient and required for the assembly of the soluble complexes observed. Together with the results demonstrating oligomerization of the recombinant COOH-terminus (section 5.1), this outcome also suggests that these complexes *in vivo* represent most likely Hcoronin 3 homooligomers formed by association via the coiled coil.

7. Phosphorylation of coronin 3

Phosphorylation by members of the protein kinase C family has been reported and suggested for different mammalian coronins. A detailed analysis has been done for coronin 1 in neutrophils, which interacts with a component of NADPH oxidase complex, p40^{phox} (Reeves et al., 1999). Both proteins are substrates of protein kinase C, and the formation of a complex including p40^{phox}, coronin 1 and PKC appeared to be a prerequisite for the phosphorylation of coronin 1. *Phox* proteins and coronin 1 have a similar distribution in neutrophils, and accumulate around the phagocytic vacuole. PMA (phorbol-12-myristate-13-acetate, a PKC activator) treatment resulted in a relocalization of both proteins from the periphery to perinuclear regions in neutrophils (Grogan et al., 1997). Also the phosphorylation of coronin 2_{se}, an isoform of coronin 2, was increased by PMA in rabbit parietal cells (Parente et al., 1999). In addition, PKC-dependent phosphorylation of another family member, coronin 5, was reported. Since coronin 3 contains several possible PKC phosphorylation target sites

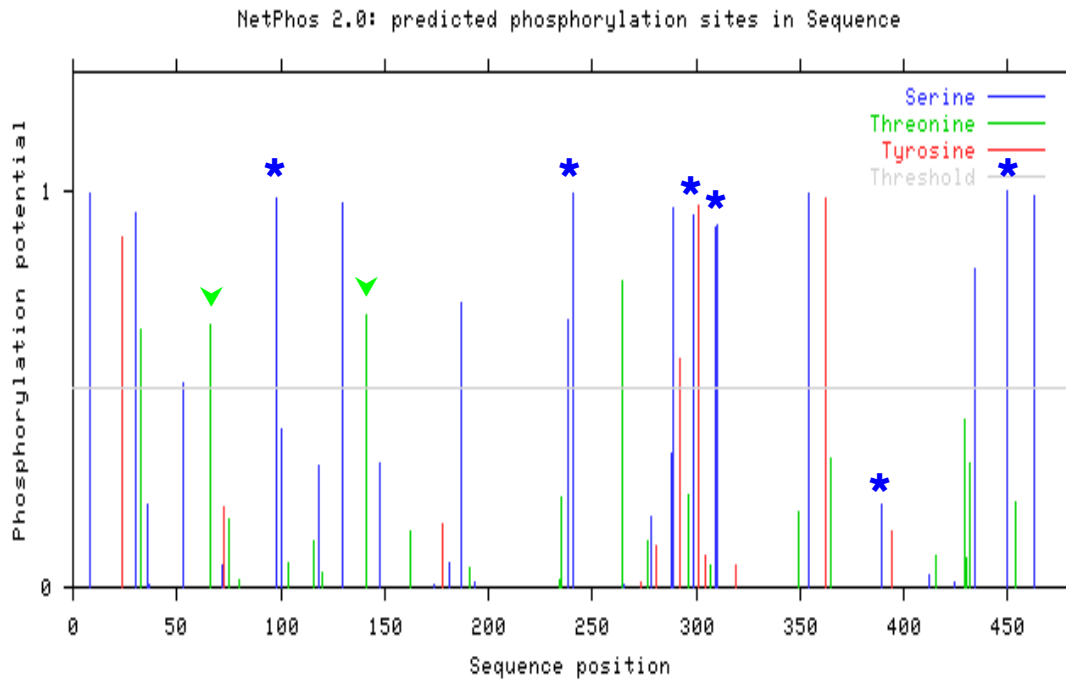


Fig. 18. The putative PKC phosphorylation site in Hcoronin 3 sequence predicted with ScanProsite program (<http://us.expasy.org/tools/scanprosite/>). Green arrowheads represent two putative PKC-consensus threonine phosphorylation sites in Hcoronin 3 sequence, which are located in the NH₂-terminus (amino acid 66-68) and in the second WD40-repeat (amino acid 141-143) respectively. Blue asterisks represent six possible PKC-consensus serine phosphorylation sites, which are located in the second WD40-repeat (amino acid 130-132), the fourth WD40-repeat (amino acid 241-243), the fifth WD40-repeat (amino acid 289-291), the unique region (amino acid 309-311,, 389-391), and the coiled coil domain (amino acid 450-452).

(Fig. 18), and Western blot analysis of different subcellular compartments revealed that coronin 3 translocates from a cytosolic pool to the cytoskeleton and membrane compartment during differentiation in Neuro-2a cells (section 7), it was reasonable to test whether coronin 3 localization may be regulated by PKC-dependent phosphorylation.

For this purpose, 2D-electrophoresis of cytosolic and particle-associated coronin 3 extracted from undifferentiated and differentiated Neuro-2a cells was performed. Although this approach does not permit conclusions concerning which or how many of the possible phosphorylation sites are actually modified, it provides information about the presence and amounts of phosphorylated proteins. The assays were performed using a Pharmacia Multiphor II system. 2,000×g supernatant, 10,000×g pellet, and 100,000×g supernatant fractions were prepared in HES buffer that was adjusted to 2D-electrophoresis buffer with urea and detergents (4% CHAPS). About 4 μg protein of each sample were subjected to 2D-gel analysis, using a pH range of 3-10 for the first and 10% polyacrylamide SDS gels for the second dimension). Coronin3 in different fractions was determined by Western blots using mAb K6-444.

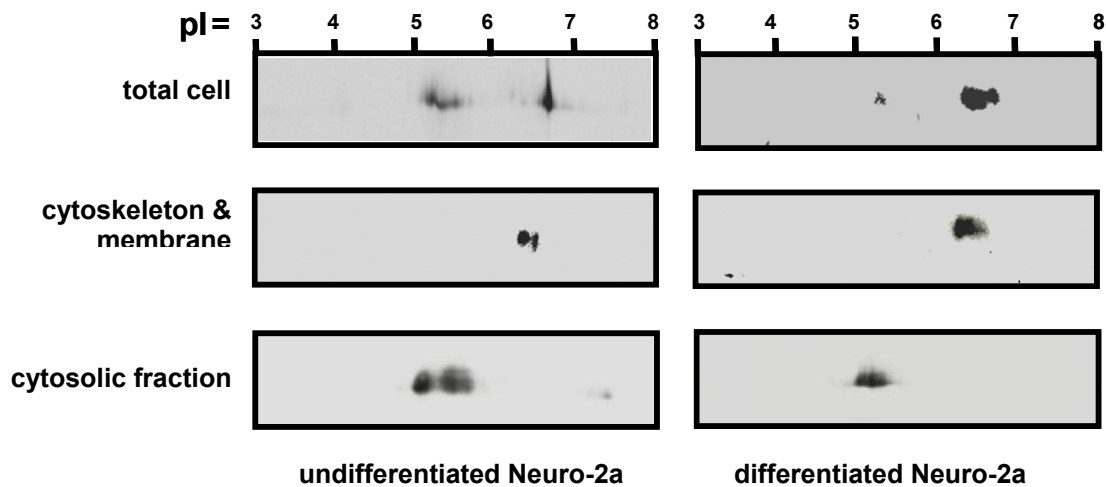


Fig. 19. 2D-gel electrophoresis of total cell extract, cytoskeleton/membrane and cytosolic fractions of undifferentiated and differentiated Neuro-2a cells. 2,000×g postnuclear supernatant, 10,000×g pellet, and 100,000×g supernatant were extracted from undifferentiated and differentiated Neuro-2a cells. Aliquots corresponding to about 8 μg of each sample were focused on immobilized Dry strips (linear pH gradient, pH 3-10) with a Pharmacia Multiphor II system. After isoelectric focussing, the samples were analyzed by SDS-PAGE (10% polyacrylamide). Coronin 3 in different fractions was detected by Western blot using mAb K6-444.

The results showed that coronin 3 exhibited two major spots in the total cell extract of undifferentiated cells (Fig. 19). One spot had a pI value of 6.7, which was consistent with the theoretical pI. This spot was also found for coronin 3 from the cytoskeleton/membrane fraction. In contrast to this, the majority of coronin 3 from the cytosolic fraction was found in a triplet-like set of spots with an apparent pI from 5.2 to 5.5. These more acidic pI values resulted most likely from phosphorylation.

Similar results were also obtained for differentiated Neuro-2a cells. More than 90% of coronin 3 in the total cell extract was focused on the site corresponding to a pI value of 6.7. This was also found for the majority of coronin 3 in the cytoskeleton fraction. Again, cytosolic coronin 3 was focused at more acidic pH with a doublet/triplet distribution pattern. However, the balance between dephosphorylated and phosphorylated state was slightly different in the total cell extracts of undifferentiated and differentiated cells. In differentiated cells, a higher amount of coronin 3 was unphosphorylated than that in undifferentiated cells (Fig. 19). Together with the observation for the subcellular distribution of coronin 3 during differentiation (section 4), this suggests that coronin 3 function during cytoskeletal rearrangements might require phosphorylation and dephosphorylation events.

8. Effect of PMA and bisindolylmaleimide on the phosphorylation of coronin 3 in Neuro-2a cells *in vivo*

The phosphorylation state of coronin 3 in response to a PKC activator and an inhibitor was also analyzed by using 2D-electrophoresis to examine the possible involvement of PKC in modification and regulation of coronin 3. Since the amount of phosphorylated coronin 3 appeared to be higher in undifferentiated cells, undifferentiated cells were used for treatment with a PKC inhibitor. On the other hand, for the test of the PKC activator PMA, differentiated cells were chosen, because the majority of coronin 3 appeared unphosphorylated in these cells and the effect of the activator would be expected to be higher than in undifferentiated cells. It was expected that incubation with a PKC activator would induce a shift to the more acidic spots if coronin 3 phosphorylation is PKC-dependent.

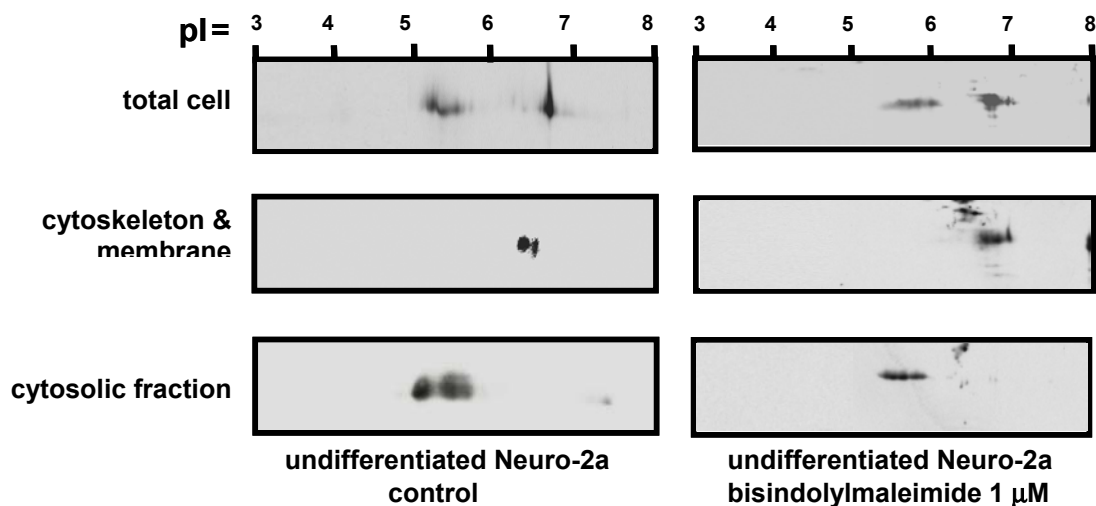


Fig. 20. Effect of bisindolylmaleimide on the phosphorylation of coronin 3 in undifferentiated Neuro-2a cells. Undifferentiated cells were treated with 1 μ M bisindolylmaleimide for 10 min. 2,000 \times g supernatant, 10,000 \times g pellet, and 100,000 \times g supernatant were then extracted from undifferentiated neuro-2a cells. About 8 μ g of each probe were focused on the immobiline Dry Strips pH 3-10 (linear) with a pharmacia Multiphor II system. After first dimensional separation, the samples were analyzed on SDS-PAGE (10% polyacrylamide). The pI of coronin 3 in different fractions was determined by Western blot using mAB K6-444. The control panel is taken from Fig. 19.

In detail, undifferentiated cells were incubated with 1 μ M bisindolylmaleimide for 15 min prior to cellular fractionation or, as a control, left untreated. In a second experiment, differentiated cells were left untreated or treated with 0.1 μ M PMA for 10 min. The different subcellular fractions were prepared as described in section 7.

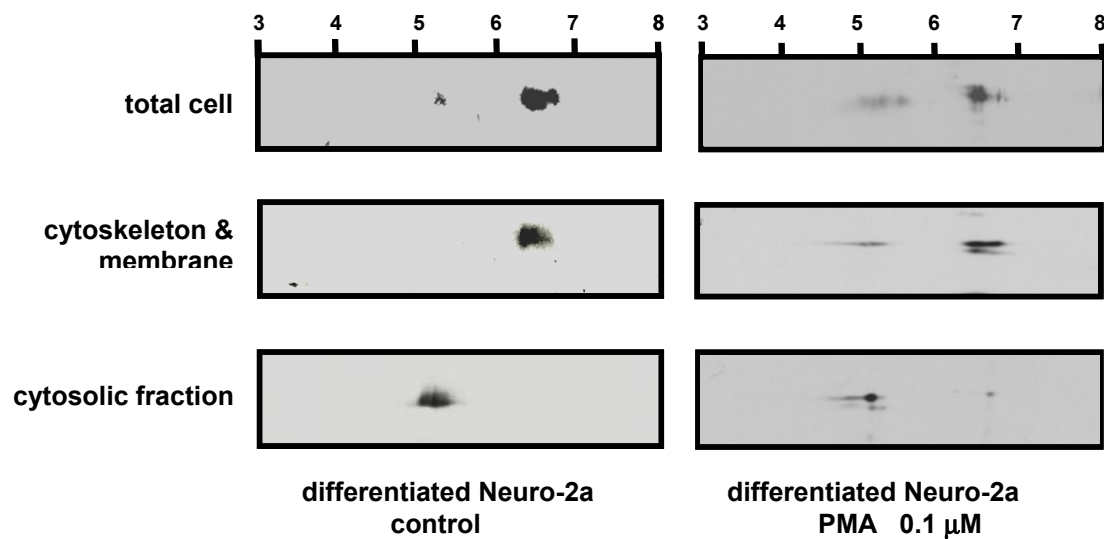


Fig. 21. Effect of PMA on the phosphorylation of coronin3 in differentiated Neuro-2a cells. Differentiated cells were incubated with 0.1 μM PMA for 5 min prior to subcellular fractionation. 2,000 \times g supernatant, 10,000 \times g pellet, and 100,000 \times g supernatant were then extracted from differentiated Neuro-2a cells. About 8 μg of each sample were focused on the immobiline Dry Strips pH 3-10 (linear) with a pharmacia Multiphor II system. After first dimensional separation, the samples were analyzed on SDS-PAGE (10% polyacryamide). The pI of coronin3 in different fractions was determined by Western blot using mAb K6-444. The control panel is taken from Fig. 19.

2D-electrophoresis indicated that in the presence of the PKC inhibitor bisindolylmaleimide the amount of coronin 3 in the acidic spots (pI 5.5) from total cell extracts of undifferentiated cells was similar to that of untreated cells (Fig. 20).

In the differentiated cells treated with PMA, unphosphorylated coronin 3 in total cell extracts and in the cytoskeleton fraction could still be detected. Furthermore, the amount of phosphorylated coronin 3 did not dramatically increase after stimulation with bisindolylmaleimide activator as compared with that of untreated and differentiated cells (Fig. 21). Thus, the effects of PKC inhibitor and PKC activator suggested that coronin 3 is not a direct substrate of PKC. However, to determine if PKC stimulation on coronin 3 phosphorylation *in vivo* is transient or time-dependent, further studies are required.

9 Effect of PMA and bisindolylmaleimide on the subcellular localization of EGFP-Hcoronin 3 in undifferentiated and differentiated Neuro-2a cells

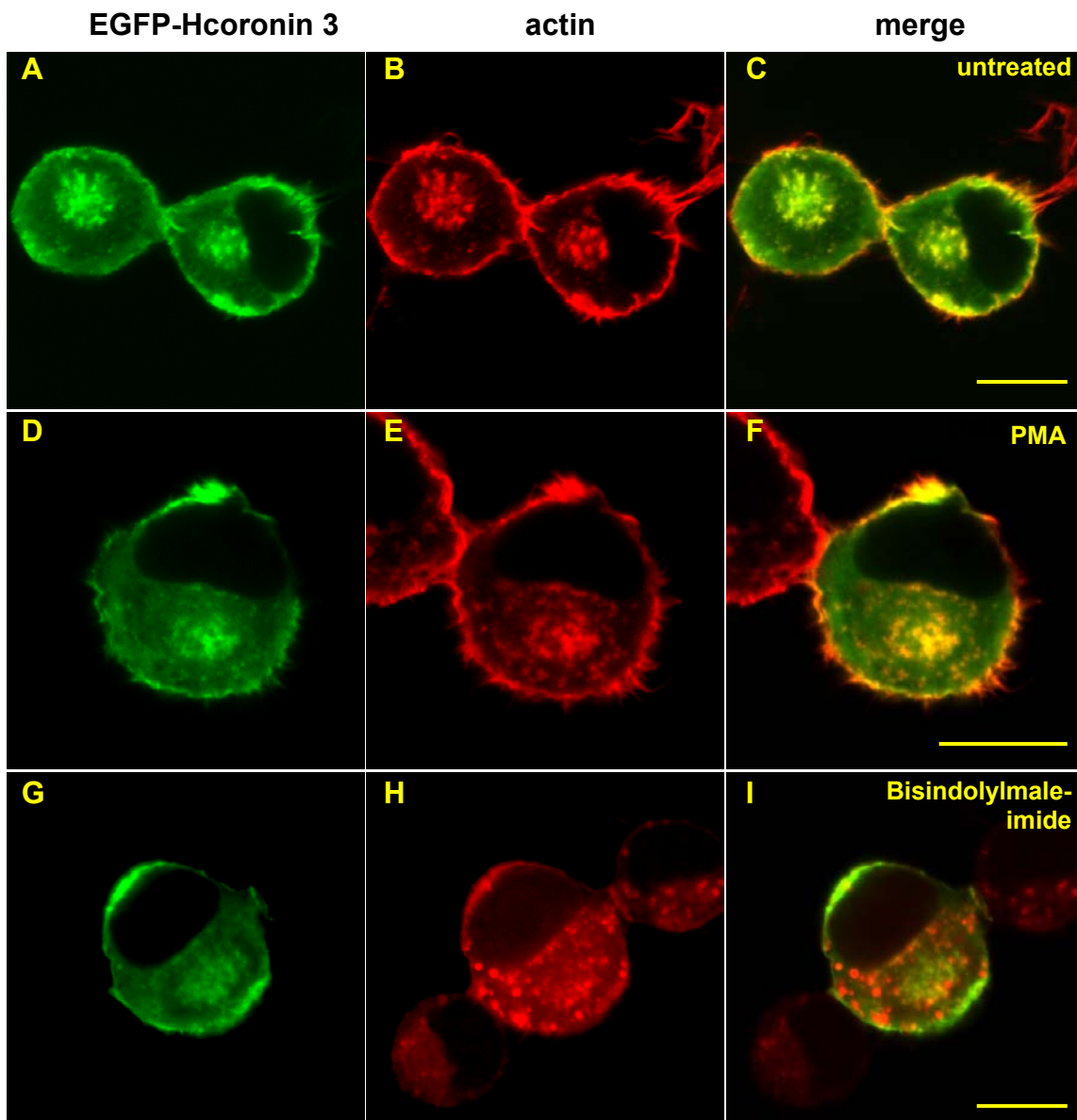


Fig. 22. Effect of PMA and bisindolylmaleimide on the subcellular localization of Hcoronin 3 in undifferentiated Neuro-2a cells. Cells expressing EGFP-fused full length Hcoronin 3 were treated with 0.1 μM PMA for 10 min (D) or 1 μM bisindolylmaleimide for 20 min (G). Cells were fixed in 3 % paraformaldehyde and permeabilized with 0.5 % Triton X-100. Actin was stained with TRITC-phalloidin. Representative cells are shown. Bars, 10 μm .

To examine the effect of PMA and bisindolylmaleimide on subcellular localization of coronin 3, undifferentiated Neuro-2a cells expressing EGFP fused to Hcoronin 3 were treated with 0.1 μM PMA (10 or 20 min) or 1 μM bisindolylmaleimide (20 or 40 min) in culture medium. As a control, cells were washed with PBS. Subsequently, cells were fixed with in 3 % paraformaldehyde and permeabilized with 0.5 % Triton X-100. To

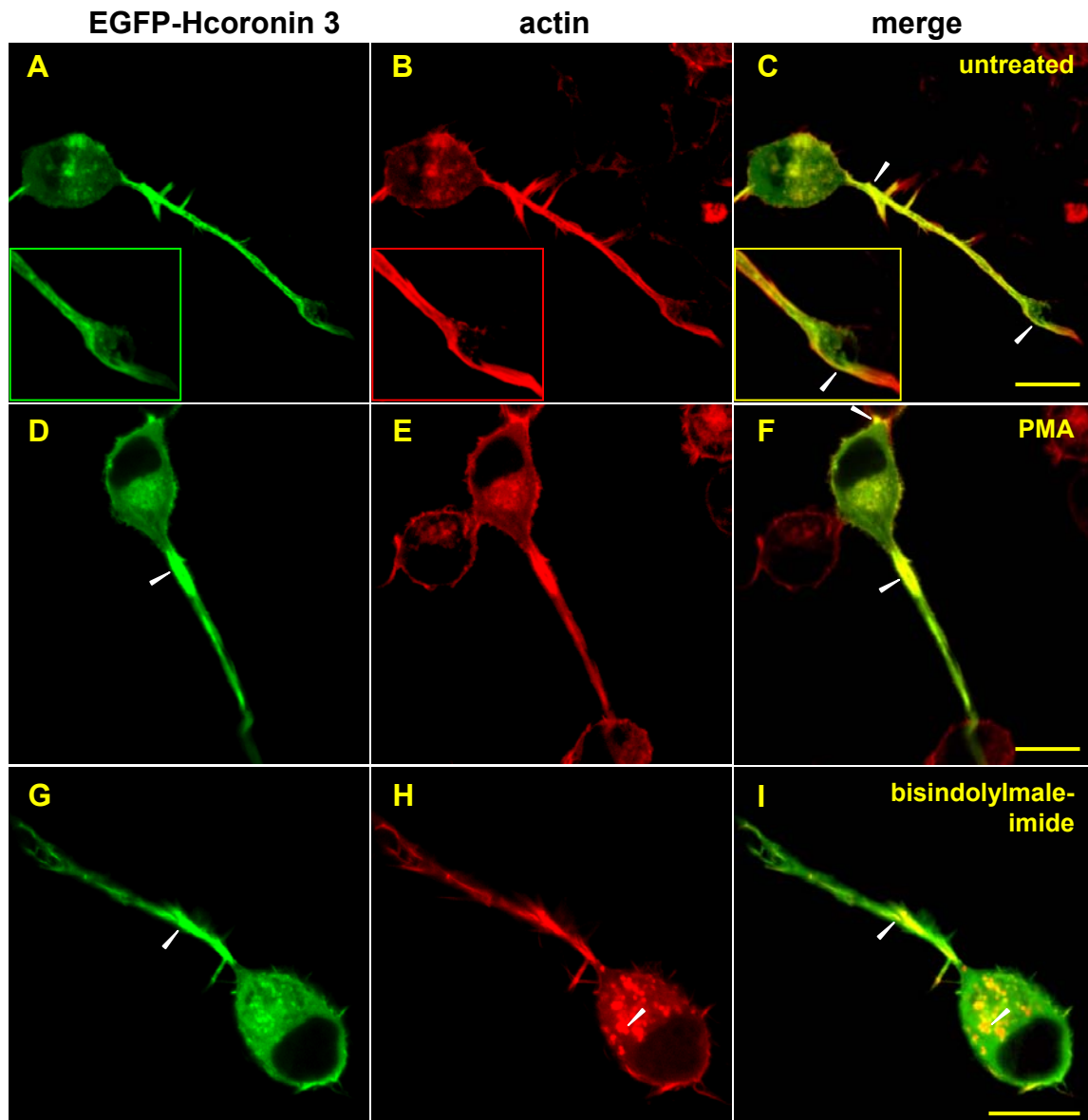


Fig. 23. Effect of PMA and bisindolylmaleimide on the subcellular localization of EGFP-Hcoronin 3 in differentiated Neuro-2a cells. Cells expressing EGFP-tagged full length coronin3 were induced to differentiate by low serum concentration for 2 days after transfection and then treated with 0.1 μ M PMA for 10 min (D) or 1 μ M bisindolylmaleimide for 20 min (G-I). Cells were fixed in 3 % paraformaldehyde, and permeabilized with 0.5 % Triton X-100. Actin was stained with TRITC-phalloidin. Representative cells are shown. Bars, 10 μ m.

test whether the actin structure is also changed in the presence of PMA or bisindolylmaleimide, fixed cells were incubated with TRITC-phalloidin. As already shown in section 2.1, EGFP-Hcoronin 3 staining in untreated undifferentiated cells was most intense in neurite outgrowth. In these cells, enrichment of EGFP-Hcoronin 3 in the cell periphery similar to the control cells could still be detected in PMA-treated cells, and the amount of EGFP-Hcoronin3 in cytosol was not significantly enhanced in response to PMA-treatment (Fig. 22). Furthermore, EGFP-Hcoronin 3

colocalized with F-actin primarily in neurite but also in the center of the cell body. The addition of bisindolylmaleimide to undifferentiated cells resulted in a change of the F-actin structures. This was also observed in differentiated cells. The localization of EGFP-Hcoronin 3 seemed not to be significantly changed after bisindolylmaleimide treatment.

As already shown in section 2.1, EGFP-Hcoronin 3 staining in untreated differentiated cells was most intense in neurite projections. In growth cones, EGFP-Hcoronin 3 was also present except for the most apical regions of the tips. This was clearly visible in the overlay picture (arrowhead, Fig. 23C). In the presence of PMA, the intracellular distribution of EGFP-Hcoronin 3 was not significantly changed as compared with the control. EGFP fluorescence was also most intense at the neurites (Fig. 23D). The amount of cytosolic coronin 3 was slightly increased. Similar results were obtained when application of PMA was prolonged to 20 min (data not shown). In the presence of bisindolylmaleimide, EGFP-Hcoronin 3 similarly accumulated in the neurite. However, an obvious effect of the treatment was that the F-actin structures of the cell were changed. In more than 95% of the cells, the number of phalloidin-positive punctate structures in the center of the cells strongly increased (arrowhead, Fig 23H). EGFP-Hcoronin 3 colocalized with these cytoplasmic structures in the cytosol (arrowhead, Fig. 23I). Such a relocation of EGFP-Hcoronin 3 as well as F-actin in response to bisindolylmaleimide did not occur in PMA-treated or untreated differentiated cells. It has been reported that addition of PMA to Swiss 3T3 cells induces the formation of lamellipodia and membrane ruffles (Nobes et al., 1995; Spoerl et al., 2002), In contrast to fibroblasts, cell morphology of Neuro-2a was not altered in the presence of bisindolylmaleimide and PMA.

10. Effect of colchicine and taxol on the subcellular localization of EGFP-Hcoronin 3 in differentiated Neuro-2a cells

It has been reported that yeast coronin (crn1p) binds to microtubules *in vitro* and that its microtubule binding is enhanced in the presence of actin filaments (Goode et al., 1999). Therefore, it was postulated that crn1p serves as a functional link between the actin and microtubule cytoskeleton in yeast. Since the tubulin content in neuronal cells makes up approximately 30 % of total protein, and neurite outgrowth is a strongly microtubule-dependent process, it was reasonable to test whether coronin 3 colocalizes with microtubules during differentiation and whether its distribution in

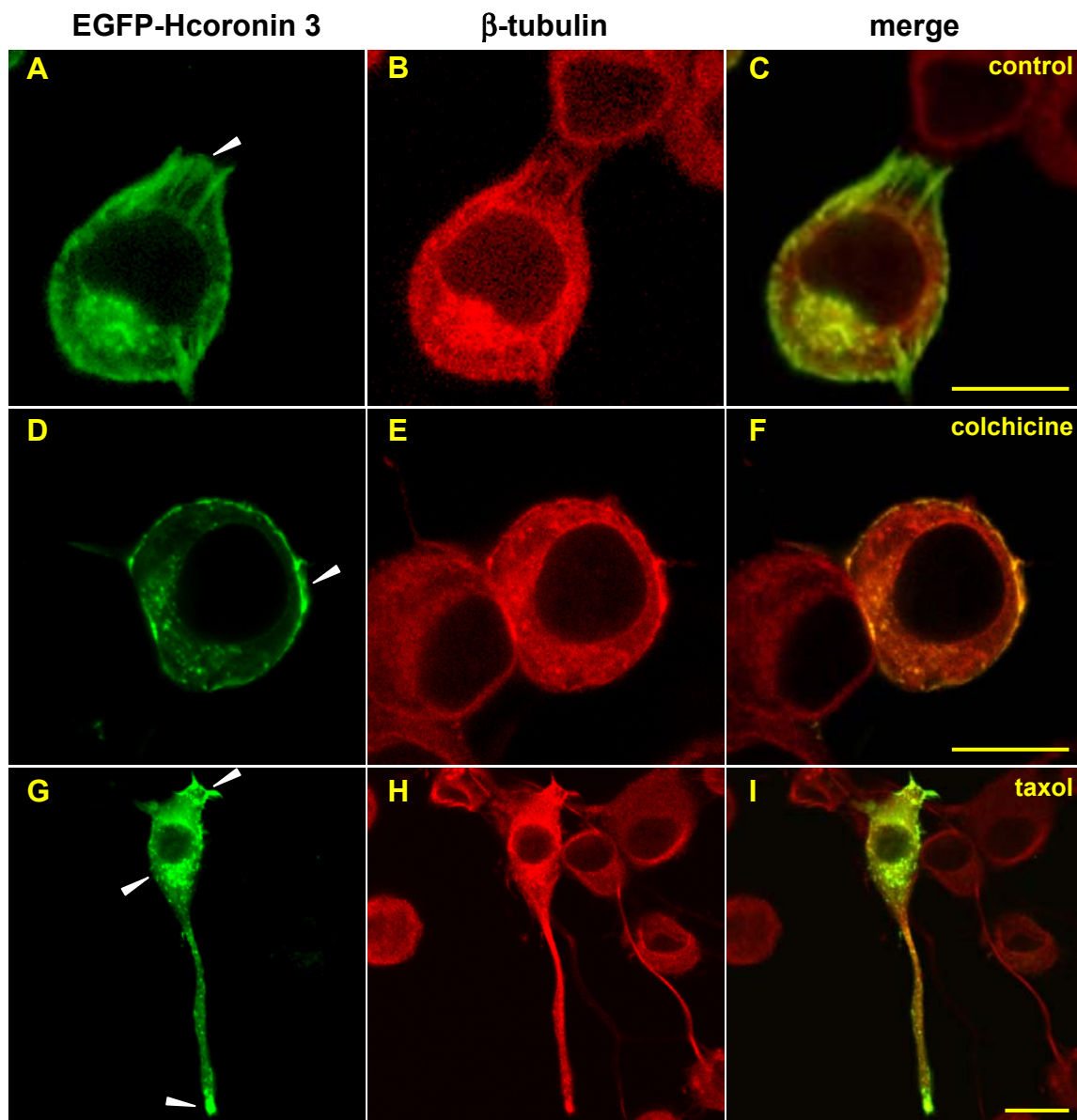


Fig. 24. Effect of colchicine and taxol on the subcellular localization of Hcoronin 3 in Neuro-2a cells. Cells expressing EGFP-tagged full length Hcoronin 3 were induced to differentiate by low serum concentration for 2 days after transfection and then treated with 0,1 $\mu\text{g}/\mu\text{l}$ of colchicine for 60 min (D) or 1 $\mu\text{g}/\mu\text{l}$ taxol for 40 min (G) at 37 °C. Cells were fixed in 95% methanol containing 5 mM EGTA at -20°C and then incubated with mouse monoclonal anti- β -tubulin antibody, followed by Cy3-conjugated goat anti-mouse IgG antibody. Representative cells are shown. Bars, 10 μm .

Neuro-2a cells is microtubule-dependent. To this end, microtubules in differentiated Neuro-2a cells expressing EGFP-coronin 3 were labeled with a mouse monoclonal anti- β -tubulin antibody, followed by Cy3-conjugated goat anti-mouse IgG antibody. More than 80% of the by Cy3-conjugated goat anti-mouse IgG antibody. More than 80% of the differentiated cells showed no colocalization of EGFP-Hcoronin 3 with tubulin (Fig. 24A, B). EGFP-Hcoronin 3 was more enriched in the cell periphery than

microtubules (Fig. 24C). To test a possible dependence of coronin 3 localization on microtubules, colchicine, a tubulin binding and thus polymerization-inhibiting drug was used. The picture D in Figure 24 shows that the addition of colchicine led to a drastic change in cell morphology, e.g. cells became round and lost their neurites as a result of microtubule depolymerization. The distribution of EGFP-Hcoronin 3 did not change pronouncedly, as it still was found in the cell periphery and at cell-cell contacts (Fig. 24D), while tubulin accumulated in the cytoplasm. This means that colchicine did not significantly change the subcellular localization of Hcoronin 3. Conversely, in the presence of taxol, a microtubule-stabilizing drug, the cells showed more pronounced neurites (Fig. 24G). EGFP-Hcoronin 3 was found not only in neurites but also in the cytoplasm, similar to untreated cells. Again, the localization of microtubules and EGFP-Hcoronin 3 did not overlap. Taken together, these experiments do not suggest any interaction of coronin 3 with the microtubule network.

11 *In vitro* F-actin interaction of recombinant Hcoronin 3 fragments

Despite some preliminary observations, the localization of the possible actin binding domain in mammalian coronins remains elusive. Studies for defining the actin binding domain of coronin-homologues from different organisms led to controversial results. The deletion of the C-terminal coiled coil domain in yeast coronin 1 (crnp1) did not have a significant effect on actin binding affinity of the protein but lost the actin crosslinking activity (Goode et al., 1999). Therefore, the WD40-repeats were referred to as a putative actin binding domain in yeast coronin. Contrarily, *Xenopus* coronin revealed a dramatic decrease of F-actin affinity by either deletion of the N-terminal 60 amino acids or truncation of the C-terminal coiled coil region. The WD40-repeat region alone showed neither interaction with actin filaments *in vitro* nor colocalization with filamentous actin *in vivo* (Mishima et al., 1999). Thus, NH₂-terminal and COOH-terminal parts of *Xenopus* coronin are postulated to be involved in the association with F-actin. Mammalian coronins have also been described to bind to F-actin and were localized in actin-rich cortical regions (Suzuki et al., 1995; Nakamura et al., 1999), however, no F-actin binding domain of mammalian coronins has been characterized so far. Sequence analysis of the amino acids 315-474 of Hcoronin 3 containing the unique region showed similarities to other F-actin binding proteins with coiled coil domains such as myosins, tropomyosins and the COOH-terminus of the vasodilator-stimulated phosphoprotein (VASP) as well as the COOH-terminal region

of *Xenopus* coronin. The subcellular localization of EGFP-Hcoronin 3 and truncated variants suggested that NH₂- and COOH-terminus are required for the colocalization with F-actin *in vivo*. Thus, it seemed possible that they might be involved in the F-actin interaction. To confirm this observation, recombinant NH₂- and COOH-terminal fragments were tested in actin binding assays.

11.1 Expression and purification of 6×His-Hcoronin 3 fragments

The following recombinant Hcoronin 3 NH₂- and COOH-terminal peptides were expressed as 6×His-tagged fusion proteins for *in vitro* actin binding and crosslinking assays (Fig. 25).

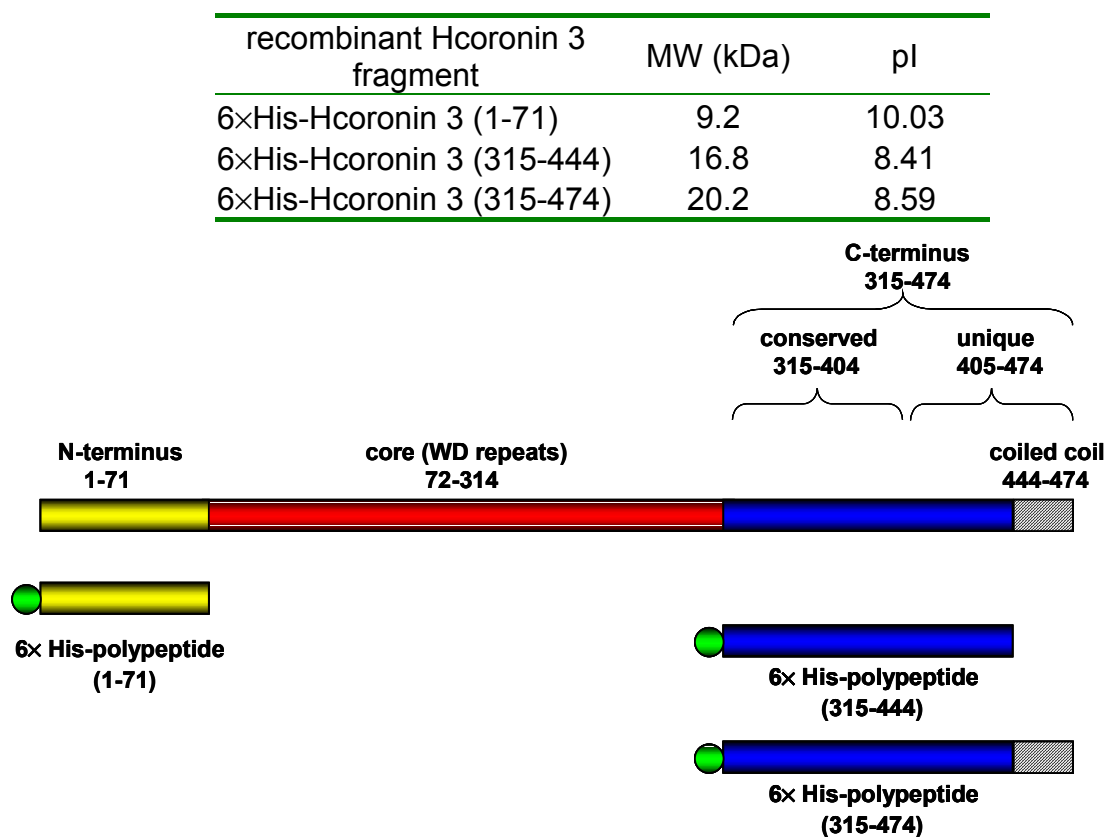


Fig. 25. Domain structure of Hcoronin 3 based on sequence analysis. Numbers represent the amino acid position in coronin 3. For the localization of actin binding domains in coronin 3, NH₂- and COOH-terminal fragments indicated were expressed as 6×His tagged protein in the pQE-30 vector and purified from *E. coli* M15.

Briefly, the respective coding sequences were cloned into pQE30 vector and expressed in *E. coli* host strain M15 (pREP4). The purification of C-terminal Hcoronin 3-(315-444) and -(315-474) peptides was done by affinity chromatography with Ni-NTA matrix under native conditions. The correct size of the recombinant proteins was

confirmed by matrix-assisted laser desorption/ionisation (MALDI). For the COOH-terminal coiled coil domain, the predicted α -helical structure served as an indicator for correct protein folding and was verified by CD-spectra.

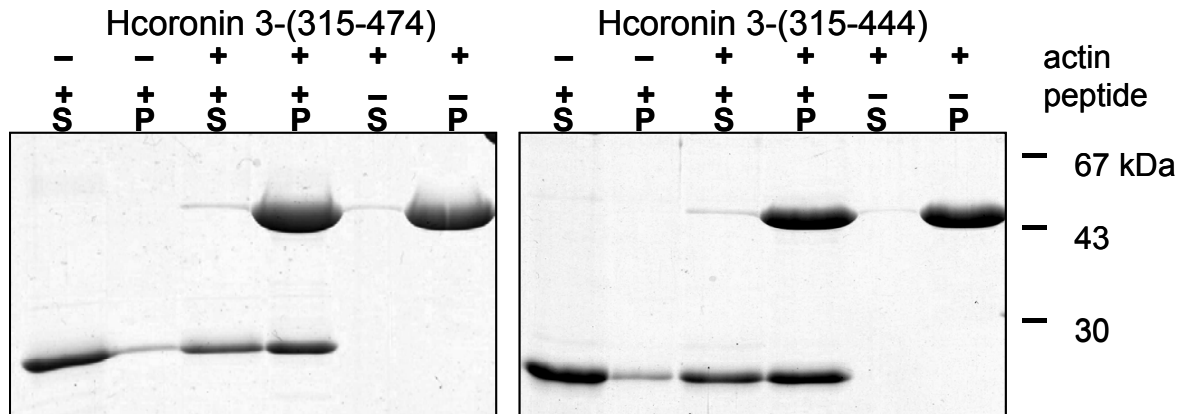


Fig. 26. *In vitro* cosedimentation of Hcoronin 3 COOH-terminal fragments with F-actin at high speed. Recombinant 6 \times His-tagged COOH-terminal Hcoronin 3 (315-474) and (315-444) were incubated in actin polymerization buffer alone or with G-actin in the same buffer. Actin filaments were pelleted at 100,000 \times g for 45 min. The pellets (P) and supernatants (S) were analyzed by 12% SDS-PAGE and the gels were stained with Coomassie blue.

11.2 Actin binding assay

11.2.1 *In vitro* binding of Hcoronin 3 NH₂- and COOH-terminal domains to F-actin

In order to examine the *in vitro* F-actin binding activity of N- and C-terminal Hcoronin 3 domains, the purified recombinant polypeptides were used for an *in vitro* actin cosedimentation assay. To avoid pelleting of possible protein precipitates in the cosedimentation assay, the purified protein and G-actin solutions were clarified at 100,000 \times g, 4 $^{\circ}$ C for 30 min. The supernatants were used for the actin binding assays. In the absence of actin, most of both C-terminal fragments remained in the supernatant after centrifugation, whereas a considerable amount of Hcoronin 3 (315-474) as well as Hcoronin 3 (315-444) pelleted with F-actin at high speed (100,000 \times g, 22 $^{\circ}$ C for 30 min, Fig. 26). The results suggest that both COOH-terminal fragments of Hcoronin 3 were active in F-actin binding and that 315-444 is sufficient for binding to F-actin. In contrast to the COOH-terminal polypeptide, the NH₂-terminal 71 amino acids did not bind F-actin (see Fig. 27).

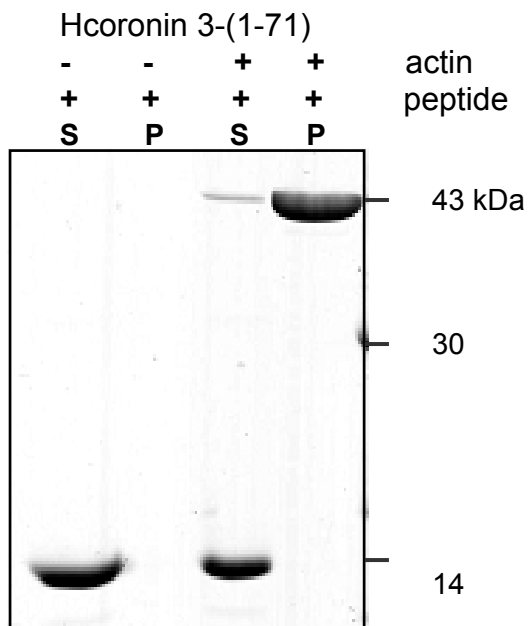


Fig. 27. *In vitro* cosedimentation of Hcoronin 3 NH₂-terminal fragments with F-actin at high speed. Recombinant 6×His-tagged Hcoronin 3 NH₂-terminal (1-71) was incubated in actin polymerization buffer alone or with G-actin in the same buffer. Actin filaments were pelleted at 100,000×g for 45 min. The pellets (P) and supernatants (S) were analyzed by 15% SDS-PAGE and the gels were stained with Coomassie blue.

11.2.2 The affinity of COOH-terminal Hcoronin 3 polypeptides to actin filaments

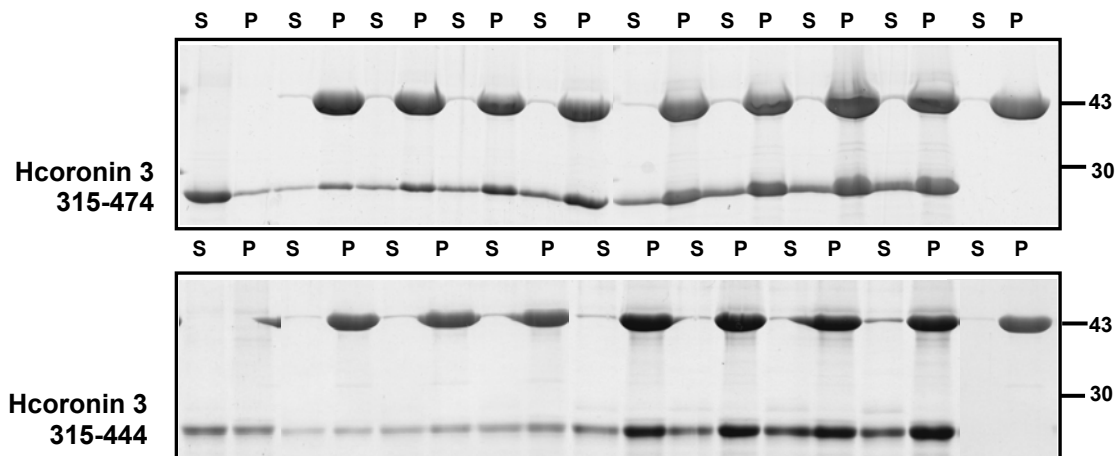


Fig. 28. The affinity of the COOH-terminal Hcoronin 3 polypeptide to actin filaments. 10 μ M G-actin were incubated with varying amounts of recombinant Hcoronin 3 (315-474) and (315-444) for 1 h. After the incubation, actin filaments were sedimented at 100,000×g for 30 min. The pellets (P) and supernatants (S) were then analyzed by 12% SDS-PAGE and the gels stained with Coomassie blue.

In order to quantify the binding of COOH-terminal Hcoronin 3 polypeptide to F-actin, a constant concentration of actin (10 μ M) was added to varying amounts of Hcoronin

3 (315-474) and (315-444) in a cosedimentation assay (Fig 28). Pellets and supernatants of each mixture were analyzed by SDS-PAGE and the concentration of free and actin-bound polypeptide was determined by laser scanning densitometry analysis of the Coomassie blue stained gels using 1 μM , 5 μM and 10 μM of BSA as a protein standard. With these data and the known concentration of the added actin (10 μM), the dissociation constant was calculated using the following formula:

$$K_d = \frac{[A][P]}{[AP]}$$

K_d = dissociation constant

[A] = concentration of actin

[P] = concentration of free polypeptide

[AP] = concentration of polypeptide bound to actin

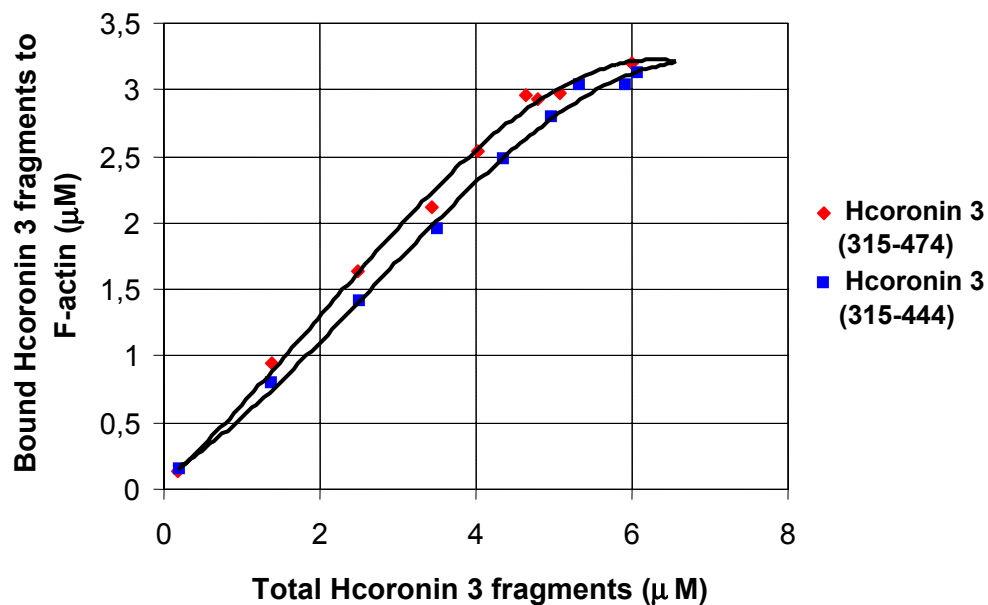


Fig. 29. Concentration-dependent binding of recombinant Hcoronin 3 (315-474) and (315-444) to F-actin. 10 μM of G-actin was incubated with varying concentration of the recombinant Hcoronin 3 fragments in a high speed cosedimentation assay. The concentrations of free and actin-bound polypeptide were calculated by laser scanning of the respective bands in Coomassie stained gels using laser densitometry. The bands for 1 μM , 5 μM and 10 μM of BSA in the same gels were used as protein standard. The concentration of bound versus total Hcoronin 3 fragments was plotted to calculate the dissociation constants of Hcoronin 3 (315-474) and (315-444) to actin.

Plotting the concentration of 6×His tagged Hcoronin 3 (315-444) and (315-474) fragments bound to F-actin versus the corresponding total free polypeptides showed a linear curve at lower concentration for both fragments. Binding reached saturation at about 3.1 μM bound polypeptide per 10 μM actin was reached (Fig. 29). The dissociation constants of both fragments were determined as the half-maximal saturation concentration with $K_d=7.1 \mu\text{M}$ for Hcoronin 3 (315-474) and $K_d=8.5 \mu\text{M}$ for Hcoronin 3 (315-444) respectively. Thus, both fragments showed a similar binding affinity to F-actin *in vitro*. F-actin binding was saturated at a 1:3 molar ratio for both COOH-terminal Hcoronin 3 fragments.

11.2.3 COOH-terminal Hcoronin 3 polypeptides crosslink and bundle F-actin filaments *in vitro*

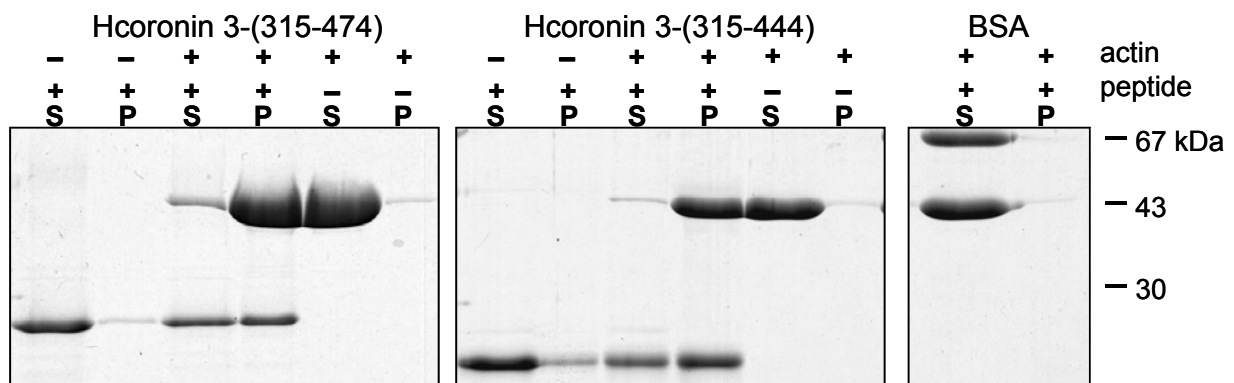


Fig. 30. The Hcoronin 3 COOH-terminal region can bundle or crosslink actin filaments *in vitro*. G-actin was incubated in actin polymerization buffer alone, with BSA or with recombinant 6×His-tagged Hcoronin3(315-444) or (315-474) for 1h and was centrifuged at low speed (12,000×g) for 30 min. The pellets (P) and supernatants (S) were analyzed by 12% SDS-PAGE and the gels were stained with Coomassie blue.

After showing that the COOH-terminal region binds to F-actin *in vitro*, an actin-bundling assay was performed. Since the COOH-terminal coiled coil domain is speculated to be responsible for self-association of coronins (de Hostos, 2000), the dimerization or multimerization of coronin would allow that the molecule crosslinks and bundles filaments. These activities require more than one actin-binding site per molecule. Therefore, the role of the coiled coil domain in F-actin interaction was further analyzed by low speed spin down assays. Bundled actin filaments can be sedimented at 12,000×g, whereas uncrosslinked filaments remain in the supernatant. Thus, actin was incubated in the actin polymerization buffer alone, with BSA or with

Hcoronin 3 (315-474) as well as with Hcoronin 3 (315-444) as described for the actin binding assay and centrifuged at 12,000×g for 30 min at room temperature. The experiments revealed that actin could be pelleted in the presence of the complete COOH-terminus or the COOH-terminal region lacking the coiled coil domain under these conditions (Fig. 30). In the controls for actin alone and actin in the presence of BSA, actin remained in the supernatant. This experiment suggests that the COOH-terminus of Hcoronin 3 is able to bundle actin filaments *in vitro* and that the coiled coil is not necessary for this activity.

11.2.4. Light microscopic observation of F-actin suprastructures formed in the presence of Hcoronin 3 COOH-terminal fragments

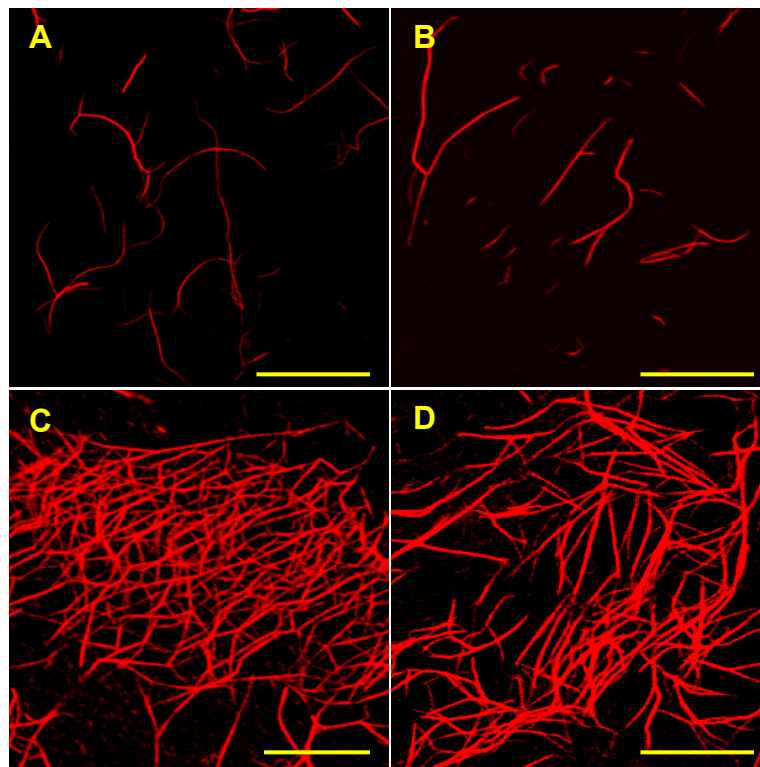


Fig. 31. Visualization of actin filaments incubated with Hcoronin 3 COOH-terminal fragment (315-474) and (315-444) lacking the coiled domain. 10 μ M F-actin was incubated in actin polymerization buffer alone (A), with 5 μ M BSA (B), with 5 μ M coronin 3 (315-474) (C), or coronin 3 (315-444) (D) at room temperature for 1 h. Aliquots of the sample were applied to poly-L-lysine-coated coverslips. After 30 min at 4°C incubation, the absorbed proteins were fixed with formaldehyde and stained with TRITC-phalloidin. Fluorescence images were obtained using a Leica laser scanning confocal microscope with a Krypton laser. Bar, 8 μ m.

This assay is based on a protocol by Korneeva and Jockusch (1996) with slight modifications. The purpose of this experiment was to visualize the change of actin filament structure in the presence of coronin 3 full length COOH-terminal region and COOH-terminal polypeptide lacking the coiled coil domain. The F-actin/full length COOH-terminus containing sample showed F-actin bundles forming extensive mesh-like suprastructures (Fig. 31C). In contrast, F-actin alone (A) and F-actin with BSA (B) was characterized by a poor filament appearance. Only occasionally, few bundles were seen in those sample. Bundles observed in the F-actin/COOH-terminal fragment lacking coiled coil domain were shorter but thicker than those of the F-actin/full length COOH-terminus containing sample. It seems that the full length COOH-terminal polypeptide and the COOH-terminal fragment lacking the coiled coil region not only crosslink but also bundle F-actin.

11.2.5 Interaction of Hcoronin 3 NH₂-terminal and COOH-terminal fragments *in vitro*

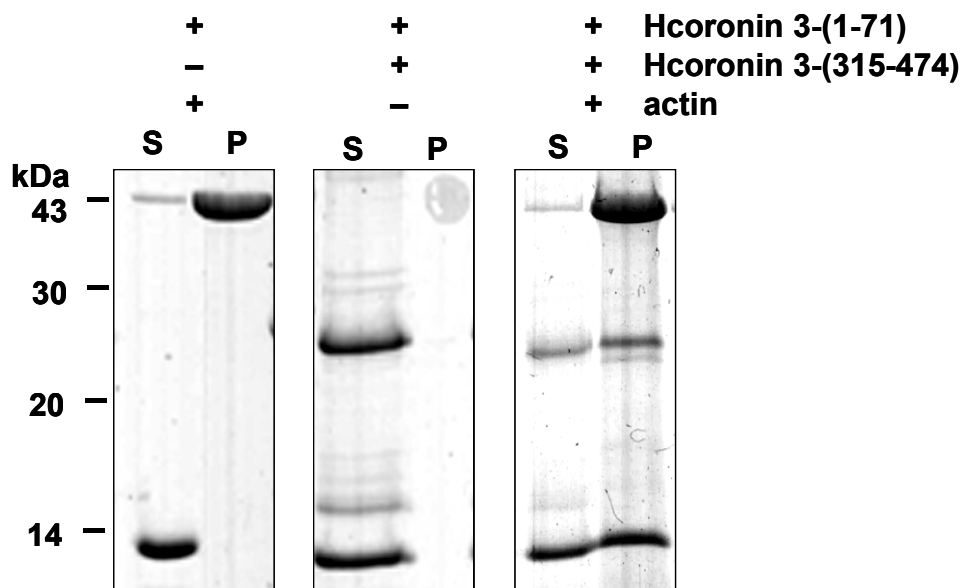


Fig. 32. The NH₂-terminus (1-71) binds to the COOH-terminus (315-474) simultaneously with F-actin. 6×His tagged recombinant Hcoronin 3 NH₂-terminus (1-71) was incubated in actin polymerization buffer with 10 μM of G-actin, COOH-terminus (315-474) or with 10 μM of G-actin and COOH-terminus (315-474). The mixture was centrifuged at 100,000×g for 45 min. The pellets (P) and supernatants (S) were analyzed by 12% SDS-PAGE and the gels were stained with Coomassie blue.

Interestingly, the NH₂-terminal fragment cosedimented with F-actin in the presence of the COOH-terminus (Fig. 32). In the control, most of the N-terminal fragments remained in the supernatant when incubated with the COOH-terminal polypeptide in the absence of F-actin. This might indicate that the COOH-terminal domain can recruit the NH₂-terminal region to actin filaments. In order to define which

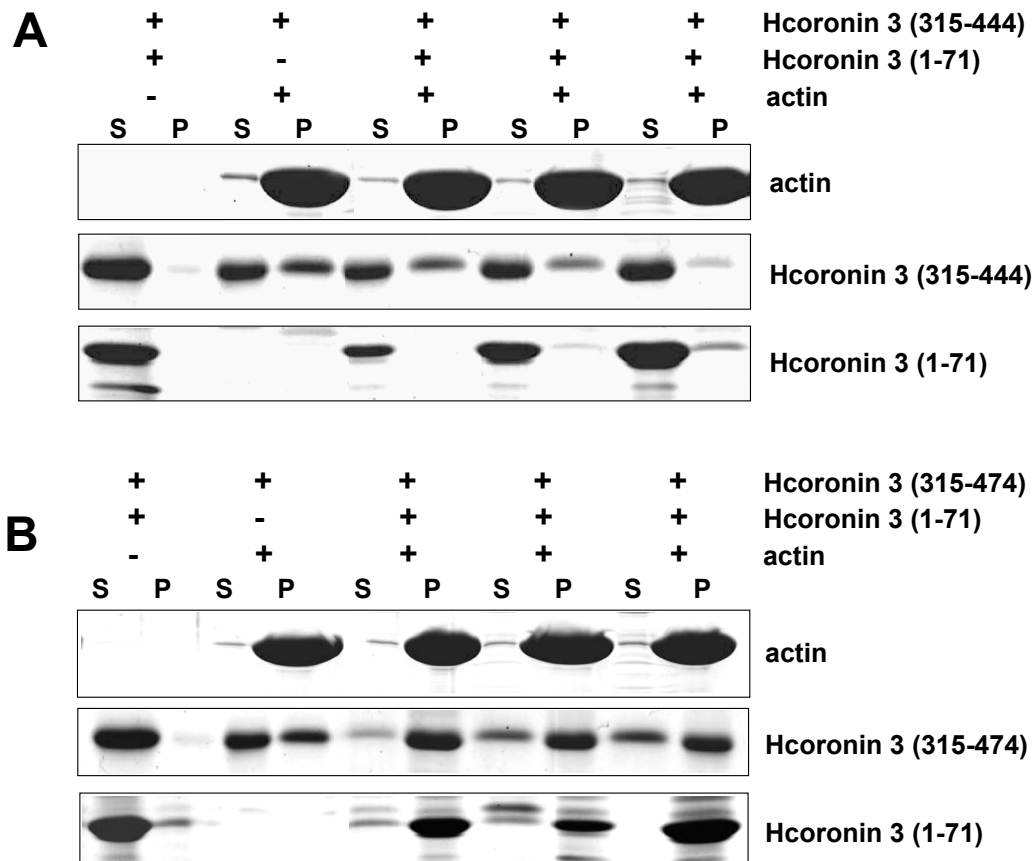


Fig. 33. The role of the coiled coil domain in the interaction of the Hcoronin 3 COOH-terminus with the NH₂-terminus *in vitro*. Constant amounts of COOH-terminal Hcoronin 3 (315-444) or (315-474) were incubated in actin polymerization buffer with NH₂-terminus alone, with 10 μ M of G-actin or with variable concentrations of NH₂-terminus in presence of 10 μ M G-actin for 1 h at room temperature. The mixture was centrifuged at high speed (100,000 \times g) for 45 min. The same volumes of pellets (P) and supernatants (S) were analyzed by 12% SDS-PAGE and the gels were stained with Coomassie blue.

of the C-terminal region is required for the binding of the NH₂-terminus, constant amounts of C-terminal Hcoronin 3 (315-444) and (315-474) were incubated with different amounts of NH₂-terminal fragment 1-71 in the presence of a constant amount of actin. It was found that the majority of the NH₂-terminal fragment remained in the supernatant in the presence of Hcoronin 3 (315-444). Moreover, increasing amounts of NH₂-terminal fragments led to a marked decrease of the binding of

Hcoronin 3 (315-444) to F-actin (A Fig. 33). This suggests that the NH₂-terminal domain could interfere with the binding of Hcoronin 3 (315-444) to F-actin.

In contrast to this, most of the NH₂-terminal fragment was found in the actin pellet in the presence of the complete COOH-terminus. Increasing concentrations of the NH₂-terminal fragment did not significantly decrease the association of Hcoronin 3 (315-474) with F-actin (B Fig. 33). These results suggest that the coiled coil domain might stabilize the interaction with F-actin. Moreover, the full length COOH-terminal domain (315-474) seemed to bind simultaneously to F-actin and the NH₂-terminal domain (1-71) *in vitro*.

IV. Discussion

A great variety of different cellular functions such as cell motility, differentiation and cytokinesis are based on the exact regulation of the cytoskeleton. A major role is exerted by the dynamic actin network. Many different actin binding proteins are involved in these events, which are able to regulate actin filament length, formation and stability upon request (Pollard, 1990; Stossel, 1993; Welch et al., 1997). One family of actin-interacting proteins is the coronin family, which are expressed in a large variety of eukaryotes from yeast to man. However, little is known about their action at the molecular level. The mammalian coronin family is composed of at least seven members, which show a similar molecular mass of about 50 to 60,000. They share considerable sequence homology except for a unique region in their COOH-terminal regions. Interestingly, their expression pattern is tissue-specific, but partially overlapping, implying that mammalian coronins possess diverse functions and do not simply replace each other in different tissues (de Hostos, 2000). Homologue-specific functions are believed to be exerted by their unique region. No function is as yet known for coronin 3. One aim of this work was thus to characterize homologue-specific domain functions of mammalian coronin 3, and the role of different domains for its subcellular localization. The second focus of this study was to determine the localization and, if possible, a role of coronin 3 in neuronal cells, since it is expressed most abundantly in the brain and may thus be predominantly required in this organ.

The role of microtubules and their associated proteins in nerve cells is well established (Kreis and Vale 1999), whereas the impact of the microfilament system on neuron function and development is just beginning to emerge. Recent studies show that Down syndrome (DS) patients reveal a reduced neuronal density in different regions of the brain, and abnormal neuronal differentiation, migration and synaptogenesis (Becker et al., 1986; Becker et al., 1991; Engidawork et al., 2001). These morphological aberrations are believed to result in mental retardation. Furthermore, Krucker et al. (2000) reported that actin and actin binding proteins play a role in the generation of memory, e.g., dynamic actin filaments were found to be essential for the stable long-term potentiation in hippocampus areas. In a search for aberrantly expressed proteins in DS fetal brain using the proteomic approach of 2D-gel electrophoresis, it was found that the expression level of the 20 kDa subunit of the actin related protein complex 2/3 (arp2/3) and of coronin 1 were significantly reduced (Weitzdoerfer et al., 2002). However, according to expression analyses of

different coronins, coronin1 is not assumed to be the major coronin in neural structures (see introduction, section 3.3). Rather, coronin 3, coronin 4 ("Clipin C") and coronin 5 are expressed more abundantly in the brain (Zaphiropoulos et al., 1996; Nakamura et al., 1999). Coronin 3 is enriched in the myelinated areas of mouse brain (M. Stumpf and A. Hasse, unpublished results), the parts containing the nerve fibers built up by axons. Thus, coronin 3 might be important for the organization of neuronal actin networks in processes like axon development, dendrite formation, and growth cone motility. It is known that all these processes require leading edge extension or growth cone protrusion in neuronal cells, which are mainly directed by polymerization or depolymerization of actin filaments in coordination with other cytoskeletal structures (Lambert and Goffinet, 2001). Thus, the analysis of the behavior of coronin 3 during the neuronal differentiation process in cell culture was one aim of these studies.

1 Subcellular localization of coronin 3

The neuroblastoma cell line Neuro-2a was derived from a spontaneous tumor of a strain A albino mouse. One feature of this cell line is that its morphology has similarity with amoeboid stem cells during differentiation. Another characteristic is that it can be easily differentiated *in vitro*. Depending on the stimulus used, Neuro-2a cells develop neurites which are predominantly of the dendrite or axon type (Klebe and Ruddle, 1969). Low serum conditions give rise to mostly axon-like neurites and were used in these studies. Another advantage is the fact that Neuro-2a cells are easily transfected with mammalian expression vectors using common methods, e.g., electroporation or cationic lipids. Therefore, this line was chosen to study the behavior of different full-length and truncated coronin 3 proteins during neuronal differentiation in culture.

The monoclonal anti-coronin 3 antibody K6-444 specifically reacts with the COOH-terminal unique region of coronin 3 in mouse and human cells. Indirect immunostaining of Neuro-2a cells with K6-444 revealed that coronin 3 was partially enriched in the cortical regions. In addition, a strong punctated coronin 3 staining was found in a region close to the nucleus in undifferentiated cells. Interestingly coronin3 was mainly concentrated in the neurites and protrusions in the cell periphery of differentiated cells, although cytoplasmic punctate staining was also observed. However, the amount of cytosolic coronin 3 in differentiated cells was reduced in comparison to undifferentiated cells. Coronin 3 localization in neurites overlapped to

some extent with that of F-actin, although, F-actin appeared to be more restricted to the cortex than coronin 3. A similar localization was also reported for coronin 5 in the human neuroblastoma cell line SH-SY5Y (Nakamura et al., 1999). These data are in agreement with the observation that *Dictyostelium* coronin is reversibly recruited from the cytoplasm and is involved in the rearrangement of the actin network (Gerisch et al., 1995). The differences in the distribution of coronin 3 of undifferentiated and differentiated cells suggest that coronin 3 may be translocated from a cytosolic pool to dynamic cortical regions, e.g., neurite protrusion areas, and may also participate in the regulation of actin filament formation, prolongation or stability in response to still unknown signal transduction pathways. This assumption is confirmed by the subcellular fractionation studies presented in this work, which show an enhanced concentration of coronin 3 in the large particulate fraction of differentiated cells as compared to undifferentiated cells.

On the whole, the localization of coronin 3 in Neuro-2a cells suggest that it could play a role in neuronal extension and growth cone advance required for neuronal plasticity, consistent with the data for other mammalian coronins which are also found at dynamic actin-rich structures of the cell cortex (Parente et al., 1999, Nakamura et al., 1999). These findings thus support the view that the common function of the coronin protein family is in the reorganization of actin networks. The nature of the perinuclear punctate coronin 3 and actin-positive structures is not known. Association of coronin with vesicles was described in *Dictyostelium* (Rauchenberger et al., 1997), however, previous results from our group show that the cytoplasmic structures do not colocalize with markers for vesicles, Golgi apparatus and endoplasmic reticulum (Spoerl et al., 2002). It is possible that the punctate pattern represents preformed protein complexes involved in actin turnover. For example, the Arp2/3 complex has a similar punctate cytoplasmic localization (Welch et al., 1997).

Arp2/3 complex is an evolutionarily conserved protein complex of actin-related proteins (Arp2 and Arp3) and five other subunits involved in the nucleation of actin polymerization (Machesky et al., 1994; Mullins et al., 1997; 1998; Welch et al., 1997; 1998). The Arp2/3 complex is also localized to protruding lamellipodia and to the *Listeria* comet tail (Welch et al., 1997). Recently, it has been demonstrated that yeast coronin (Crn1p) physically interacts with the Arp2/3 complex and may restrict its activity to the sides of actin filaments (Humphries et al., 2002). The authors reported that proper localization of Crn1p to actin patches *in vivo* and association of Crn1p

with the Arp2/3 complex require its COOH-terminal coiled coil domain. Based on sequence alignment, the COOH-terminal region of coronin 3 and Crnp1 shares little homology to each other (10.5%). Whether coronin 3 also interacts with the Arp2/3 complex *in vivo* is unknown.

When expressed as an EGFP fusion protein in Neuro-2a cells, localization was essentially consistent with that of the endogenous protein. Also EGFP-Hcoronin 3 was pronouncedly enriched in neurites and dynamic growth cones, overlapping with actin filaments in those regions, and at punctate structures close to the nucleus. In addition to the localization to the cell periphery, EGFP-Hcoronin 3 as well as the endogenous protein were also found in small actin-rich structures in the perinuclear region in Neuro-2a cells.

Another feature reported for yeast Crn1p is its association with microtubules via its unique region (Goode et al. 1999). The affinity to microtubules is enhanced in the presence of actin filaments. The authors postulated that Crn1p acts as a functional link between the actin and microtubule cytoskeleton. In neuronal cells of mammals, about 30 % of the total protein in neuronal cell is tubulin (Alberts et al., 1994). Axon elongation strongly depends on microtubule structure. Therefore, a possible interaction of coronin 3 with microtubules during the differentiation of Neuro-2a cells was investigated by immunofluorescence. However, no colocalization could be detected. Furthermore, distribution of EGFP-Hcoronin 3 was not affected by drugs that act on the microtubule system, suggesting that in contrast to its yeast orthologue, coronin 3 did not interact with microtubules.

2 Overexpression of full-length and a truncated EGFP-Hcoronin 3 changes cell morphology

An interesting outcome of our studies was the finding that overexpression of EGFP-Hcoronin 3 induced morphological changes in Neuro-2a cells. The most evident effect was these it caused formation of abundant actin-rich filopodia. Furthermore, the neurites were slightly longer than that of untransfected cells. Even more dramatic was the strong inhibitory effect of EGFP-Hcoronin 3 (72-404) that lacked both the NH₂- and COOH-terminus on neurite elongation in Neuro-2a cells. The majority of the cells transfected with this construct had a shorter neurite (between 11 and 20 μm) than that of wild type cells (21-30 μm , Fig. 10). Isopycnic separation of total cell extracts showed that this fusion protein encompassing only the five WD-repeats was

predominantly present in the cytosolic fraction and not in the membrane fraction, which was the case for the full length protein (Fig. 12). Subcellular localization studies confirmed these results. These observations suggest that coronin 3 might be involved in the organization of the neurite actin cytoskeleton, and that exogenous EGFP-Hcoronin 3 (72-404) acts in a dominant-negative fashion by competing with endogenous coronin 3 for putative interacting proteins different from actin or for upstream regulatory signals.

The WD repeat is believed to serve as a motif for protein-protein interaction and have a function in signal transduction by forming multi-protein complexes (Smith et al., 1999). Gerisch et al. (1995) suggested that coronin binds not only to actin but also to other proteins, thus coupling regulatory proteins to the actin-myosin system. Mishima and Nishida (1999) proposed that the coronin core might directly interact with small GTPases and thus block signal pathways to downstream targets. They hypothesized that Xcoronin may function downstream of Rac-mediated intracellular signaling to the actin cytoskeleton. The effects of full-length EGFP-Hcoronin 3 and EGFP-Hcoronin 3 (72-404) on cell morphology can also be explained by the assumption that, similar to yeast coronin, coronin 3 is able to interact with the Arp2/3 complex. Overexpression of the functional full-length protein may lead to enhanced branching of the cortical actin network, while the truncated version that lacks the coiled-coil region responsible for Arp2/3 interaction in yeast may block transduction of upstream signal to the Arp2/3 complex (Humphries et al., 2002). However, this view does not explain why the truncated protein lacking only the coiled coil region did not change the shape of the cells.

3. Oligomerization of the COOH terminus

The COOH-terminal coiled coil domain was suggested to mediate self-interaction of coronins (de Hostos 1999; Goode et al., 1999; Asano et al., 2001). Dimerization was demonstrated for *Xenopus* coronin (Asano et al., 2001). This activity might also be necessary for the F-actin cross-linking and bundling activity of coronin 3. The low speed spin down assay showed that the COOH-terminal amino acids 315-444 lacking the coiled coil region has essentially the same activity as the complete COOH-terminus (315-474) to bundle or crosslink F-actin *in vitro*. This result is confirmed by the light microscopic assay of F-actin suprastructures formed in the presence of either one of these two recombinant proteins. The latter findings suggest

that the complete COOH-terminal polypeptide both bundles and crosslinks F-actin, whereas the COOH-terminal fragment lacking the coiled coil region has mainly F-actin bundling activity.

Gel filtration of both recombinant polypeptides confirmed the self-association mediated by the coiled-coil region. The polypeptide (315-474) containing the coiled coil region (calculated MW 20.2 kDa) migrated as a complex of a molecular mass of more than 60 kDa, probably representing a tri- or tetramer rather than a dimer, whereas the polypeptide (315-444), lacking the coiled coil domain eluted with an apparent mass below 40 kDa, possibly forming dimers and monomers (Fig.13). All these data obtained *in vitro* suggest that coronin 3 COOH-terminal region contains an F-actin binding domain that does not depend on oligomerization.

The data from gel filtration of cytosolic and cytoskeletal fraction reveal that endogenous coronin 3 also behaves as an oligomer *in vivo*, with an apparent mass of about 150-200 kDa. To exclude weaker possible binding partners, coronin 3 was extracted by 0.6 M KCl from both soluble and particulate subcellular fractions. The high ionotropic condition dissolves actin-myosin complexes (Berryman et al., 1995). This suggests that coronin 3 exists exclusively in the form of oligomers also *in vivo* and that oligomerization depends on hydrophobic rather than electrostatic interactions. The gel filtration analyses of cytosolic fractions from HEK 239 cells stably expressing EGFP-Hcoronin 3 and different truncated versions suggest that the COOH-terminus is sufficient and required for incorporation into this complex *in vivo* (Fig.17). This further supports the notion that the observed cytosolic complexes are identical to or at least require coronin 3 homooligomers formed via the coiled coil. Interestingly, expression of truncated EGFP-Hcoronin 3 (1-444) also changes the size of the endogenous coronin 3 complex (Fig.17). One explanation is that exogenously expressed EGFP-tagged protein interacted with endogenous coronin 3 via a region distinct from the coiled coil domain, thus interfering with complex formation. Findings presented in this study indicate that the COOH-terminal non coiled coil region may still form homodimers and that the coronin 3 NH₂-terminus is able to interact with the COOH-terminus *in vitro*. The intermolecular interaction between the NH₂-terminus of exogenous EGFP-coronin 3 and the COOH-terminus of endogenous coronin 3 might be involved in the formation of cytosolic complex.

It is possible that different coronins might form different homomers, which may be related to their specific function, e.g. by extending the number of multiple protein-

protein interactions. In a similar manner to coronin 3, the COOH-terminal region of mammalian VASP, vasodilator-stimulated phosphoprotein, which is implicated in the regulation of the actin cytoskeleton (Bachmann et al., 1999), has been shown to mediate oligomerization, F-actin binding, and cross-linking activities. The COOH-terminus of coronin 3 has characteristics similar to that of VASP, which also comprises a putative coiled coil region and contains one F-actin binding site per molecule. The coiled coil mediates VASP tetramerization, which is essential for F-actin bundling. The COOH-terminus of coronin 3 exhibits a weak homology to that of VASP. This might indicate a functional relationship between both molecules. It is as yet unknown whether coronin 3 also possesses F-actin bundling or cross-linking activity *in vivo*. However, the fact that overexpression of EGFP-Hcoronin 3 in Neuro-2a cells induces the formation of abundant actin-rich filopodia and longer neurite projections (Fig. 8, 10) could support this assumption.

The data presented here provide no information about the composition of cytoskeletal coronin 3 complexes except for the fact that coronin 3 seems to be present in the form of homooligomers also in the particle-associated fraction. For coronin 5, it has been reported that this protein is a component of the cross-bridge between the actin cytoskeleton and that of the plasma membrane and interacts with the focal adhesion protein vinculin in human neuroblastoma cells (Nakamura et al., 1999). In contrast to this, coronin 3 did not localize to focal adhesions in our experiments. To further analyze the change of cytosolic and cytoskeletal coronin 3 complex *in vivo*, GTPase/protein kinase activators or inhibitors can be used to identify regulators of the equilibrium of coronin 3 in both subcellular pools.

4 Definition of an F-actin binding domain of coronin 3

Fluorescence microscopy revealed that EGFP-Hcoronin 3 (72-474) lacking the NH₂-terminus and of EGFP-Hcoronin 3 (1-315) lacking the COOH-terminus failed to colocalize with F-actin. The major part of these EGFP fusion proteins was diffusely distributed throughout the cytosol. EGFP-Hcoronin 3 (1-444) showed partial localization in outgrowing neurites, and expression of this polypeptide induced the formation of extra filopodia in differentiated Neuro-2a cells. The most remarkable change in localization was found for the EGFP-tagged polypeptide (72-404) that contained only the WD-repeat core region. This protein not only failed to colocalize with actin filaments but also affected the shape of the cells. EGFP-Hcoronin 3 (315-

474) containing the COOH-terminus alone retained weak colocalization with cortical F-actin. All these observations suggest that both termini are involved in association with F-actin and WD-repeats alone seem not to participate in F-actin interaction. This observation resembles that for *Xenopus* coronin (Mishima et al., 1999).

4.1 *In vitro* F-actin binding assay

Although association of coronins with F-actin has been demonstrated *in vitro* and *in vivo*, the data about the regions involved in actin binding *in vitro* and *in vivo* are controversial. In yeast Crn1p, the highly conserved part including the WD-repeats are regarded as possible actin binding domain (Goode et al., 1999), whereas the WD repeat region of *Xenopus* coronin (Xcoronin) showed neither association with actin filaments *in vitro* nor colocalization with F-actin *in vivo* (Mishima et al., 1999). Truncation of either NH₂-terminus or COOH-terminus resulted in a significant decrease in the affinity of Xcoronin to F-actin. Therefore, both NH₂-terminal and COOH-terminal region are possible candidate regions for interaction with F-actin. The COOH terminus of coronin 3 contains regions homologous to *Xenopus* coronin as well as unique sequences. Furthermore, sequence analysis of amino acids 315-474, containing the unique region revealed homology to other actin binding proteins such as COOH-terminus of VASP, to myosins and tropomyosins. The data suggest that the polypeptide containing the residues 315-474 and 315-444 are able to bind rabbit skeletal muscle filamentous actin *in vitro* with similar binding affinity (K_d 7.1 μ M for polypeptide 315-474; K_d 8.5 μ M for polypeptide 315-444 respectively). This means that the amino acids 315-444 were sufficient for F-actin binding *in vitro* and the coiled coil domain has no significant influence on this interaction. The calculated dissociation constant (K_d 7.1 μ M for full length COOH-terminus) is similar to that of the actin binding domain (ABD) of alpha-actinin (K_d 4 μ M) and lower than that of the ABD of dystrophin (K_d 44 μ M) (Way et al., 1992a; 1992b). Compared with yeast Crn1p (K_d 6 nM, Goode et al., 1999), both polypeptides have a much lower affinity to F-actin. One reason could be that the K_d , obtained from F-actin cosedimentation assay, represents the affinity of the isolated COOH-terminal fragment in contrast to that of the full-length yeast Crn1p. Another explanation for the different affinity may be due to the different experimental conditions. We did not use phalloidin to stabilize actin filaments during spin-down assays, and the K_d may be dependent on the stability of actin filaments *in vitro*. Furthermore, for quantification of bound and free

proteins, the corresponding band in Coomassie-stained gels was determined by Molecular Dynamics laser Scanner in our experiments instead of immunoblotting for determining K_d for yeast Crn1p.

One of the surprising outcomes of this study is that the binding of both polypeptides to F-actin is saturated at a molar ratio of 1 COOH-terminal polypeptide to 3 actin monomers. This result suggests that the COOH-terminal region either contains three actin binding sites or forms more F-actin binding sites through intermolecular interaction. Most actin binding assays reported a stoichiometry of 1 to 1, e.g. for the spectrin proteins of the α -actinin superfamily (Moore and Kendrick-Jones, 2000). The fact that the 6×His epitopic tag could enhance the affinity of fusion proteins to F-actin should also be taken into account (Stock et al., 1999). Poly-cations such as poly-histidine and poly-lysine have been reported to bind and bundle actin filaments (Tang et al., 1996). This could result from the electrostatic interaction of the positively charged residues of the 6×His tag with the negatively charged actin filaments. Thus, the change in pI of recombinant COOH-terminal fragments has been taken into account by predicting the pI change based on protein sequence analysis. It was found that the 6×His epitopic tag does not significantly change the overall positive charges which could have an effect on the interaction with F-actin. The pI of coronin 3 (315-474) is 8.57 without 6×His tag and 8.59 with 6×His tag. The pI of coronin 3 (315-444) is 8.37 without 6×His tag and 8.41 with 6×His tag. The pI of coronin 3 (1-71) is 10.01 without 6×His tag and 10.03 with 6×His tag. The fact that 6×His tagged NH₂-terminal fragment (1-71) does not bind to F-actin under the same experimental condition rules out the possibility that the His tag might serve as a mediator for the association of the fusion protein with F-actin.

4.2 Interaction of the NH₂- and COOH-terminal region

Cosedimentation assay of the combined NH₂- and COOH-terminal peptides *in vitro* suggests that the NH₂-terminus interacts with the COOH-terminus (Fig.32,). This observation is also confirmed in coimmunoprecipitation experiments *in vivo* (A. Hasse, personal communication). The observation that addition of the NH₂-terminus to the COOH-terminal fragment (315-444) pronouncedly reduced F-actin binding of this COOH-terminal part may indicate that the region of the COOH-terminus necessary for the binding to the NH₂-terminus and to F-actin are close to each other and may even overlap (Fig.33). However, no clear reduction of F-actin

cosedimentation was found for the complete COOH-terminus in the presence of the NH₂-terminus. Rather, the complete COOH-terminus (residues 315-474) seemed to interact with F-actin and the NH₂-terminus simultaneously (Fig. 33), whereas the fragment (315-444) did not. This means that although amino acids 315-444 were sufficient for F-actin binding *in vitro*, the coiled coil region also has an influence on this interaction. One explanation is that the coiled coil part provides additional F-actin-interacting sites. Alternatively, the oligomerization of the complete COOH-terminus may allow for simultaneous interaction with both the N-terminus and F-actin, which is not possible for the monomer. Furthermore, binding of the oligomers by more actin binding sites may allow for synergistic interaction with F-actin.

In contrast to this, it is not possible to draw conclusions for the *in vivo* role of the NH₂-terminus. However, the failure of the NH₂-terminally deleted constructs to colocalize with F-actin *in vivo* could suggest a regulatory role of the first 71 amino acids in the spatial regulation of F-actin binding. It is also possible that intramolecular interactions between NH₂- and COOH-terminus are necessary for the proper formation of the WD40-propeller structure. On the other hand, intermolecular interactions between NH₂ and COOH termini of different coronin 3 molecules could be involved in the stable or transient interaction with F-actin fibers in a way similar to ERM proteins (Bretscher 1999). However, these putative roles for the NH₂-terminus *in vivo* do not explain why the NH₂-terminally truncated EGFP-Hcoronin 3 (72-474) failed to be enriched in outgrowing neurites, whereas the even shorter version, EGFP-Hcoronin 3 (315-474) was in part found at the cell periphery. The truncation of the NH₂-terminus may also lead to problems in protein folding *in vivo*, and misfolding of the whole protein could also abolish the functions of the COOH-terminus.

5. Phosphorylation of coronin 3

Subcellular distribution of coronin 3 in undifferentiated and differentiated Neuro-2a cells showed that enhanced translocation of the protein from a cytosolic pool to the submembranous cytoskeleton takes place during differentiation. Immunofluorescence demonstrated that endogenous coronin 3 is enriched along the axon and at the growth cone (Fig. 6, 11). Growth cone development is related to leading edge extension (Lambert and Goffinet 2001). The leading edge extension is based on microfilament polymerization that is orchestrated by different actin binding proteins upon extracellular or intracellular cues. Therefore, it is tempting to propose that

coronin 3 might play a functional role in neurite outgrowth. However, it is unknown which events lead to accumulation of coronin 3 in outgrowing neuritis. Coronin 3 is present in the form of homooligomers both in the cytosolic and the particulate fraction, and deletion of the coiled-coil responsible for self-association leads to impaired membrane localization. Thus, the shift of the protein between both compartments is most likely not regulated by its oligomerization, although self-association is a prerequisite for correct localization. It was thus attempted to identify other processes governing translocation of the protein. For several reasons, phosphorylation is one likely factor. It has been reported that protein kinase C-dependent phosphorylation of human coronin 1 occurs in neutrophils. Incorporation of coronin 1 into a complex of p40^{phox} and PKC (Grogan et al., 1997) is a prerequisite for its phosphorylation, which in turn is necessary for appropriate localization in the cytosol, whereas coronin 1 in the cytoskeleton fraction was not phosphorylated (Grogan et al., 1997; Reeves et al., 1999). PKC inhibitors inhibit coronin 1 phosphorylation, thus blocking the dissociation of coronin 1 as well as F-actin from phagosomes (Itoh et al., 2002). Therefore, the authors hypothesized that PKC-mediated phosphorylation of coronin 1 induces its dissociation from phagosomes, which could be essential for the fusion of phagosomes with lysosomes. Furthermore, coronin 2_{se}, an isoform of coronin 2, seems to be also regulated by PKC in rabbit gastric parietal cells. In contrast to coronin 1, the phosphorylation of coronin 2_{se} induces the recruitment of this protein into the actin network, and results in the formation of curtain-like lamellopodia (Parente et al., 1999).

For coronin 3, 2D electrophoresis revealed that the pI of the cytosolic protein is different from that in the particulate fraction not only in undifferentiated but also in differentiated cells. The bulk of soluble coronin 3 has a pI more acidic (5.2-5.5) than the predicted one (6.65). The triplet or quartet-like spot pattern in the 2D-gels suggests that cytosolic coronin 3 is phosphorylated at several sites. In contrast to this, the majority of coronin 3 in the particulate fraction was unphosphorylated and showed the predicted pI. Although coronin 3 contains eight possible PKC phosphorylation sites (Fig. 18), undifferentiated Neuro-2a cells treated with the PKC inhibitor revealed a similar spot pattern as untreated cells in 2D gels. Also, the addition of the PKC activator PMA to differentiated Neuro-2a cells does not significantly change the 2D pattern. Furthermore, treatment of EGFP-Hcoronin 3 expressing differentiated cells with these compounds did not cause obvious changes

in the distribution of the protein. Expectedly, actin filaments seemed to be sensitive to the PKC inhibitor, which was a control for the activity of this compound (Djafarzadeh et al., 1997; Meberg et al., 1998). Phalloidin-positive punctuate structures accumulated in the cell body after addition of bisindolylmaleimide, showing that the drug was functionally active. These findings are different from the data for coronin 1 (Grogan et al., 1997; Reeves et al., 1999) and coronin 2_{se} (Parente et al., 1999). One explanation is that the effect of PMA or bisindolylmaleimide on the putative phosphorylation of coronin 3 might be time dependent. On the other hand, Neuro-2a cells are sensitive to toxic effects of PMA and bisindolylmaleimide. Most cells died after exposure to PMA for more than 20 minutes. However, this time is usually more than enough to observe affects of PMA on PKC. Probably, other approaches, like phosphoamino acid analysis of coronin 3 extracted from ³²P-labeled cells or mutation of suspected phosphorylation sites will be helpful tools for the characterization of the pathways and kinases involved in coronin 3 phosphorylation and regulation.

V Summary

Coronin, an F-actin binding protein, is expressed in a variety of organisms from *Dictyostelium* to humans. The mammalian coronin family comprises at least seven members, six of which show a similar size and domain structure. Their expression patterns are tissue-specific but overlapping, implying that they possess diverse functions. Little is known about mammalian coronin 3, which was studied in this work. This protein is expressed in different amounts in many mouse tissues, being most abundant in the brain. Due to this, mouse neuroblastoma (Neuro-2a) cells were chosen for the *in vivo* studies presented here.

By immunofluorescence, endogenous coronin 3 was detected both in F-actin-rich structures like growth cones, neurites and intracellular small particles, and in the cytosol. Treatment of cells with colchicine and taxol did not provide any hints that coronin 3 localization depends on microtubules. Proper localization of EGFP-Hcoronin 3 required both the NH₂- and COOH-terminus. Expression of EGFP-Hcoronin 3 (72-404) that lacked both termini had an inhibitory effect on neurite elongation, which was not the case for the proteins truncated at either terminus. This suggests that coronin 3 is involved in the generation of F-actin-rich cortical extensions.

Subcellular fractionation and 2D gel electrophoresis demonstrated that during differentiation of Neuro-2a cells, endogenous coronin 3 translocated from a phosphorylated cytosolic pool to an unphosphorylated membrane- and F-actin associated fraction. A role of PKC in the regulation of other coronins has been reported in the literature. However, addition of the PKC activator PMA and the inhibitor bisindolylmaleimide to differentiated Neuro-2a cells did not significantly change the pI value of coronin 3 in cytosolic and cytoskeletal fractions, nor did it change the localization of the protein. This indicates that the phosphorylation of coronin 3 is independent of protein kinase C.

In further experiments, the role of distinct coronin 3 domains for protein function was tested *in vitro* and *in vivo*. It turned out that the C-terminal part harbored several features required for molecular interactions. Gel filtration analysis showed that, in contrast to other coronins, coronin 3 is exclusively extracted as an oligomer from both the cytosolic and cytoskeletal fraction. Under native conditions, the cytosolic pool resides in a large complex and the COOH-terminal coiled-coil is essential for the formation of this complex. The COOH-terminal region mediated oligomerization of

recombinant fragments *in vitro*. Furthermore, F-actin cosedimentation assays showed that the COOH-terminal amino acid residues 315-444 without the coiled coil domain are sufficient for F-actin binding and crosslinking *in vitro*. In contrast to this, the NH₂-terminal region had no affinity for F-actin. The fragment coronin 3 (315-474) that contained the coiled coil was capable of recruiting the NH₂-terminal coronin 3 (1-71) domain to actin filaments *in vitro*, implying that intramolecular or intermolecular interactions between the NH₂- and COOH-terminal parts might be involved in the association with actin filaments *in vivo*.

VI Zusammenfassung

Coronin, ein F-Aktin bindendes Protein, ist in eukaryotischen Organismen von *Dictyostelium* bis *Homo sapiens* weitverbreitet. In Säugetieren existiert eine Familie Coronin-ähnlicher Proteine mit 7 bisher bekannten Mitgliedern. Die Coronin-Homologe zeigen gewebsspezifische, jedoch teilweise überlappende Expressionsmuster. Dies deutet darauf hin, dass die Säuger-Coronine divergierende Funktionen entwickelt haben, die über die in Einzellern bekannten hinausgehen. In dieser Arbeit wurde die Funktion von Coronin 3 untersucht, die noch nahezu unbekannt ist. Coronin 3 ist in vielen Mausgeweben exprimiert, jedoch am stärksten im Gehirn. Es wurden daher Neuro-2a Neuroblastomzellen für die *in vivo*-Experimente ausgewählt.

Immunfluoreszenz zeigte, dass das endogene Coronin 3 einerseits an F-Aktinreichen Strukturen, z.B. „growth cones“, Neuriten und intrazellulären Partikeln, andererseits auch stark zytosolisch lokalisiert ist. Die Behandlung der Zellen mit Colchicin und Taxol ergab keine Hinweise auf eine Mikrotubuli-abhängige Lokalisierung von Coronin 3 wie sie für das Hefehomolog beschrieben wurde. Die Untersuchung von verkürzten EGFP-Hcoronin 3-Fusionsproteinen zeigte, dass sowohl der NH₂- als auch der COOH-Terminus notwendig für die korrekte Lokalisation sind. Expression des Proteins EGFP-Hcoronin 3 (72-404), das nur die zentrale WD40-repeat-Domäne enthält, zeigte einen hemmenden Effekt auf die Neuritenelongation, welcher bei Deletion des NH₂- oder COOH-Terminus alleine nicht auftrat. Dies deutet darauf hin, dass Coronin 3 bei der Generation von F-Aktinreichen kortikalen Strukturen eine Rolle spielt.

Subzelluläre Fraktionierung und 2D Gel-Elektrophorese zeigten, dass endogenes Coronin 3 während der Neuro-2a Differenzierung von einer phosphorylierten zytosolischen Fraktion zu einer dephosphorylierten Membran- und F-Aktin-assoziierten Fraktion wandert. Im Gegensatz zu anderen Coroninen, für die in der Literatur PKC-abhängige Phosphorylierung dokumentiert ist, hatten weder der Proteinkinase C-Aktivator PMA noch der spezifische Inhibitor Bisindolylmaleimid einen deutlichen Einfluß auf den pI von Coronin 3 in zytosolischen und partikulären Fraktionen oder auf seine Lokalisation in Neuro-2a-Zellen. Dies weist darauf hin, dass die Phosphorylierung des Proteins von PKC unabhängig ist.

Weiterhin wurde die Rolle bestimmter Coronin 3-Domänen *in vitro* und *in vivo* untersucht. Es zeigte sich, dass die COOH-terminale Region für unterschiedliche Eigenschaften wichtig ist. Gelfiltrationsergebnisse weisen darauf hin, dass Coronin 3 im Gegensatz zu anderen Coroninen ausschließlich als Oligomer in der Zelle vorkommt. Unter nativen Bedingungen liegt Coronin 3 im Zytosol als Komplex vor, dessen Bildung von der COOH-terminalen coiled coil Domäne abhängt. Die letzten 30 Aminosäuren waren auch für die Oligomerisierung des rekombinanten COOH-Terminus *in vitro* notwendig.

F-Aktin-Kosedimentationsversuche ergaben, dass die COOH-terminalen Aminosäuren 315-444 außerdem für die Bindung an Aktinfilamente hinreichend sind. Dagegen zeigten die NH₂-terminalen Aminosäuren 1-71 keine Assoziation mit Mikrofilamenten. Es konnte aber nachgewiesen werden, dass das COOH-terminale Fragment (315-474) den NH₂-terminus (1-71) zu Aktinfilamenten rekrutieren kann. Dies deutet darauf hin, dass intramolekulare oder intermolekulare Interaktionen zwischen NH₂- und COOH-Terminus bei der Assoziation mit Aktinfilamenten eine Rolle spielen.

VII. References

- Adams, A.E., Shen, W., Lin, C.S., Leavitt, J., Matsudaira, P.** (1995) Isoform-specific complementation of the yeast *sac6* null mutation by human fimbrin. *Mol Cell Biol* **15**, 69-75.
- Alberts, B., Bray, D., Lewis, J., Raff, M., Roberts, K., Watson, J.D.** (1994) *Molecular Biology of the Cell*, 3rd edition, Garland Publishing New York and London
- Asano, S., Mishima, M., Nishida, E.** (2001) Coronin forms a stable dimer through its C-terminal coiled coil region: an implicated role in its localization to cell periphery. *Genes Cells* **6**, 225-35.
- Bachmann, C., Fischer, L., Walter, U., Reinhard, M.** (1999) The EVH2 domain of the vasodilator-stimulated phosphoprotein mediates tetramerization, F-actin binding, and actin bundle formation. *J Biol Chem* **274**, 23549-57.
- Bailly, M., Ichetovkin, I., Grant, W., Zebda, N., Machesky, L.M., Segall, J.E., Condeelis, J.** (2001) The F-actin side binding activity of the Arp2/3 complex is essential for actin nucleation and lamellipod extension. *Curr Biol* **11**, 620-5.
- Becker, L.E., Armstrong, D.L., Chan, F.** (1986) Dendritic atrophy in children with Down's syndrome. *Ann Neurol* **20**, 520-6.
- Becker, L., Mito, T., Takashima, S., Onodera, K.** (1991) Growth and development of the brain in Down syndrome. *Prog Clin Biol Res* **373**, 133-52.
- Berryman, M., Gary, R., Bretscher, A.** (1995) Ezrin oligomers are major cytoskeletal components of placental microvilli: a proposal for their involvement in cortical morphogenesis. *J Cell Biol* **131**, 1231-42.
- Bolton, S.J., Barry, S.T., Mosley, H., Patel, B., Jockusch, B.M., Wilkinson, J.M., Critchley, D.R.** (1997) Monoclonal antibodies recognizing the N- and C-terminal regions of talin disrupt actin stress fibers when microinjected into human fibroblasts. *Cell Motil Cytoskeleton* **36**, 363-76.
- Bradford, M.M.** (1976) A rapid and sensitive method for the quantitation of microgram quantities of protein utilizing the principle of protein-dye binding. *Anal Biochem* **72**, 248-54.
- Bretscher, A.** (1999) Regulation of cortical structure by the ezrin-radixin-moesin protein family. *Curr Opin Cell Biol* **11**, 109-16.
- Bricheux, G., Coffe, G., Bayle, D., Bruggerolle, G.** (2000) Characterization, cloning and immunolocalization of a coronin homologue in *Trichomonas vaginalis*. *Eur J Cell Biol* **79**, 413-22.
- Brown, M.R., Chew, C.S.** (1989) Carbachol-induced protein phosphorylation in parietal cells: regulation by [Ca²⁺]_i. *Am J Physiol* **257**, G99-110.

- Chew, C.S., Zhou, C.J., Parente, J.A., Jr.** (1997) Ca²⁺-independent protein kinase C isoforms may modulate parietal cell HCl secretion. *Am J Physiol* **272**, G246-56.
- Condeelis, J.** (1995) Elongation factor 1 alpha, translation and the cytoskeleton. *Trends Biochem Sci* **20**, 169-70.
- David, V., Gouin, E., Troys, M.V., Grogan, A., Segal, A.W., Ampe, C., Cossart, P.** (1998) Identification of cofilin, coronin, Rac and capZ in actin tails using a *Listeria* affinity approach. *J Cell Sci* **111**, 2877-84.
- de Hostos, E.L., Bradtke, B., Lottspeich, F., Guggenheim, R., Gerisch, G.** (1991) Coronin, an actin binding protein of *Dictyostelium discoideum* localized to cell surface projections, has sequence similarities to G protein beta subunits. *Embo J* **10**, 4097-104.
- de Hostos, E.L., Rehfuess, C., Bradtke, B., Waddell, D.R., Albrecht, R., Murphy, J., Gerisch, G.** (1993) *Dictyostelium* mutants lacking the cytoskeletal protein coronin are defective in cytokinesis and cell motility. *J Cell Biol* **120**, 163-73.
- de Hostos, E.L.** (1999) The coronin family of actin-associated proteins. *Trends Cell Biol* **9**, 345-50.
- Didichenko, S.A., Segal, A.W., Thelen, M.** (2000) Evidence for a pool of coronin in mammalian cells that is sensitive to PI 3-kinase. *FEBS Lett* **485**, 147-52.
- Djafarzadeh, S., Niggli, V.** (1997) Signaling pathways involved in dephosphorylation and localization of the actin-binding protein cofilin in stimulated human neutrophils. *Exp Cell Res* **236**, 427-35.
- Engidawork, E., Lubec, G.** (2001) Protein expression in Down syndrome brain. *Amino Acids* **21**, 331-61.
- Ferrari, G., Langen, H., Naito, M., Pieters, J.** (1999) A coat protein on phagosomes involved in the intracellular survival of mycobacteria. *Cell* **97**, 435-47.
- Fratti, R.A., Vergne, I., Chua, J., Skidmore, J., Deretic, V.** (2000) Regulators of membrane trafficking and *Mycobacterium tuberculosis* phagosome maturation block. *Electrophoresis* **21**, 3378-85.
- Fuchs, E., Weber, K.** (1994) Intermediate filaments: structure, dynamics, function, and disease. *Annu Rev Biochem* **63**, 345-82.
- Fukui, Y., Engler, S., Inoue, S., de Hostos, E.L.** (1999) Architectural dynamics and gene replacement of coronin suggest its role in cytokinesis. *Cell Motil Cytoskeleton* **42**, 204-17.
- Fukui, Y., de Hostos, E., Yumura, S., Kitanishi-Yumura, T., Inou** (1999) Architectural dynamics of F-actin in eupodia suggests their role in invasive locomotion in *Dictyostelium*. *Exp Cell Res* **249**, 33-45.

- Gaertner, A., Ruhnau, K., Schroer, E., Selve, N., Wanger, M., Wegner, A.** (1989) Probing nucleation, cutting and capping of actin filaments. *J Muscle Res Cell Motil* **10**, 1-9.
- Garcia-Higuera, I., Fenoglio, J., Li, Y., Lewis, C., Panchenko, M.P., Reiner, O., Smith, T.F., Neer, E.J.** (1996) Folding of proteins with WD-repeats: comparison of six members of the WD-repeat superfamily to the G protein beta subunit. *Biochemistry* **35**, 13985-94.
- Gerisch, G., Albrecht, R., De Hostos, E., Wallraff, E., Heizer, C., Kreitmeier, M., Muller-Taubenberger, A.** (1993) Actin-associated proteins in motility and chemotaxis of Dictyostelium cells. *Symp Soc Exp Biol* **47**, 297-315.
- Gerisch, G., Albrecht, R., Heizer, C., Hodgkinson, S., Maniak, M.** (1995) Chemoattractant-controlled accumulation of coronin at the leading edge of Dictyostelium cells monitored using a green fluorescent protein- coronin fusion protein. *Curr Biol* **5**, 1280-5.
- Goode, B.L., Wong, J.J., Butty, A.C., Peter, M., McCormack, A.L., Yates, J.R., Drubin, D.G., Barnes, G.** (1999) Coronin promotes the rapid assembly and cross-linking of actin filaments and may link the actin and microtubule cytoskeletons in yeast. *J Cell Biol* **144**, 83-98.
- Goode, B.L., Drubin, D.G., Barnes, G.** (2000) Functional cooperation between the microtubule and actin cytoskeletons. *Curr Opin Cell Biol* **12**, 63-71.
- Grogan, A., Reeves, E., Keep, N., Wientjes, F., Totty, N.F., Burlingame, A.L., Hsuan, J.J., Segal, A.W.** (1997) Cytosolic phox proteins interact with and regulate the assembly of coronin in neutrophils. *J Cell Sci* **110**, 3071-81.
- Hacker, U., Albrecht, R., Maniak, M.** (1997) Fluid-phase uptake by macropinocytosis in Dictyostelium. *J Cell Sci* **110**, 105-12.
- Hanahan, D.** (1983) Studies on transformation of Escherichia coli with plasmids. *J Mol Biol* **166**, 557-80.
- Haus, U., Hartmann, H., Trommler, P., Noegel, A.A., Schleicher, M.** (1991) F-actin capping by cap32/34 requires heterodimeric conformation and can be inhibited with PIP2. *Biochem Biophys Res Commun* **181**, 833-9.
- Heil-Chapdelaine, R.A., Tran, N.K., Cooper, J.A.** (1998) The role of Saccharomyces cerevisiae coronin in the actin and microtubule cytoskeletons. *Curr Biol* **8**, 1281-4.
- Holmes, D.S., Quigley, M.** (1981) A rapid boiling method for the preparation of bacterial plasmids. *Anal Biochem* **114**, 193-7.
- Hug, C., Jay, P.Y., Reddy, I., McNally, J.G., Bridgman, P.C., Elson, E.L., Cooper, J.A.** (1995) Capping protein levels influence actin assembly and cell motility in dictyostelium. *Cell* **81**, 591-600.

- Humphries, C.L., Balcer, H.I., D'Agostino, J.L., Winsor, B., Drubin, D.G., Barnes, G., Andrews, B.J., Goode, B.L.** (2002) Direct regulation of Arp2/3 complex activity and function by the actin binding protein coronin. *J Cell Biol* **159**, 993-1004.
- Iizaka, M., Han, H.J., Akashi, H., Furukawa, Y., Nakajima, Y., Sugano, S., Ogawa, M., Nakamura, Y.** (2000) Isolation and chromosomal assignment of a novel human gene, CORO1C, homologous to coronin-like actin-binding proteins. *Cytogenet Cell Genet* **88**, 221-4.
- Itoh, S., Suzuki, K., Nishihata, J., Iwasa, M., Oku, T., Nakajin, S., Nauseef, W.M., Toyoshima, S.** (2002) The role of protein kinase C in the transient association of p57, a coronin family actin-binding protein, with phagosomes. *Biol Pharm Bull* **25**, 837-44.
- Kaiser, D.A., Pollard, T.D.** (1996) Characterization of actin and poly-L-proline binding sites of *Acanthamoeba* profilin with monoclonal antibodies and by mutagenesis. *J Mol Biol* **256**, 89-107.
- Klebe, R.J., Ruddle, F.H.** (1969) Neuroblastoma: Cell culture analysis of a differentiating stem cell system. *J Cell Biol* **43**, 69A
- Kobayashi, T., Tsunawaki, S., Seguchi, H.** (2001) Evaluation of the process for superoxide production by NADPH oxidase in human neutrophils: evidence for cytoplasmic origin of superoxide. *Redox Rep* **6**, 27-36.
- Korneeva, N.L., Jockusch, B.M.** (1996) Light microscopic analysis of ligand-induced actin filament suprastructures. *Eur J Cell Biol* **71**, 351-5.
- Krause, M., Sechi, A.S., Konradt, M., Monner, D., Gertler, F.B., Wehland, J.** (2000) Fyn-binding protein (Fyb)/SLP-76-associated protein (SLAP), Ena/vasodilator-stimulated phosphoprotein (VASP) proteins and the Arp2/3 complex link T cell receptor (TCR) signaling to the actin cytoskeleton. *J Cell Biol* **149**, 181-94.
- Kreis, T., Vale, R.** (1999) Guidebook to the Cytoskeletal and Motor Proteins 2nd edition, A Sambrook & Tooze publication at Oxford University Press
- Krucker, T., Siggins, G.R., Halpain, S.** (2000) Dynamic actin filaments are required for stable long-term potentiation (LTP) in area CA1 of the hippocampus. *Proc Natl Acad Sci U S A* **97**, 6856-61.
- Kung, C., Thomas, M.L.** (1999) Genomic organization and chromosomal localization of mouse coronin-1. *Mamm Genome* **10**, 523-5.
- Kwiatkowski, D.J., Stossel, T.P., Orkin, S.H., Mole, J.E., Colten, H.R., Yin, H.L.** (1986) Plasma and cytoplasmic gelsolins are encoded by a single gene and contain a duplicated actin-binding domain. *Nature* **323**, 455-8.
- Laemmli, U.K.** (1970) Cleavage of structural proteins during the assembly of the head of bacteriophage T4. *Nature* **227**, 680-5.
- Lambert de Rouvroit, C., Goffinet, A.M.** (2001) Neuronal migration. *Mech Dev* **105**,

47-56.

Lewis, A.K., Bridgman, P.C. (1992) Nerve growth cone lamellipodia contain two populations of actin filaments that differ in organization and polarity. *J Cell Biol* **119**, 1219-43.

Machesky, L.M., Cole, N.B., Moss, B., Pollard, T.D. (1994) Vaccinia virus expresses a novel profilin with a higher affinity for polyphosphoinositides than actin. *Biochemistry* **33**, 10815-24.

Machesky, L.M., Reeves, E., Wientjes, F., Mattheyse, F.J., Grogan, A., Totty, N.F., Burlingame, A.L., Hsuan, J.J., Segal, A.W. (1997) Mammalian actin-related protein 2/3 complex localizes to regions of lamellipodial protrusion and is composed of evolutionarily conserved proteins. *Biochem J* **328**, 105-12.

Machesky, L.M., Way, M. (1998) Actin branches out. *Nature* **394**, 125-6.

Machesky, L.M., Insall, R.H. (1998) Scar1 and the related Wiskott-Aldrich syndrome protein, WASP, regulate the actin cytoskeleton through the Arp2/3 complex. *Curr Biol* **8**, 1347-56.

Maniak, M., Rauchenberger, R., Albrecht, R., Murphy, J., Gerisch, G. (1995) Coronin involved in phagocytosis: dynamics of particle-induced relocalization visualized by a green fluorescent protein Tag. *Cell* **83**, 915-24.

Meberg, P.J., Ono, S., Minamide, L.S., Takahashi, M., Bamburg, J.R. (1998) Actin depolymerizing factor and cofilin phosphorylation dynamics: response to signals that regulate neurite extension. *Cell Motil Cytoskeleton* **39**, 172-90.

Meyer, G., Feldman, E.L. (2002) Signaling mechanisms that regulate actin-based motility processes in the nervous system. *J Neurochem* **83**, 490-503.

Mishima, M., Nishida, E. (1999) Coronin localizes to leading edges and is involved in cell spreading and lamellipodium extension in vertebrate cells. *J Cell Sci* **112**, 2833-42.

Moores, C.A., Keep, N.H., Kendrick-Jones, J. (2000) Structure of the utrophin actin-binding domain bound to F-actin reveals binding by an induced fit mechanism. *J Mol Biol* **297**, 465-80.

Morrisette, N.S., Gold, E.S., Guo, J., Hamerman, J.A., Ozinsky, A., Bedian, V., Aderem, A.A. (1999) Isolation and characterization of monoclonal antibodies directed against novel components of macrophage phagosomes. *J Cell Sci* **112**, 4705-13.

Mullins, R.D., Heuser, J.A., Pollard, T.D. (1998) The interaction of Arp2/3 complex with actin: nucleation, high affinity pointed end capping, and formation of branching networks of filaments. *Proc Natl Acad Sci U S A* **95**, 6181-6.

Muralikrishna, T., Begum, Z., Swamy, C.V., Khar, A. (1998) Molecular cloning and characterization of a tumor rejection antigen from rat histiocytoma, AK-5. *DNA Cell*

Biol **17**, 603-12.

Nagasaki, A., de Hostos, E.L., Uyeda, T.Q. (2002) Genetic and morphological evidence for two parallel pathways of cell- cycle-coupled cytokinesis in Dictyostelium. *J Cell Sci* **115**, 2241-51.

Nakamura, T., Takeuchi, K., Muraoka, S., Takezoe, H., Takahashi, N., Mori, N. (1999) A neurally enriched coronin-like protein, ClipinC, is a novel candidate for an actin cytoskeleton-cortical membrane-linking protein. *J Biol Chem* **274**, 13322-7.

Neujahr, R., Heizer, C., Gerisch, G. (1997) Myosin II-independent processes in mitotic cells of Dictyostelium discoideum: redistribution of the nuclei, re-arrangement of the actin system and formation of the cleavage furrow. *J Cell Sci* **110**, 123-37.

Nobes, C.D., Hall, A. (1995) Rho, rac, and cdc42 GTPases regulate the assembly of multimolecular focal complexes associated with actin stress fibers, lamellipodia, and filopodia. *Cell* **81**, 53-62.

Noegel, A.A., Luna, J.E. (1995) The Dictyostelium cytoskeleton. *Experientia* **51**, 1135-43.

Noegel, A.A., Schleicher, M. (2000) The actin cytoskeleton of Dictyostelium: a story told by mutants. *J Cell Sci* **113**, 759-66.

Oku, T., Itoh, S., Okano, M., Suzuki, A., Suzuki, K., Nakajin, S., Tsuji, T., Nauseef, W.M., Toyoshima, S. (2003) Two Regions Responsible for the Actin Binding of p57, a Mammalian Coronin Family Actin-Binding Protein. *Biol Pharm Bull* **26**, 409-16.

Okumura, M., Kung, C., Wong, S., Rodgers, M., Thomas, M.L. (1998) Definition of family of coronin-related proteins conserved between humans and mice: close genetic linkage between coronin-2 and CD45- associated protein. *DNA Cell Biol* **17**, 779-87.

Olmsted, J.B., Carlson, K., Klebe, R., Ruddle, F., Rosenbaum, J. (1970) Isolation of microtubule protein from cultured mouse neuroblastoma cells. *Proc Natl Acad Sci* **65**, 129-36.

Parente, J.A., Jr., Chen, X., Zhou, C., Petropoulos, A.C., Chew, C.S. (1999) Isolation, cloning, and characterization of a new mammalian coronin family member, coroninse, which is regulated within the protein kinase C signaling pathway. *J Biol Chem* **274**, 3017-25.

Pollard, T.D., Cooper, J.A. (1986) Actin and actin-binding proteins. A critical evaluation of mechanisms and functions. *Annu Rev Biochem* **55**, 987-1035.

Pollard, T.D., Doberstein, S.K., Zot, H.G. (1991) Myosin-I. *Annu Rev Physiol* **53**, 653-81.

Rappleye, C.A., Paredes, A.R., Smith, C.W., McDonald, K.L., Aroian, R.V. (1999) The coronin-like protein POD-1 is required for anterior-posterior axis formation and

cellular architecture in the nematode *Caenorhabditis elegans*. *Genes Dev* **13**, 2838-51.

Rauchenberger, R., Hacker, U., Murphy, J., Niewohner, J., Maniak, M. (1997) Coronin and vacuolin identify consecutive stages of a late, actin-coated endocytic compartment in *Dictyostelium*. *Curr Biol* **7**, 215-8.

Reeves, E.P., Dekker, L.V., Forbes, L.V., Wientjes, F.B., Grogan, A., Pappin, D.J., Segal, A.W. (1999) Direct interaction between p47phox and protein kinase C: evidence for targeting of protein kinase C by p47phox in neutrophils. *Biochem J* **344 Pt 3**, 859-66.

Reha-Krantz, L.J. (1985) The *Escherichia coli* strain JM105 contains partial supE activity. *Gene* **38**, 275-6.

Robinson, D.N., Ocon, S.S., Rock, R.S., Spudich, J.A. (2002) Dynacortin is a novel actin bundling protein that localizes to dynamic actin structures. *J Biol Chem* **277**, 9088-95.

Sambrook, J., Fritsch, E.F., Maniatis, T. (1989). Molecular cloning. A laboratory manual., Cold Spring Harbour Laboratory, Cold Spring, NY.

Schafer, D.A., Hug, C., Cooper, J.A. (1995) Inhibition of CapZ during myofibrillogenesis alters assembly of actin filaments. *J Cell Biol* **128**, 61-70.

Schafer, D.A., Cooper, J.A. (1995) Control of actin assembly at filament ends. *Annu Rev Cell Dev Biol* **11**, 497-518.

Schuller, S., Neefjes, J., Ottenhoff, T., Thole, J., Young, D. (2001) Coronin is involved in uptake of *Mycobacterium bovis* BCG in human macrophages but not in phagosome maintenance. *Cell Microbiol* **3**, 785-93.

Schulze, A. (2001) Charakterisierung von Coronin 7, einem neuen Coronin-ähnlichen Protein. *Diplomarbeit*, Institut für Biochemie I, Universität zu Köln

Smith, T.F., Gaitatzes, C., Saxena, K., Neer, E.J. (1999) The WD repeat: a common architecture for diverse functions. *Trends Biochem Sci* **24**, 181-5.

Spoerl, Z., Stumpf, M., Noegel, A.A., Hasse, A. (2002) Oligomerization, F-actin interaction, and membrane association of the ubiquitous mammalian coronin 3 are mediated by its carboxyl terminus. *J Biol Chem* **277**, 48858-67.

Stock, A., Steinmetz, M.O., Janmey, P.A., Aebi, U., Gerisch, G., Kammerer, R.A., Weber, I., Faix, J. (1999) Domain analysis of cortexillin I: actin-bundling, PIP(2)-binding and the rescue of cytokinesis. *Embo J* **18**, 5274-84.

Stossel, T.P. (1993) On the crawling of animal cells. *Science* **260**, 1086-94.

Sutherland, J.D., Way, M. (2002) Looking over the edge: a new role for Ena/VASP proteins in lamellipodial dynamics. *Dev Cell* **2**, 692-4.

- Suzuki, K., Nishihata, J., Arai, Y., Honma, N., Yamamoto, K., Irimura, T., Toyoshima, S.** (1995) Molecular cloning of a novel actin-binding protein, p57, with a WD repeat and a leucine zipper motif. *FEBS Lett* **364**, 283-8.
- Tang, J.X., Janmey, P.A.** (1996) The polyelectrolyte nature of F-actin and the mechanism of actin bundle formation. *J Biol Chem* **271**, 8556-63.
- Tardieux, I., Liu, X., Poupel, O., Parzy, D., Dehoux, P., Langsley, G.** (1998) A Plasmodium falciparum novel gene encoding a coronin-like protein which associates with actin filaments. *FEBS Lett* **441**, 251-6.
- Way, M., Pope, B., Cross, R.A., Kendrick-Jones, J., Weeds, A.G.** (1992a) Expression of the N-terminal domain of dystrophin in *E. coli* and demonstration of binding to F-actin. *FEBS Lett* **301**, 243-5.
- Way, M., Pope, B., Weeds, A.G.** (1992b) Evidence for functional homology in the F-actin binding domains of gelsolin and alpha-actinin: implications for the requirements of severing and capping. *J Cell Biol* **119**, 835-42.
- Weber, I., Niewohner, J., Faix, J.** (1999) Cytoskeletal protein mutations and cell motility in Dictyostelium. *Biochem Soc Symp* **65**, 245-65.
- Weihing, R.R.** (1985) The filamins: properties and functions. *Can J Biochem Cell Biol* **63**, 397-413.
- Weitzdoerfer, R., Fountoulakis, M., Lubec, G.** (2002) Reduction of actin-related protein complex 2/3 in fetal Down syndrome brain. *Biochem Biophys Res Commun* **293**, 836-41.
- Welch, M.D., DePace, A.H., Verma, S., Iwamatsu, A., Mitchison, T.J.** (1997) The human Arp2/3 complex is composed of evolutionarily conserved subunits and is localized to cellular regions of dynamic actin filament assembly. *J Cell Biol* **138**, 375-84.
- Welch, M.D., Iwamatsu, A., Mitchison, T.J.** (1997) Actin polymerization is induced by Arp2/3 protein complex at the surface of *Listeria monocytogenes*. *Nature* **385**, 265-9.
- Welch, M.D., Mallavarapu, A., Rosenblatt, J., Mitchison, T.J.** (1997) Actin dynamics in vivo. *Curr Opin Cell Biol* **9**, 54-61.
- Whalen, R.G., Butler-Browne, G.S., Gros, F.** (1976) Protein synthesis and actin heterogeneity in calf muscle cells in culture. *Proc Natl Acad Sci U S A* **73**, 2018-22.
- Wientjes, F.B., Reeves, E.P., Soskic, V., Furthmayr, H., Segal, A.W.** (2001) The NADPH oxidase components p47(phox) and p40(phox) bind to moesin through their PX domain. *Biochem Biophys Res Commun* **289**, 382-8.
- Wuestehube, L.J., Luna, E.J.** (1987) F-actin binds to the cytoplasmic surface of ponticulín, a 17-kD integral glycoprotein from Dictyostelium discoideum plasma membranes. *J Cell Biol* **105**, 1741-51.

Zaphiropoulos, P.G., Toftgard, R. (1996) cDNA cloning of a novel WD repeat protein mapping to the 9q22.3 chromosomal region. *DNA Cell Biol* **15**, 1049-56.

Zheng, P.Y., Jones, N.L. (2003) Helicobacter pylori strains expressing the vacuolating cytotoxin interrupt phagosome maturation in macrophages by recruiting and retaining TACO (coronin 1) protein. *Cell Microbiol* **5**, 25-40.

Erklärung

Ich versichere, dass ich die von mir vorgelegte Dissertation selbständig angefertigt, die benutzten Quellen and Hilfsmittel vollständig angegeben und die Stellen der Arbeit - einschließlich Tabellen und Abbildungen -, die anderen Werken im Wortlaut oder dem Sinn nach entnommen sind, in jedem Einzelfall als Entlehnung kenntlich gemacht habe; dass diese Dissertation noch keiner anderen Fakultät oder Universität zur Prüfung vorgelegen hat; dass sie – abgesehen von unten angegebenen beantragen Teilpublikationen – noch nicht veröffentlicht ist, sowie, dass ich eine Veröffentlichung vor Abschluss des Promotionsverfahrens nicht vornehmen werde. Die Bestimmungen dieser Promotionsordnung sind mir bekannt. Die von mir vorgelegte Dissertation ist von Frau Professor Dr. Angelika Anna Noegel betreut worden.

Köln, den 05.05.2003

Ziqiang Spoerl

Teilpublikation

Spoerl, Z., Stumpf, M., Noegel, A.A., Hasse, A. (2002) Oligomerization, F-actin interaction, and membrane association of the ubiquitous mammalian coronin 3 are mediated by its carboxyl terminus. *J Biol Chem* **277**, 48858-67.

Acknowledgements

My profound gratitude is to Professor Dr. Angelika Anna Noegel, Institute of Biochemistry I, Medical Faculty, University of Cologne for her offering me the opportunity to work in her research group and excellent working condition, constructive comments on the results, and valuable suggestions on the preparation of this thesis.

An ordinary "appreciation" for my adviser, Dr. Andreas Hasse is entirely inadequate to express how grateful I am for his valuable guidance, creative suggestion, fruitful discussion, and constant encouragement during the course of present work. His scientific and personal support is a decisive factor to the present work. His logical and analytical comments on the manuscript are deeply appreciated.

I am grateful to Professor Dr. Helmut W. Klein for overtaking the coreferrance.

I owe my indeed thanks to Dr. Elena Korenbaum for providing rabbit skeletal muscle G-actin. For the help of Dr. Budi Tunggal on computer software and Dr. Francisco Rivero on confocal laser microscopy I am deeply grateful.

My appreciation goes to Maria for her endless support upon request during the work, especially for her generous gift of mAB K6-444. The constant assistance of Berthold in cell culture and in computer programs is unforgettable. I am very grateful to the members of lab 12 for the pleasant working atmosphere.

I am indebted to Thorsten for his help in the quantification of the bands with a Molecular Dynamics scanner and ImageQuant software. For several techniques and nice suggestions used, I would like to thank Rosemarie and Rolf.

My thanks go to Frau Michel and Bettina for their patience and all of the necessary administrative works.

For the friendly cooperation, I am grateful to the members of our department including: Alfred, Monika, Tina, Christoph, Marija, Michael, Nandu, Deen, Bärbel, Roberto, Sonia, Soraya, Henning, Akis, and all other lab colleagues.

I shall always appreciate my German mother for her deep understanding and incredible affection and continuous encouragement during completing this work. I would like to thank all of my friends for their interests and indisputable balance.

Lebenslauf

Name: Ziqiang Spoerl
Geburtsdatum: 15.05.64
Geburtsort: Shanghai, China
Staatsangehörigkeit: Deutsch
Anschrift: Kolbergerstr. 13, 50997 Köln

Schulausbildung:

September 1970 - Juli 1975 Shanghai Zhangshou Grundschule

September 1975 - Juli 1981 Shanghai Jinyuan Gymnasium
Abschluß: Abitur

Studium:

September 1981 - Juli 1984 1. Studium am Shanghai Medical Instrumentation College
Studiengang: Medizintechnik
Abschluß: Diplom-Medizintechniker

April 1996 - Dez. 1999 2. Studium an der Universität zu Köln,
Studiengang: Diplom-Chemie
Schwerpunkt: Biochemie
Abschluß: Diplom-Chemiker

Januar - Juli 2000 Diplomarbeit am Institut für Biochemie der Med. Fakultät
der Universität zu Köln bei Prof. Dr. Angelika A. Noegel
Thema: Charakterisierung der Aktinbindung von
rekombinantem humanen Coronin-3

Tätigkeit:

Juli 1984 - Februar 1993 Wissensch. Mitarbeiter am Medical Research Center
der Shanghai Railway Medical College

März 1993 - Januar 1994 Wissensch. Mitarbeiter am Institut für Pharmakologie und
Toxikologie, med. Fakultät der Technischen Universität
München

Februar 1994 - März 1996 Wissensch. Mitarbeiter am Institut für Physiologie, med.
Fakultät der Universität zu Köln

August 2000 – Mai 2003 Promotion an der Mathematische-
Naturwissenschaftlichen Fakultät der Universität zu Köln
Praktische Arbeit am Institut für Biochemie I der Med.
Fakultät der Universität zu Köln
bei Prof. Dr. Angelika A. Noegel
Thema: Functional analysis of mammalian coronin3

Köln, den 05 Mai 2003

Ziqiang Spoerl

Curriculum Vitae

Personal data

Name: Ziqiang Spoerl
Date of birth: 15.05.1964
Place of birth: Shanghai, China
Nationality: German
Address: Kolbergerstr. 13, 50997 Cologne, Germany

Education

September 1970 - July 1975 Shanghai Zhangshou primary school
September 1975 - July 1981 Shanghai Jinyuan secondary school

University Education

September 1981 - July 1984 Shanghai Medical Instrumentation College
Major: Medical Instrumentation
Diplom-Medical Technician
April 1996 – July 2000 University of Cologne
Major: Chemistry
Diplom-Chemist

Employments

July 1984 – February 1993 Research assistant, Medical research center
Shanghai Railway Medical College
March 1993 – January 1994 Research assistant,
Institute of Pharmacology and Toxicology
Medical Faculty, Technical University of Munich
February 1994 – March 1996 Research assistant,
Institute of Physiology, Medical Faculty,
University of Cologne
August 2000 – May 2003 Doctoral studies,
Advisor: Professor Dr. Angelika A. Noegel
Institute of Biochemistry I
Medical Faculty, University of Cologne
Thesis: Functional analysis of mammalian coronin3

Cologne, May 05, 2003

Ziqiang Spoerl